Technical Report for ESA/ESTEC No. 1/1999
January 1999

[Report for ESTEC contract no. 12954/98/NL/GD,
WP 110: Review of sampling requirements and mission scenarios]

Review of Sampling Requirements and Mission Scenario Study

J. Ramsauer and G. Kirchengast
Institute for Meteorology and Geophysics, University of Graz (IMG/UoG)
A-8010 Graz, Halbärthgasse 1, Austria

Contents

1 Introduction

The 'generic GRAS'-related spatial and temporal sampling requirements for operational meteorology given in the "Report of the GRAS-SAG" are briefly reviewed concerning their suitability for modern NWP.

These requirements include horizontal and vertical sampling, both of which are intrinsically associated (by the nature of this satellite-to-satellite sounding technique) with characteristic temporal sampling requirements for a given GNSS/LEO satellite constellation. Horizontal sampling, expressed (to zeroth order) by the average sampling distance between individual occultation profiles within a desired area (e.g., full globe), depends strongly on the time interval allowed for a single sampling cycle, i.e., on the required time resolution. Vertical sampling, expressed by the average vertical distance of individual occultation rays sampled within a suitable height interval (e.g., stratosphere), depends strongly on the sampling rate of the GNSS receiver(s) in LEO (in turn this sampling rate should be compliant with the instruments observational bandwidth in order to avoid aliasing).

These interdependencies have to be kept in mind when focusing on reviewing the constellation-relevant requirements in the GRAS-SAG report. One implication of them is that the vertical sampling requirement only weakly depends on given constellation; thus it can be considered an off-line topic w.r.t. constellation studies. The mission scenario study work performed and this written report therefore concentrate on the sampling of the geographical (horizontal) space.

It is also practically very important to take into account typical natural constraints on GNSS/LEO constellations. The GNSS side is very strongly constrained by prescribed layout of the existing GPS and GLONASS space segments so that these can be used, favorably, as firm-fixed reference constellations.

The LEO side, however, has much more degrees of freedom. Without assuming some basic constraints for this side, the investigation of optimal constellations is prohibitive due to the very large basin space of options. To this end, sensible a priori constraints, as we introduce below, help to greatly reduce the basin space of scenario options. In turn, this then allows a tractable number of scenarios to be studied with proper quantitative rigor.

2 Generic GRAS Observational Requirements

2.1 The Requirements for Operational Meteorology

This report is concerned with the planning for a suitable satellite constellation for atmospheric temperature and humidity measurements for NWP using the radio occultation technique. The expected advantages of the occultation technique for the purposes of NWP were already discussed in several ESA-Reports (e.g., see the EUMETSAT-ESA document "Report of the GRAS-SAG", where GRAS means Global navigation satellite system Receiver for Atmospheric Sounding and SAG denotes the GRAS Science Advisory Group) and several papers in the scientific literature.

To take the full advantage of the occultation method, one should use the whole Global Navigation Satellite Systems (GNSS) (i.e. the USA's Global Positioning System, GPS,

and the Russian Global Navigation Satellite System, GLONASS) using their high performance radio transmitters in high orbits along with sophisticated receivers on low Earth orbiting (LEO) satellites. This combination allows to make radio occultation measurements for the Earth's atmosphere with an accuracy useful for applications in operational meteorology, or NWP, as well as in climate and in ionospheric research.

Table 2.1 gives, following the GRAS-SAG report, a compact overview of the needed accuracies for performing operational meteorology at a substantially improved level (especially concerning the absolute data accuracy and the really global distribution of the measurements, provided the satellite constellation is properly designed).

		Temperature	**Humidity**	**Bending Angle**
Horizontal Domain		Global	Global	Global
Horizontal Sampling(1)		< 300 km(2)	< 300 km(2)	< 300 km(2)
Vertical Domain		surface to 1 hPa (0 - 50 km)	surface to 300 hPa (0 - 10 km)	surface to 80 km
Vertical Resolution		0.5 - 1.0 km	0.5 km	< 0.5 km or equivalent in time sampling
Time Resolution		1 - 6 hrs	1 - 6 hrs	1 - 6 hrs
Absolute Accuracy	0 - 30 km	< 1 K	< 10 % or < 0.2 g/kg(3)	< 1 μrad or 0.4 %(3)
	30 - 50 km	< 2 K	n/a	< 1 μrad or 0.4 %(3)
Timeliness		2 - 3 hrs	2 - 3 hrs	2 - 3 hrs

Table 2.1: Generic GRAS Requirements for Operational Meteorology

Notes: (1) This would be the mean sampling distance between atmospheric profiles.
(2) This assumed 20 to 25 satellites carrying GRAS.
(3) Whatever is larger.

2.2 Brief Review

The important improvements compared to present weather data collection systems (as readily seen from Table 2.1) are the globally distributed horizontal sampling with mean inter-event distances of less than 300 km (and with a reasonable time resolution of the order of less than 6 hrs) combined with a vertical resolution of about 0.5 - 1 km for all measured parameters. Also the needed absolute accuracies for the measured physical parameters are perhaps only achievable with such (very carefully designed) GRAS instruments and by using sophisticated atmospheric models.

Given the most modern global NWP systems, which achieve resolutions of T319 (50 - 100 km) horizontally (e.g., the ECMWF state-of-the-art medium range forecast model), the horizontal resolution (achieved within $\sim$ 6 hrs) could even be much better than 300 km, allowing still to gain further information. And Local Area Models (LAMs), which achieve today resolutions of $\sim$ 10 km could in principle exploit data with even higher geographic resolution.

The point important to note in relation to the GNSS occultation method is, however, that this is a method unique in vertical resolution and absolute accuracy but - being a

limb sounding method - its horizontal resolution is best suited to resolve all scales down to the mesoscale (i.e., down to $\sim$ 100 km) but not finer scales. Even when thinking of a comparatively large constellation of $\sim$ 100 LEO receivers, the scales resolved will be typically $>$ 100 km (within a 6 hrs sampling cycle). The physical resolution of a profile from a single event is $\sim$ 200 - 300 km. It seems thus reasonable to assume a "maximum" constellation of $\sim$ 25 satellites, geometrically resolving all scales down to the physical resolution measure of a single event, as a quite reasonable implementation.

In other words, such a constellation seems to be an ideal backbone of a global operational meteorology observing system for horizontal scales down to some 100 km - and it delivers vertical profiling of unique capability at this "grid size"; for the horizontal scales smaller than 100 km it should be complemented by other observing systems (e.g., high-spectral resolution downlooking sounders).

We will below, based on this brief review and evaluation of reasonable horizontal resolution "requirements" of GNSS occultation, choose the largest constellations to consist of 24 satellites. Since good NWP impact can be expect already with a significantly lower number of satellites, we will study also smaller constellation scenarios comprising either 6 or 12 satellites.

3 Basic Considerations for Mission Scenario Studies

3.1 Constraints

For our satellite constellation study, the horizontal sampling requirements in conjunction with the given time resolution requirement are the major challenge to be fulfilled. Before actually designing specific satellite constellations, we shall take a short look to several useful general mission constraints, in order to reduce the basin space of scenario options. We will only afterwards fix the main orbital design parameters within the subspace obeying these constraints.

As said earlier, we want to use the whole GNSS constellation of (ideally) 24 GPS and 24 GLONASS satellites for our purposes. The GPS and GLONASS satellites are orbiting the Earth in groups of 6-8 satellite per orbital plane (using 3-4 different orbital planes) in circular orbits about 20,000 km above the Earth's surface. These systems form our basic GNSS system of ultra-stable radio transmitters in High Earth orbit and are therefore a fixed quantity for us.

For the LEO segment of our satellite network (the core of this study) there is (theoretically) a lot more freedom in designing the orbital parameters, the satellite numbers per orbit plane, etc., but for practical reasons (size, complexity, and last but not least the system costs) we introduce some reasonable a priori constraints in advance before we start to hard-quantify different LEO satellite scenarios.

- We fixed the height of the LEO's to $\simeq$ 800 km (i.e., $a \simeq 7170$ km, a is the semimajor axis of the satellite orbit) above ground. There are several good reasons for doing this (e.g., to design near-polar sun-synchronous orbits, where the LEO crosses always at the same local time the equator, to avoid large air drag but to dig not too deep into the Van Allen belts, etc.). It is also well known that the price per mass unit grows with orbit height (and the LEO mass would be about the same for all potential orbits). Also recommended, and used, is a nearly circular orbit in order to render the

occultation conditions about the same all over the orbit. (eccentricity of $e \simeq 0.001$ will be tolerated; and will be our fixed setting).

- The argument of the perigee will be tendatively placed at $\omega \simeq 90°$ (and is in fact fixed there) to best fit Earth's ellipticity effects for high-inclined orbits.
- The epoch does not alter at all in this study and was fixed to $T = 96213.5$ (31. July 96, 12.00 hrs) to match the epochs in the gps/glo *.tle files. Absolute time is not relevant for this study.

After fixing the first three Kepler parameters, we concentrate now on the three remaining orbital quantities. So what can be changed is Ω the node, I the inclination, and M the mean anomaly of the LEO satellite orbit at the given epoch. It is useful for further work to make also some constraints on these more free parameters:

- For a given number of orbits, the individual orbit nodes Ω shall be equally separated along the equator as baseline. In case of deviations from this rule it will be separately mentioned.
- Constraints for the mean anomaly are that given some satellites per orbit, the satellites shall be equally separated in the orbit as baseline (e.g., 3 LEO's will be separated by 120°). In case of deviations from this rule it will be separately mentioned.
- Theoretically the orbital inclination I, finally, is an almost free parameter, which can vary from $0° \leq I \leq 180°$, but practically $0° \leq I \leq 98°$ (i.e., sun-synchronous orbits are the most retrograde ones allowed) shall be used without significant loss of generality.

With these orbital geometry constraints defined we move on to also make reasonable assumptions for several other relvant parameters, before we can construct one "real" satellite scenario. Despite all the limitations the number of possible constellation scenarios is otherwise still much to large. These other settings include:

- The total number of satellites in LEO N shall be limited to $N \leq 24$ (in order to limit run-time, in view of the OSSE study to be performed as a next step, but to nevertheless allow to reach the 300 km/6 hrs horizontal resolution goal set out by Table 2.1 above).
- One occultation event simulation shall generally run for 0.5 days (12 hrs), half of which (6 hrs) will finally be used for computing the presented statistical measures (the other half is for verification purposes).
- The simulation domain shall be global.
- The rays (GNSS-LEO) shall be straight line.
- The Earth figure shall be spherical.
- Visibilities are not of interest as baseline.

- Occultation antennae are generally $-\vec{v}$ & $+\vec{v}$ antennae with typical azimuths (180°/0°), elevations (27°) and a TPBW of 90° (TPBW means Threshold Power Beam Width).
- Occultation events are geolocated computing at a single height level (we chose 1 km height above sea level, to be matched with an accuracy of 100 m). This 1 km target height for straight line rays represents well, based on experience, the tropopause-crossing locations of real events (for bended rays).

Based on the constraints above, the basin space for constellation scenarios is still big (i.p., since the total number of satellites and the inclination range is rather wide), so we select in a next step some useful sampling of the scenario basin space by trial scenarios.

3.2 Basic Scenarios

We selected 21 single-orbit baseline cases for further evaluation. Common for all of them is that they use only one orbital plane (O=1) for the different satellite configurations. This single orbit plane contains 1, 3, or 6 satellites (S$\epsilon\{1,3,6\}$), and the inclination varies, in 7 (unequal) steps, from an equatorial 0° to a sun-synchronous 98° orbit. A list of these basic scenarios is given for convenience by Table 3.1.

O=1	O=1	O=1
S=1	S=3	S=6
I=98	I=98	I=98
I=90	I=90	I=90
I=80	I=80	I=80
I=70	I=70	I=70
I=60	I=60	I=60
I=30	I=30	I=30
I=0	I=0	I=0

Table 3.1: Basic LEO Satellite Constellation Scenarios

Notes: O denotes the number of orbital plane(s).
S is the number of satellites per orbital plane.
I marks the inclination of the orbital plane(s).

The mean anomaly (in-orbit) spacing for the 3-satellite cases is 120°, for the 6-satellite cases it is 60°. These 21 baseline runs were necessary in order to get basic quantitative information and a good feeling for sensibly defining a reasonable sample of so-called real scenario cases later on (chapter 5).

3.3 Calculations of the Baseline Scenarios

3.3.1 Tangent Point Calculations with EGOPS

The next step in the evaluation of the 21 baseline scenarios is to calculate the tangent points of the straight-line GNSS-LEO rays with respect to the surface of the Earth. For this purpose, the EGOPS simulation tool was used (EGOPS is the End to end GNSS Occultation Performance Simulator, a software developed 1997/98 under the leadership of IMG/UoG for ESA). The MAnPl (Mission Analysis and Planning) tool of EGOPS is ideally suited for performing the simulations required here.

Before working with MAnPl under EGOPS, the so-called leo*.tle files for the LEO sats had to be calculated (EGOPS uses standard NASA/NORAD "two-line-element (tle) files", which contain all needed parameters for defining the satellite(s) orbit(s) (epoch of perigee, inclination, right ascension of ascending node, eccentricity, argument of the perigee, etc.). In the simplest case (only one satellite is orbiting, as in the first 7 cases) a *.tle file contains all necessary orbital parameter information in only two lines - therefore the name of these files. For calculation of leo*.tle files, EGOPS' "CreateTLEs" routine was used (this had to be done for every different satellite constellation).
For the GNSS space segment of our satellite configuration, we took the standard gps*.tle and glo*.tle files contained in the EGOPS package (gps96213.tle and glo96213.tle — these contain full 24-satellite GPS/GLONASS standard constellations). Before beginning with the MAnPl simulations, all needed leo*.tle files had to be stored in the /orbitelem subdirectory of EGOPS.

Now the EGOPS-MAnPl tool can be used for calculation of the so-called *.sgd files (sgd means simulated geometry data). These files contain (beside other information), the geographical coordinates of the tangent points of all occultation events within a simulated time range. For calculating those results, we need as EGOPS input parameters the UT Range, the Height Levels, the Geographic Area of Interest for the Occultation Events, the GNSS-LEO Ray Treatment, the Earth Figure Model, the GRAS Antennae Specifications, and the LEO- and the GNSS Specifications. A 12 hr simulation time was chosen, from which a 6 hr time interval was cut out for data processing and analysis. Using a single Height Level was also sufficient for this kind of geographical coverage study. Typical values for these input parameters can be seen in Table 3.2, which shows the actual MAnPl input for basic case 2 (one LEO circling the Earth in an orbit with an inclination of 90° so that the satellite passes over both poles every orbit). The orbital period of our chosen LEO sats is near 100 min, whereas the orbital period for the GNSS satellites is near 12 hrs (orbit height $\sim$ 20,000 km).

3.3.2 Analysis of occultation event location results

With the tangent points obtained with the aid of EGOPS, we are now ready for statistical post-processing of these results to achieve better knowledge of the value of our basic satellite constellation scenario.

We chose to calculate the following 5 main statistical measures, which will also form the basis for a performance assessment of mission scenarios at a later stage:

[*UT Range*]	
Start_Time	= 960801.000000 [yymmdd.hhmmss]
Simul_Time_Range	= 0120000 [hhhmmss]
[*Height Levels*]	
Hlo1 Hhi1 HStep1 dh1	= 1.0 1.0 0.0 0.10 [km]
[*Geographic Area of Interest for Occ.Events*]	
GeogrAreaChoice	= Global
[*GNSS-LEO Ray Treatment*]	
RayTreatmentChoice	= Straight Line Rays
[*Earth Figure Model*]	
EarthFigModelChoice	= Spherical
[*GRAS Antennae Specifications*]	
-V AntennnaChoice	= Used
-V BoresightElevation	= 27.0 [deg]
-V BoresightAzimuth	= 180.0 [deg]
-V FOVChoice	= Conical
-V TPBW Vertical	= 90.0 [deg]
-V TPBW Horizontal	= 90.0 [deg]
+V AntennaChoice	= Used
+V BoresightElevation	= 27.0 [deg]
+V BoresightAzimuth	= 0.0 [deg]
+V FOVChoice	= Conical
+V TPBW Vertical	= 90.0 [deg]
+V TPBW Horizontal	= 90.0 [deg]
[*LEO Specifications*]	
LEOOrbElemFilename	= leoO1S1I90.tle
LEOOrbModelChoice	= Keplerian Orbits
[*GNSS Specifications*]	
GPS SatSystemChoice	= Standard
GPSOrbElemFilename	= gps96213.tle
GLON SatSystemChoice	= Standard
GLONOrbElemFilename	= glo96213.tle
GNSSOrbitModelChoice	= Keplerian Orbits

Table 3.2: Typical MAnPl Input for a Basic Scenario

- N $(= N_{occ}^{(\Delta T)}(A))$ $[1/(1000km)^2]$ is the total number of occultation events per unit area within a given sampling time (ΔT) in a given geographic area A.

- $\overline{d}$ $(= \overline{d}_{occ}^{(\Delta T)}(A))$ $[km]$ denotes the mean horizontal sampling distance between neighbor occultation events within a given sampling time (ΔT) in a given geographic area A; $\overline{d} = \frac{1}{n_A}\sum_{i=1}^{n_A} d_i$, with n_A the number of events in $\{(\Delta T), A\}$.

- σ_d $(= \sigma_{docc}^{(\Delta T)}(A))[km]$ is a sampling distance dispersion measure (rms deviation about mean) for given $\{(\Delta T), A\}$; $\sigma_d = \left[\frac{1}{n_A - 1}\sum_{i=1}^{n_A}\left(d_i - \overline{d}\right)^2\right]^{\frac{1}{2}}$.

- $\overline{t}$ $(= \overline{t}_{occ}^{(\Delta T)}(A))$ $[min]$ is the mean time separation between neighbor occultation events for given $\{(\Delta T), A\}$; $\overline{t} = \frac{1}{n_A}\sum_{i=1}^{n_A} t_i$.

- σ_t $(= \sigma_{tocc}^{(\Delta T)}(A))[min]$ is the time separation dispersion measure for given $\{(\Delta T), A\}$; $\sigma_t = \left[\frac{1}{n_A - 1}\sum_{i=1}^{n_A}(t_i - \overline{t})^2\right]^{\frac{1}{2}}$.

Furthermore, as global indices/single figures of merit, the following values were routinely calculated as scalar quantities:

- $\sigma_N^{gl} = \left[\frac{1}{N_A - 1}\sum_{i=1}^{N_A}\left(N_i^A - N^{gl}\right)^2\right]^{\frac{1}{2}}$ & $\tilde{\sigma}_N^{gl} = \frac{\sigma_N^{gl}}{N^{gl}}$ represent the "coverage inhomogenity indices", i.e., global absolute & relative measures, respectively, of how (un)equally distributed the occultation events are in general (N_i^A is the number of events collected in region A, N_A is the number of areas).

- σ_d^{gl} & $\tilde{\sigma}_d^{gl} = \frac{\sigma_d^{gl}}{\overline{d}^{gl}}$ are the "geographic irregularity indices", i.e., global absolute & relative measures, respectively, of how (ir)regularly the occultation events are distributed over geographic space.

- σ_t^{gl} & $\tilde{\sigma}_t^{gl} = \frac{\sigma_t^{gl}}{\overline{t}^{gl}}$ are the "time irregularity indices", i.e., global absolute & relative measures, respectively, of how (ir)regularly the occultation events are ordered in time.

The two further external parameters required to be set for the analysis are $\{(\Delta T), A\}$:

As noted earlier a (ΔT) of 6 hrs was used for our study (it is the upper bound of the time sampling requirement spec according to Table 2.1). We confirmed for our post-processing computations that our results are virtually invariant w.r.t. the specific choice of the 6-hr window within the basic 12-hr interval available from the basic tangent point location processing by EGOPS. All result shown were taken from the center of the 12 hrs time interval, i.e., from 3-9 UT).

For better regional analysis of our data several different areas A were used . For computing the global values, we computed the required statistical measures for the whole Earth. For all other values, we limited the computations, for computational speed, to the northern hemisphere or subregions of it. This no real restriction at all, however, we just sensibly exploit the perfect north-south symmetry inherent in circular satellite orbits. This symmetry is indeed only broken to an irrelevant degree in our context, as we confirmed for all measures by routinely computing a hemispheric asymmetry factor (see further below). (It is slightly broken, especially for few satellites, given that the total time span is not an integer multiple of the orbit period).

Specifically we analyzed the following 49 different sub-global areas (together with "global" there are 50):

- Northern Hemisphere (NH).

- 6 Latitude Bands $\epsilon\{0° - 15°, 15° - 30°, 30° - 45°, 45° - 60°, 60° - 75°, 75° - 90°\}$ in NH.

- 6 Longitude Bands $\epsilon\{0° - 60°, 60° - 120°, 120° - 180°, 180° - 240°, 240° - 300°, 300° - 360°\}$ in NH.

- 6 x 6 Cells $\epsilon\{$the 36 15° x 60° LatLon cells from using the above bands$\}$ in NH.

We produced a computer code to compute these chosen statistical measures (the d_i's, t_i's, etc.) from the given occultation event tangent point locations (ϕ_i, λ_i) stored in the respective *.sgd files of the mission scenarios. All five measures (and the three global indices, plus a hemispheric asymmetry factor) were calculated for all chosen areas. Thus, for example, the latitude averages for one measure are *not* just averaged results form the individual cell values making up this latitude band. This is important, since such operation were actually wrong given that there is no "superposition principle" valid in this context.

As first step in the computation process, the size of the individual areas was determined by integrating over the respective spherical surface. This provides us with 50 different values, beginning from the area of the whole planet (about 510 x $10^6 km^2$) to the area of the smallest pieces (the 6 circumpolar cells $\geq 75°$). Using this for normalization and counting the number of events, i.e., tangent points which happen to fall into a given area, the computation of N is straightforward.

For computation of $\overline{d}$ and σ_d, respectively, it was necessary, for having a robust general algorithm, to proceed as follows: We need to calculate the average distance d_i from each tangent point location to its neighbor tangent points. This was accomplished by dividing the surrounding of the tangent point into 4 equal azimuth ranges (a north-, west-, south-, and east range), then computing the distance to the closest neigbor in each azimuth sector and averaging over the four minimum distances found. This yields, after performed for all events in an area, all d_i values. The calculation of $\overline{d}$ and σ_d is then straightforward based on the formulae given above.
With this method one obtains good results even in sparse-event situations, where more straightforward methods fail due to difficulties to deal with small event numbers in a given area.

The same method was chosen for the computation of $\overline{t}$ and σ_t, respectively, as it is obvious that time separations between neighbor events, t_i, can be handled in close link to the computation of the distances d_i. After the four closest neigbors are found as outlined above we take the Universal Times when these events occurred and average them to obtain t_i. Having these values the computation of $\overline{t}$ and σ_t is readily done based on the respective formulae above.
It should be noted that tight "clouds" of tangent point locations over a given area do not imply that they are also closely packed in time. This is due to the somewhat intricate way in which GNSS occultation events are sampled.

After preparing the 5 measures for all defined areas, the 6 global indices (σ_N^{gl}, $\tilde{\sigma}_N^{gl}$; σ_d^{gl}, $\tilde{\sigma}_d^{gl}$; σ_t^{gl}, $\tilde{\sigma}_t^{gl}$) were calculated, which is straightforward (see their definition above). The hemispheric asymmetry factor, computed for each measure, is finally obtained as $DX^{hem/gl} = 100(X^{NH} - X^{gl})/X^{gl}$ (units [%]), with X denoting one of the 5 measures.

The results of these post-processing computations, together with some major orbital information defining the satellite constellations, are now ready for being visualized and inspected in a comparative manner.

4 Visualization of the Baseline Scenario Results

4.1 The Format and Structure of all Result Plots

For optimum visualization of the results we used a plot concept comprising two panels per page with a 7 x 7 cell arrangement per panel. We give here a short description on how to understand the plots. Since all plot panels shown in this report have a common structure, we provide this description just on this single place here for both the baseline scenarios following below and for the realistic scenarios following in chapter 5. We will explain the plot panel contents from top to bottom of panel.

At the top of each plot panel there are two header lines. The first line contains, at its first position, the name of the plot parameter (i.e., statistical measure) displayed, together with its physical unit. The following abbreviations are used for describing the 5 measures:

- Event No N/$(1000km)^2$ $[Mm^2]$, for the occultation event number density per square megameter.
- Mean HDist md [km], for the Mean Horizontal Distance between neighbor occultation events, measured in kilometers.
- HDistDisp sd [km], for the Horizontal Distance Dispersion (rms distance about mean), measured also in kilometers.
- MeanTSep mt [min], for the Mean Time Separation between neighbor occultation events, measured in minutes.
- TSepDisp st [min], for the Time Separation Dispersion (rms separation about mean), measured also in minutes.

If there is more than one different satellite scenario plotted (up to 4 are possible per panel, each visualized by a histogram bar), the measure displayed for the different scenarios is of course one and the same for all scenarios.

The next three groups of acronyms in the first line give the main satellite constellation information. Beginning with the left one, O is the number of orbital planes used (O can be 1, 2 or 4 in our case), S is the number of individual satellites per orbital plane (S can be 1, 3, or 6 for "symmetrical" scenarios or 2, 4 or 8 for "asymmetrical" scenarios; see details on that in the description of the realistic scenarios), and I denotes the inclination of the orbital planes (I can be 00, 30, 60, 70, 80, 90 or 98 degrees). In case more than one scenario is plotted (we generally plotted, in order to save trees, 3 or 4 scenarios per panel), the individual values for O, S, and I, respectively, of the specific scenarios shown are separated by vertical lines for better recognition of the respective values (the leftmost value is associated with the leftmost histogram bars plotted in each of the 7 x 7 cells, the second-left value with the second-left histogram bars, and so on). In case more than one plane is involved (O greater than 1) the values for S and I comprise the information on the number of satellites in a plane and on the inclination of a plane, respectively, for all planes. For example, if O=2 (2 orbit planes), then S=42 and I=8030 if the first plane holds 4 satellites at 80 deg inclination and the second plane holds 2 satellites at 30 deg inclination. If the plot panel shows three different scenarios, typically different due to trying different inclinations, this may look like O=2—2—2, S=42—42—42, I=8030—8055—9830 (i.e.,

the number of orbits and the distribution of satellites into the orbit is the same for all three scenarios, but the orbit inclination are varied).

The second header line shows, for the plotted measure, the two global indices defined above in section 3.3.2 (the absolute and relative global irregularity measures sX^{gl} and rsX^{gl}, respectively, with X denoting one of the 5 measures). This provides quantitative information, which supplements the displayed information in form of giving single figures of merit for the global behavior of the results presented. The second line also gives the value of the hemispheric asymmetry factor ($DX^{hem/gl}$, with X denoting one of the 5 measures) in order to routinely see how well the NH represents the globe. In full analogy to the first header line, the values corresponding to the different scenarios shown are separated by bars.

The actual results for a given statistical measure are visualized as histogram bars in a 7 x 7 cell arrangement, where the 36 single cell results (60 deg longitude cells x 15 deg latitude cells) are plotted in a 6 x 6 cell structure, the longitude band results in a 1 x 6 cell structure beneath the 6 x 6 cells, the latitude band results in a 1 x 6 cell structure to the right of the 6 x6 cells, and the total NH (northern hemisphere) results in the lower-right cell, respectively. While we fixed the size of the cells we left the ordinate axis scale adjustable to best fit the magnitude of values of any given measure (for enforcing clarity, this scale is only adjustable for all 49 cells together).

As mentioned earlier, each grid cell can contain from 1 to 4 histogram bars, representing results of 1 to 4 different mission scenarios. Note that, basically, the scenarios can be different in the number of orbital planes, their respective satellite numbers per plane, and in the inclinations (this will be visible from the first header line), but also in other paramters like right ascension of node, mean anomalies, etc. (which is not made visible but needs to be logged externally and mentioned in the caption/plot explanation as appropriate). For enhancing the quantitative information content of the plot, each histogram bar is tagged with its corresponding numerical value.

4.2 General Figure Structure of Baseline Scenario Results

The following Figure structure description for the baseline results serves also as an indicator for the structure of the realistic scenario Figures following further below.

The Figures are regularly arranged in groups of 5 Figure sheets (each sheet includes two separate plot panels), whereby each individual Figure of the group shows one of the five statistical measures. The first sheet of such a group contains always the occultation event number density N, the second the mean distance md, the third the distance dispersion sd, the fourth the mean time separation mt, and the fifth time separation dispersion st, respectively.

Each individual Figure visualizes the results of 7 (in some real scenario cases 6) scenarios for one statistical measure.

Common to those 7 (or 6) different satellite constellation scenarios is always, as we arranged it, the number of orbital planes (O) and the numbers of LEO sats per orbit (S). The main difference is in the different inclinations (I) of the orbital planes. For example, for all baseline scenarios (Figures 4.1 to 4.15), I starts with an inclination of 0 deg for the leftmost histogram bars in the upper plot panel and ends with an inclination of 98 deg for rightmost histogram bars in the lower plot panel, the results "in between" corresponding to inclinations of 30, 60, and 70 degrees (upper panel) and of 80 and 90 degrees (lower

panel). This can be directly seen from the first header line of the panels as explained in section 4.1 above.

The partitioning into separate packages of 7 (or 6) mission scenarios (visualized by one specific 5 Figure group in all 5 measures) has been performed considering the following three main criteria:

- Different orbital planes (used for the real scenarios, chapter 5).
- Varying satellite numbers per orbital plane (used for the baseline scenarios and for the real scenarios).
- Maximum or minimum orbital plane (orbital node) separation, $\Delta\Omega$, relevant for drifting (i.e., non-sunsync) orbits where this separation continuously, and periodically, changes over time (used for scenarios with planes that have different inclinations). For scenarios with different orbital planes but identical inclinations (as purely sun-synchronous constellations orthogonal separation is used as a single case, since here no different orbit plane precession takes place because we have chosen circular orbits with all orbits at the same orbital heights).

Involving the insights gained from the results for the baseline scenarios presented below in section 4.3 we will then proceed to create a more "realistic" sample of satellite scenarios (which we call real or realistic scenarios), the results of which are presented in chapter 5.

4.3 Figure Caption for Figures 4.1 - 4.5

4.3.1 Contents

Figures 4.1 - 4.5 contain the results for the left hand column of the basic satellite scenario table shown in chapter 3 (Table 3.1). For these simplest of our scenarios we assumed only one orbit plane with only LEO satellite. This serves as a reference scenario for true constellations.

4.3.2 Special Remarks

A quick look at Figure 4.1 shows that the number of occultation events is very unevenly distributed over the globe, with a maximum event number density reached of 3.5 [Mm^{-2}]. As expected, scenarios with low inclination give better densities near the equator, while constellations with higher inclined orbits have a better spreading of the occultation events. It is very obvious that these 1 satellite scenarios are certainly far from reaching the requirements set out in Table 2.1.

Figures 4.2 and 4.3 extend the results of Fig. 4.1. Large fluctuations of the mean distance and the mean horizontal distance dispersion can be seen everywhere in these two pictures.

For Figures 4.4 and 4.5 the situation is about the same. The mean time separation and the time separation dispersion are varying from neighbor events occurring nearly simultaneously to time differences of nearly 3 hours between them (2 hours for the dispersion).

A primary reason for this irregularity is certainly that a single orbit plane allows to cover only about half of the globe with occultation events.

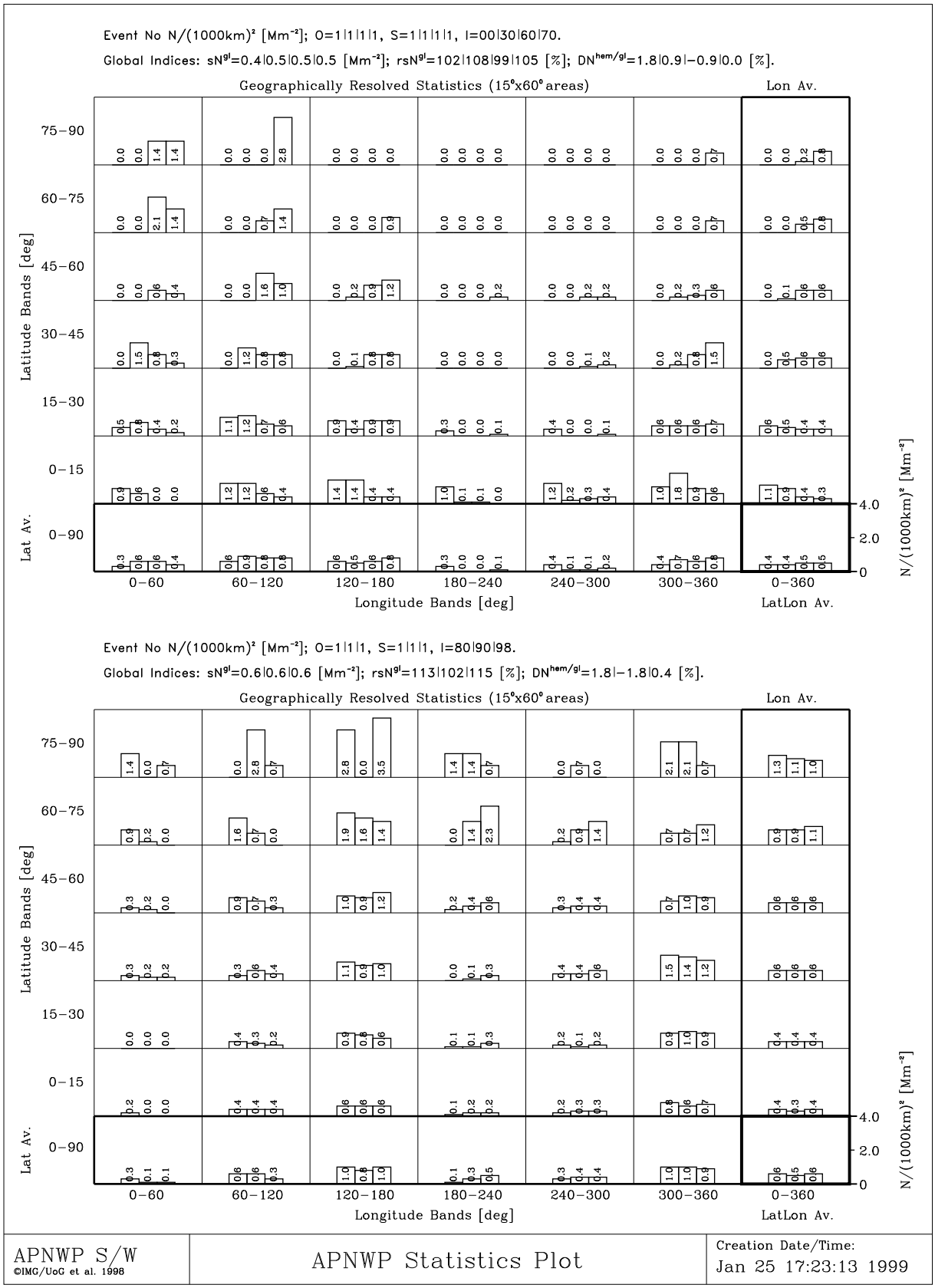

Figure 4.1: Occultation event number densities $N/(1000km)^2$ $[Mm^{-2}]$.

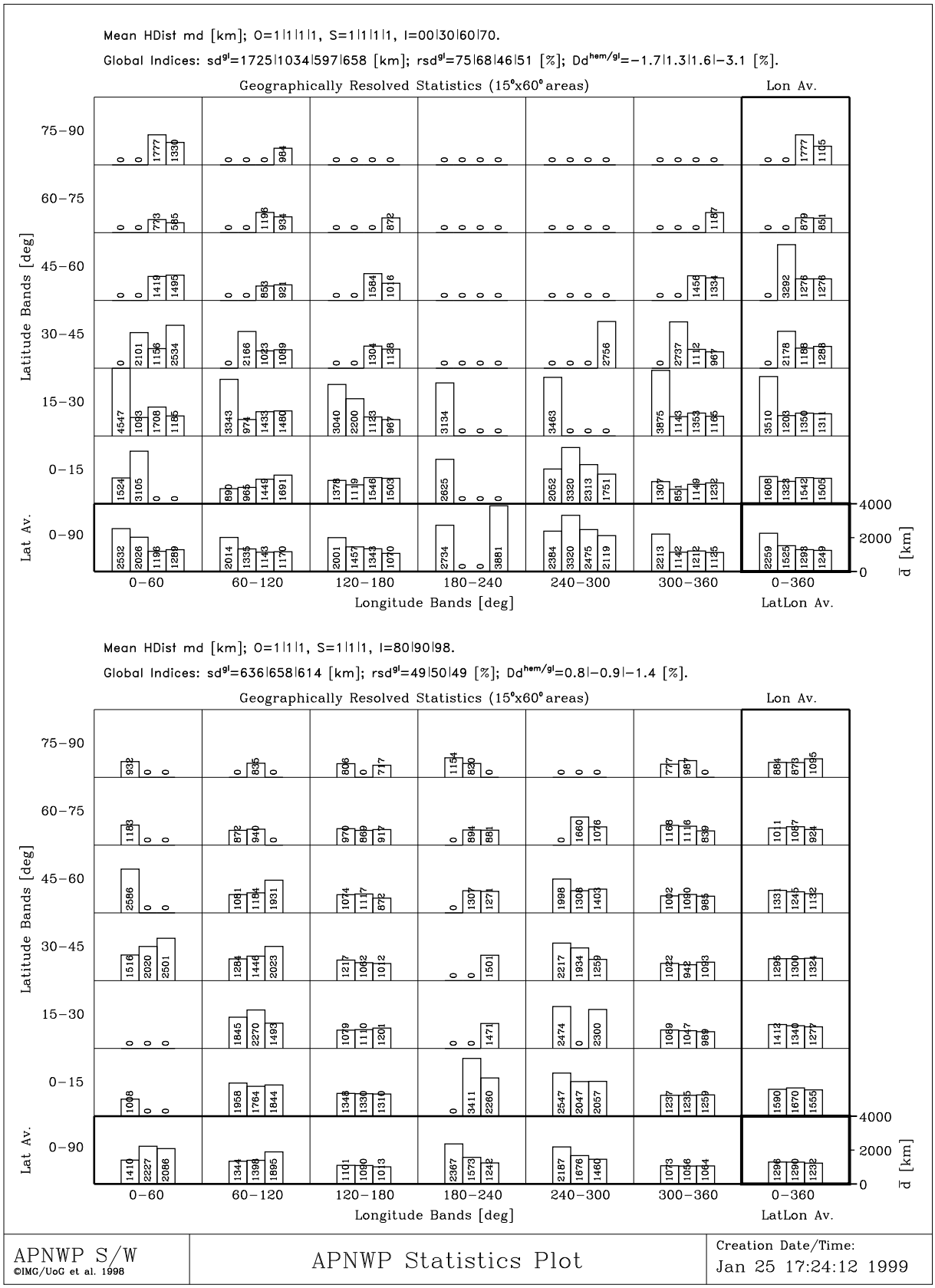

Figure 4.2: Mean horizontal distances $\overline{d}$ $[km]$.

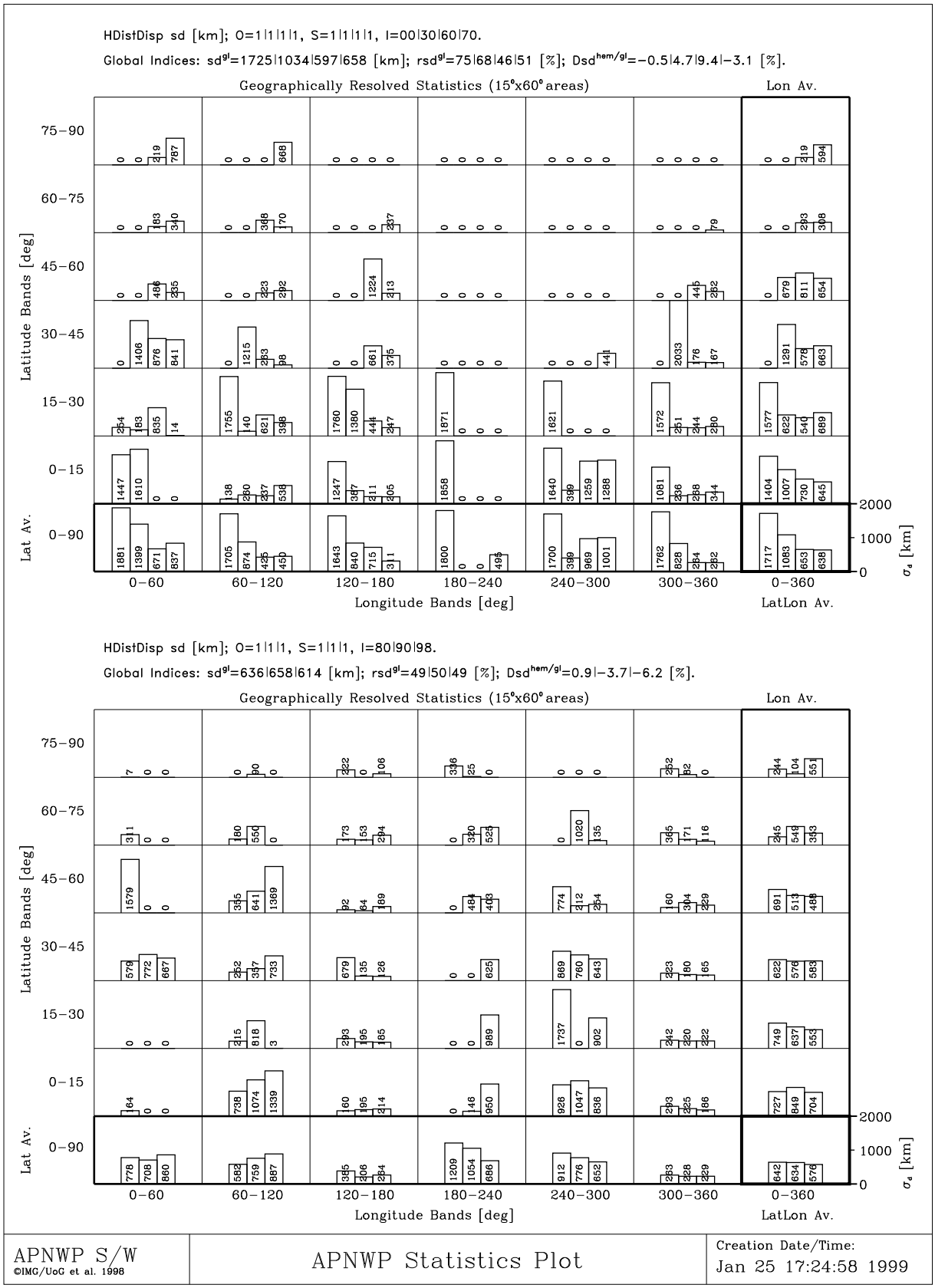

Figure 4.3: Horizontal distance dispersion σ_d $[km]$.

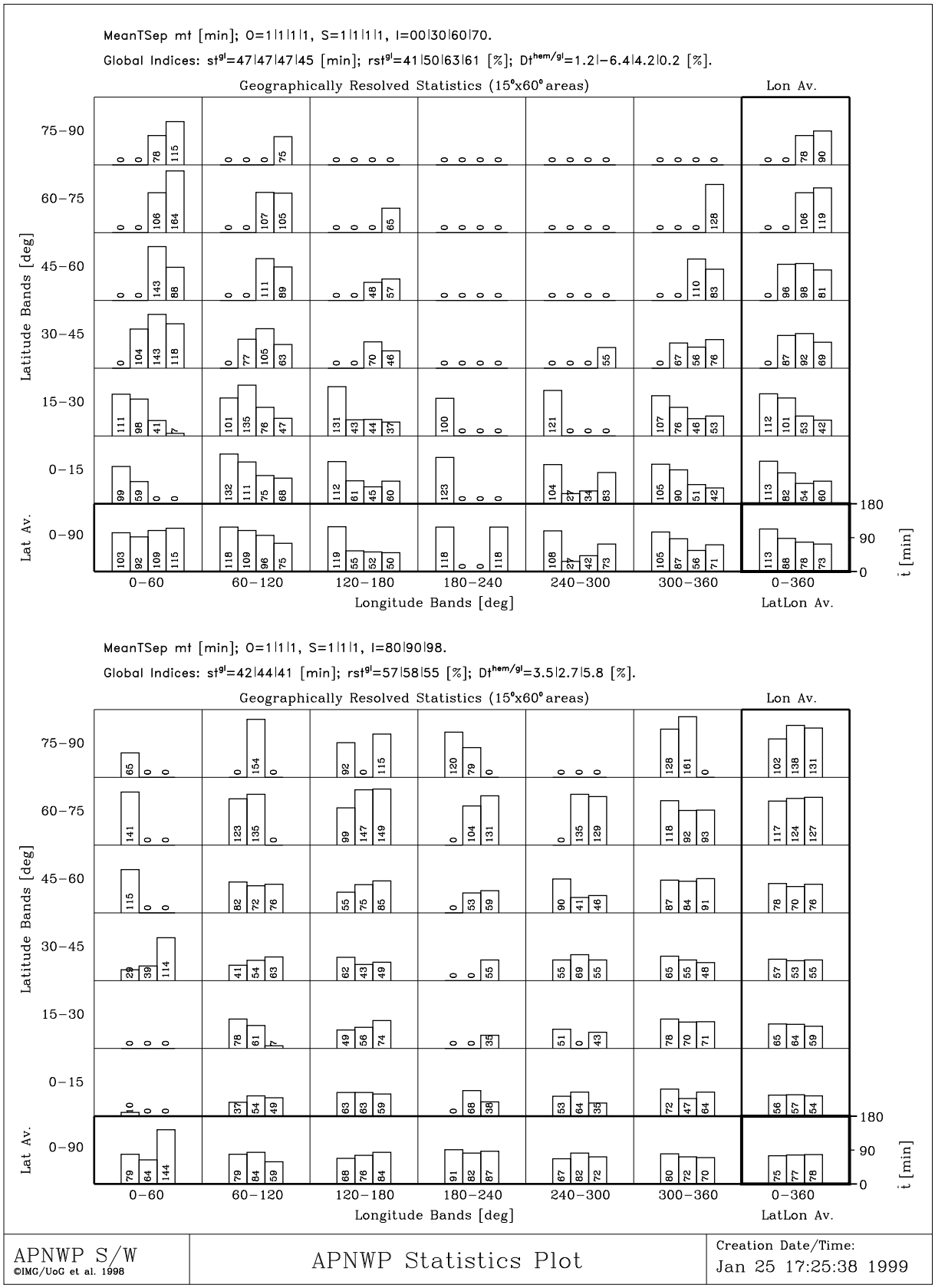

Figure 4.4: Mean time separation $\bar{t}$ $[min]$.

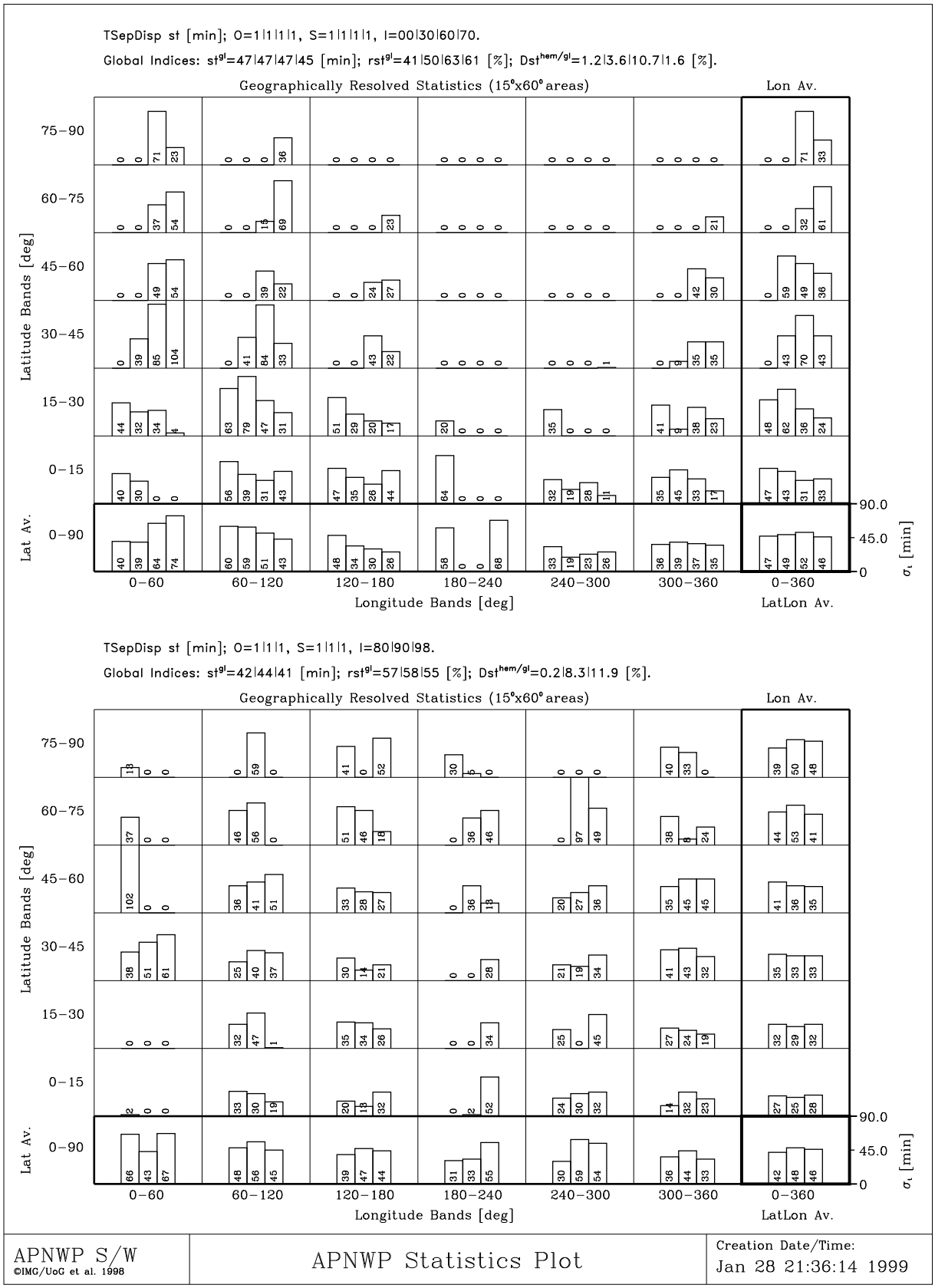

Figure 4.5: Time separation dispersion σ_t $[min]$.

4.4 Figure Caption for Figures 4.6 - 4.10

4.4.1 Contents

Figures 4.6 - 4.10 contain the results for the middle column of the basic satellite scenario table shown in chapter 3 (Table 3.1). We still deliberately assume only one orbit plane and again have the 7 scenarios differing by inclination, but here we use 3 satellites instead of one. According to our "weak constraints" baselined in section 3.1, the 3 satellites are equi-spaced by 120 deg in the orbit.

4.4.2 Special Remarks

A quick look at Figure 4.6 shows that the number of occultation events is still very unevenly distributed over the globe (we still have one orbital plane only which does not allow to cover the full globe withn 6 hours), the maximum number density now reaches 5.5 [Mm^{-2}]. As expected, scenarios with low inclination give better densities near the equator, while constellations with higher inclined orbits have a better spreading of the occultation events. In comparison to Figure 4.1 it is obvious that average occultation event density has increased as should be natural for this 3 satellite constellation. Nevertheless this scenario is of course also very far away from fulfilling the requirements set out in Table 2.1.

Figures 4.7 and 4.8 extend the results of Fig. 4.6. Large fluctuations of the mean distance and the mean horizontal distance dispersion can be seen everywhere in these two pictures. The mean distances are clearly shrinking, however, if one compares the results of Figure 4.7 with Figure 4.2.

Figures 4.9 and 4.10 express the same qualitative picture as their predecessors, Figures 4.4 and 4.5. The mean time separation and the time separation dispersion are varying from neighbor events occurring only a few minutes apart to time differences of nearly 3 hours (2 hours for the dispersion). In general, however, the 3 satellite constellation already leads to a somewhat smoother time separation (and time dispersion) relative to the single-satellite case.

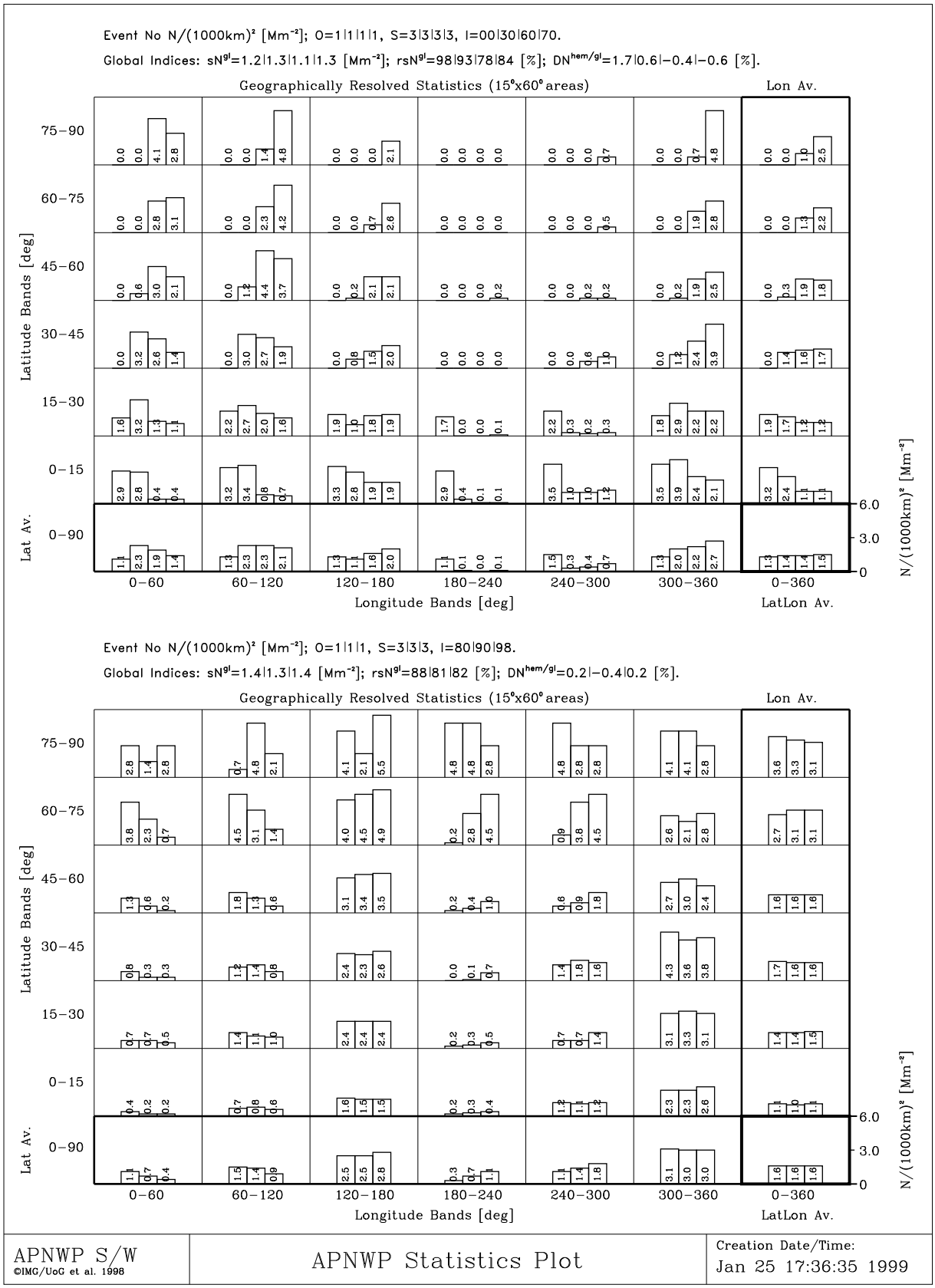

Figure 4.6: Occultation event number densities $N/(1000km)^2$ $[Mm^{-2}]$.

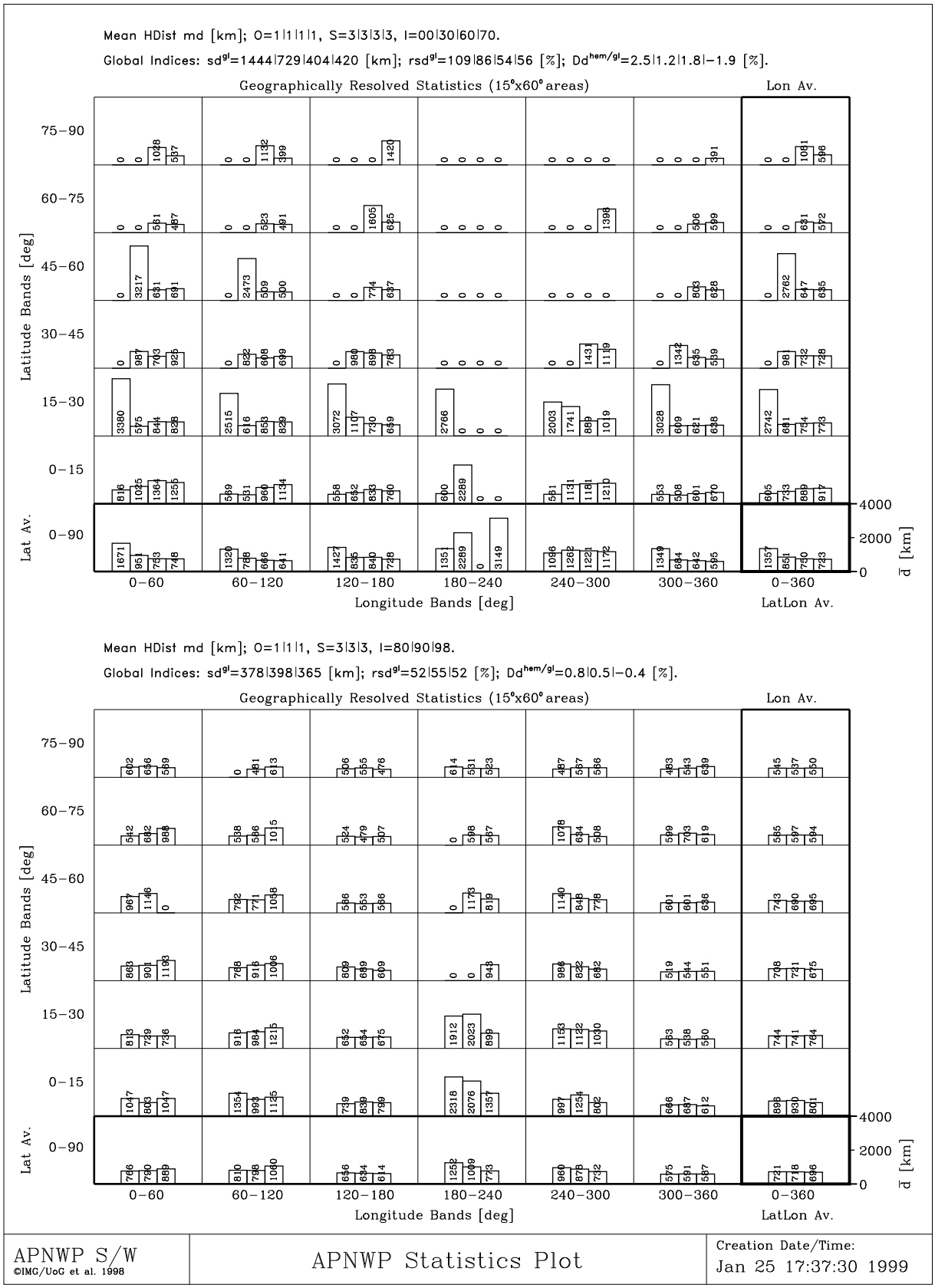

Figure 4.7: Mean horizontal distances $\overline{d}$ $[km]$.

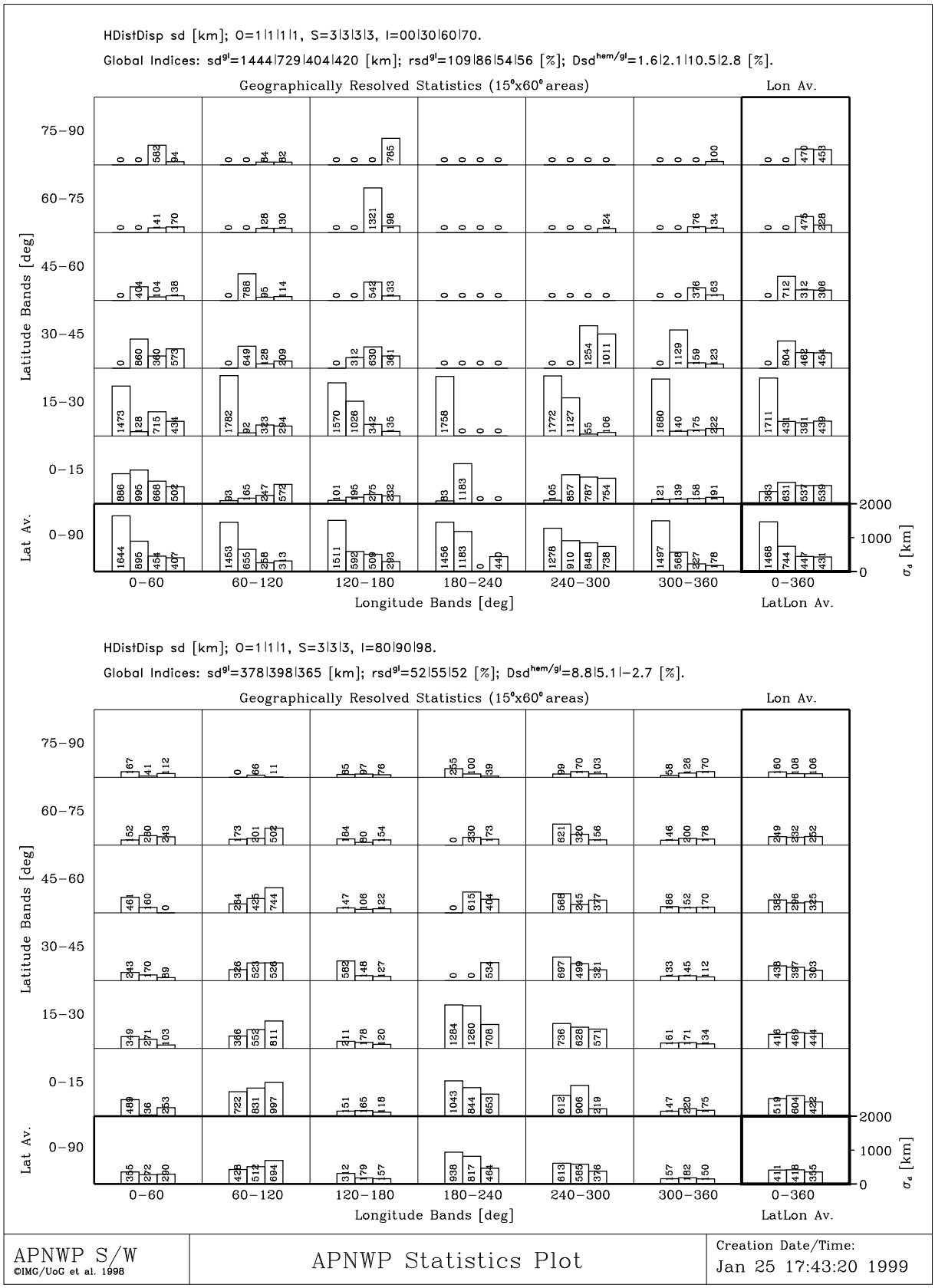

Figure 4.8: Horizontal distance dispersion σ_d $[km]$.

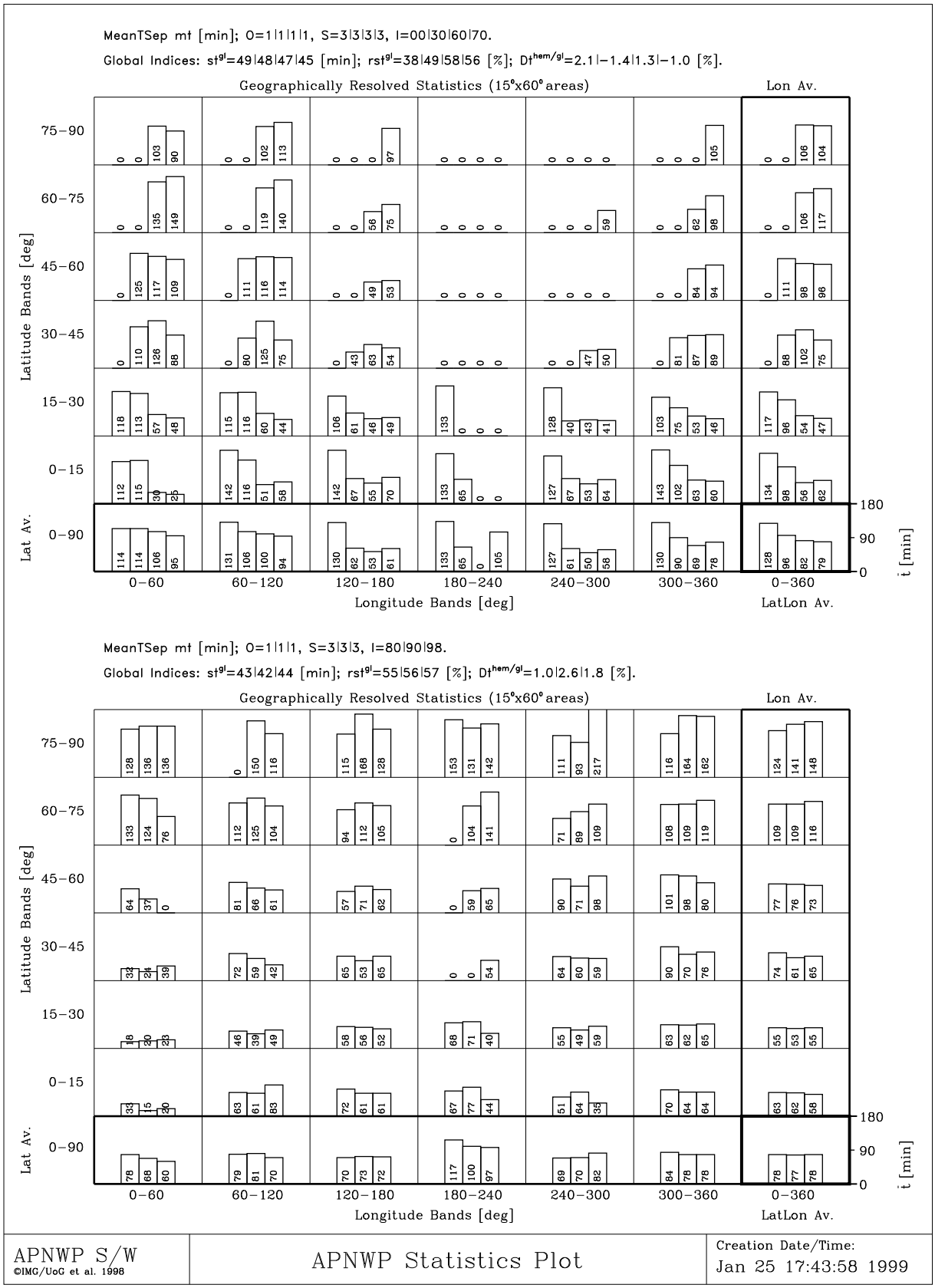

Figure 4.9: Mean time separation $\bar{t}$ $[min]$.

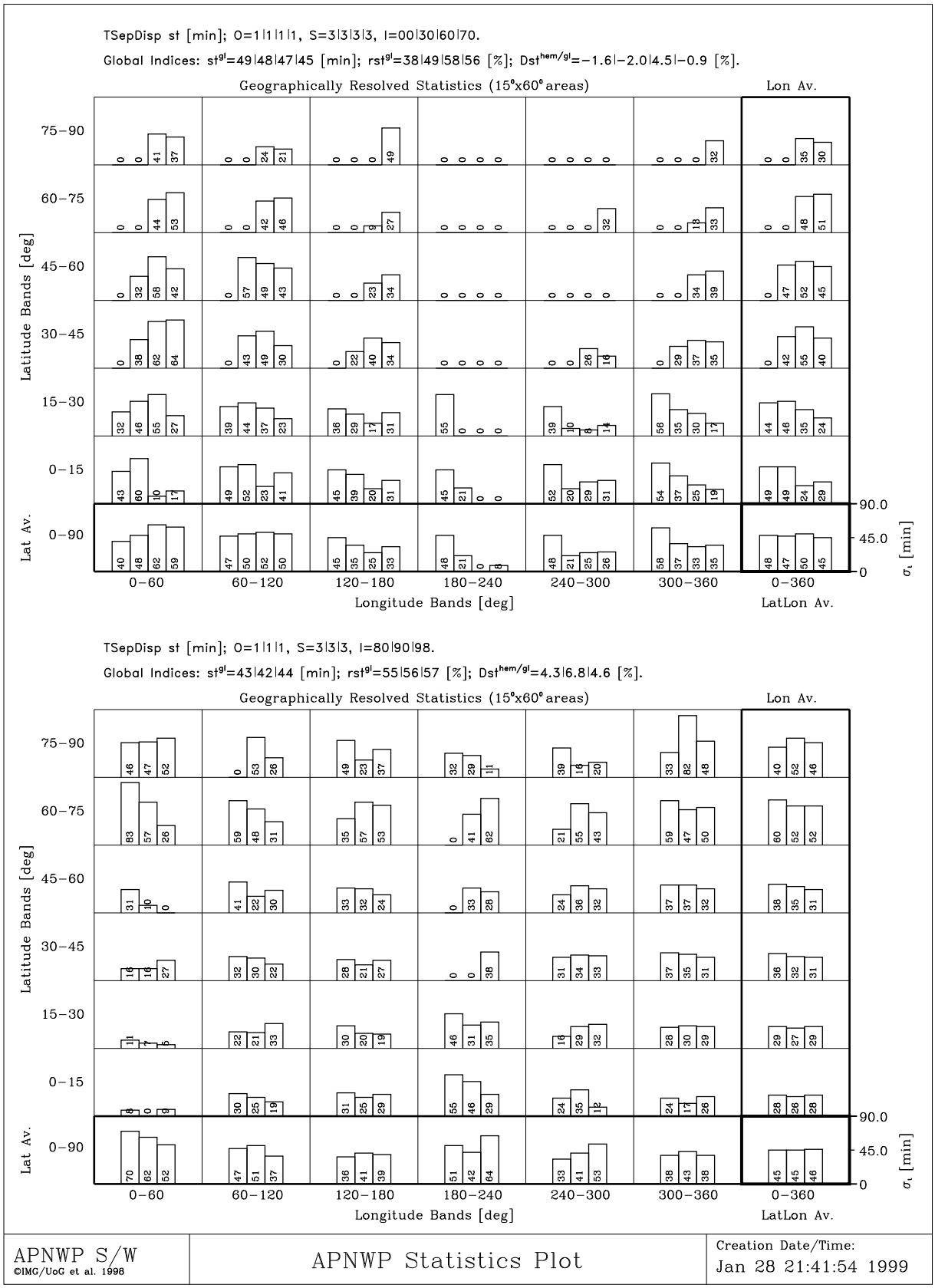

Figure 4.10: Time separation dispersion σ_t $[min]$.

4.5 Figure Caption for Figures 4.11 - 4.15

4.5.1 Contents

Figures 4.11 - 4.15 contain the full set of results for the right hand column of the basic satellite scenario table shown in chapter 3 (Table 3.1). Though we still deliberately assume only one orbit plane and again have the 7 scenarios differing by inclination, we now check the situation for 6 satellites instead of one or three as before. According to our "weak constraints" baselined in section 3.1, the 6 satellites are equi-spaced by 60 deg in the orbit.

4.5.2 Special Remarks

A quick look at Figure 4.11 demonstrates that the number of occultation events is, not surprisingly, still very unevenly distributed over the globe. The maximum density has reached now nearly 12 [Mm^{-2}], however. As still well visible, scenarios with low inclination give better densities near the equator, while constellations with higher inclined orbits have a better spreading of the occultation events. As a rough statement one can say that these 6-satellite scenarios are looking promising in several viewed areas but on the other hand there are still large gaps to fill for a more even distribution of occultation events.

Figures 4.12 and 4.13 extend the results of Fig. 4.11. There are still, in several regions, large fluctuations of the mean distance and the mean horizontal distance dispersion, on the other hand also more smooth areas are now definitely appearing at different places.

The situation for Figures 4.14 and 4.15 is basically still comparable with that of the predecessors figures (Fig. 4.9 and fig. 4.10). However, the mean time separation and the time separation dispersion are now again more smoothly distributed, especially moderate changes in inclination do not change too much. Nevertheless the average time separation and time separation dispersion values are in the still in the same range of magnitude as their predecessors.

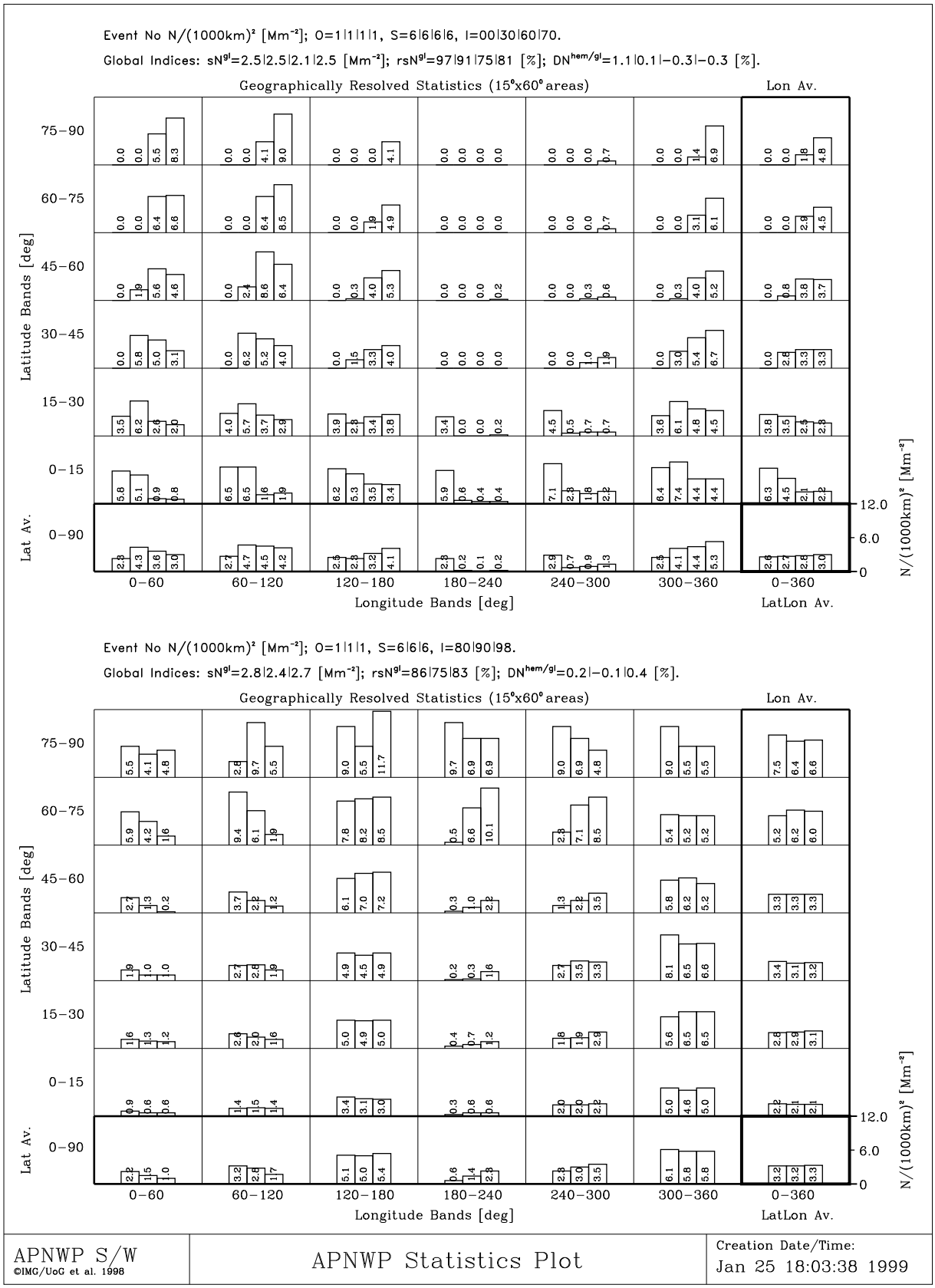

Figure 4.11: Occultation event number densities $N/(1000km)^2$ $[Mm^{-2}]$.

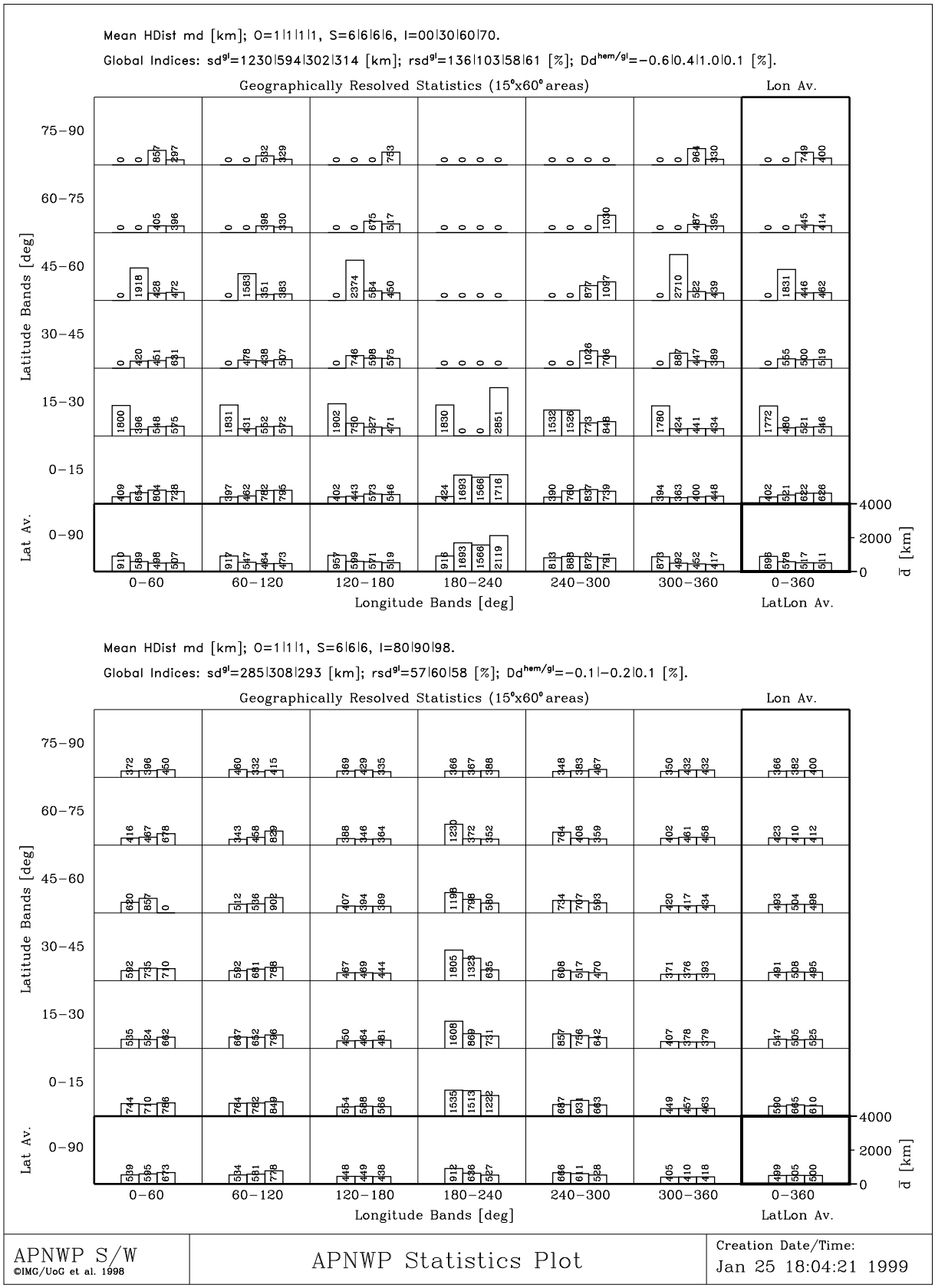

Figure 4.12: Mean horizontal distances $\overline{d}$ $[km]$.

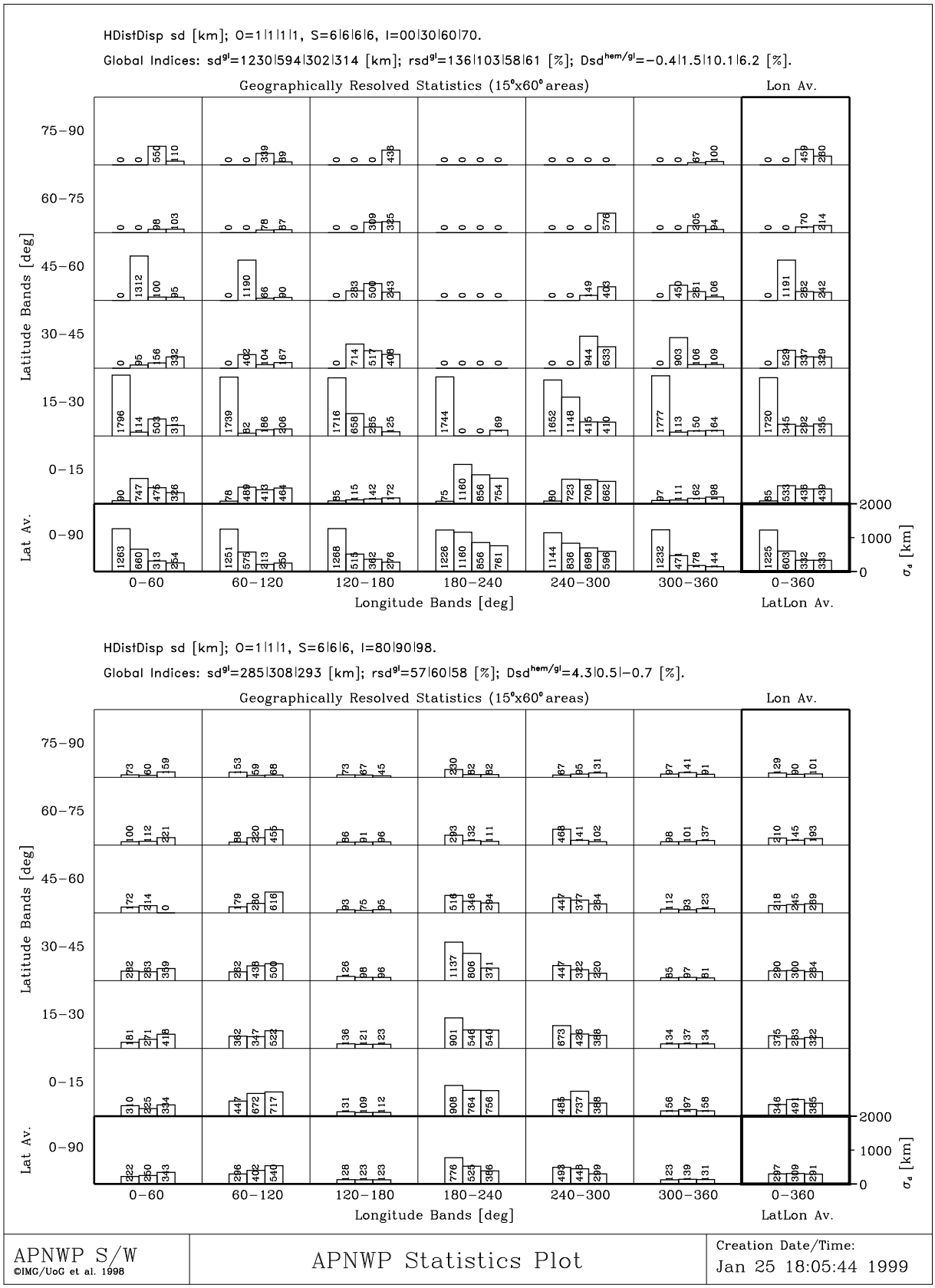

Figure 4.13: Horizontal distance dispersion σ_d $[km]$.

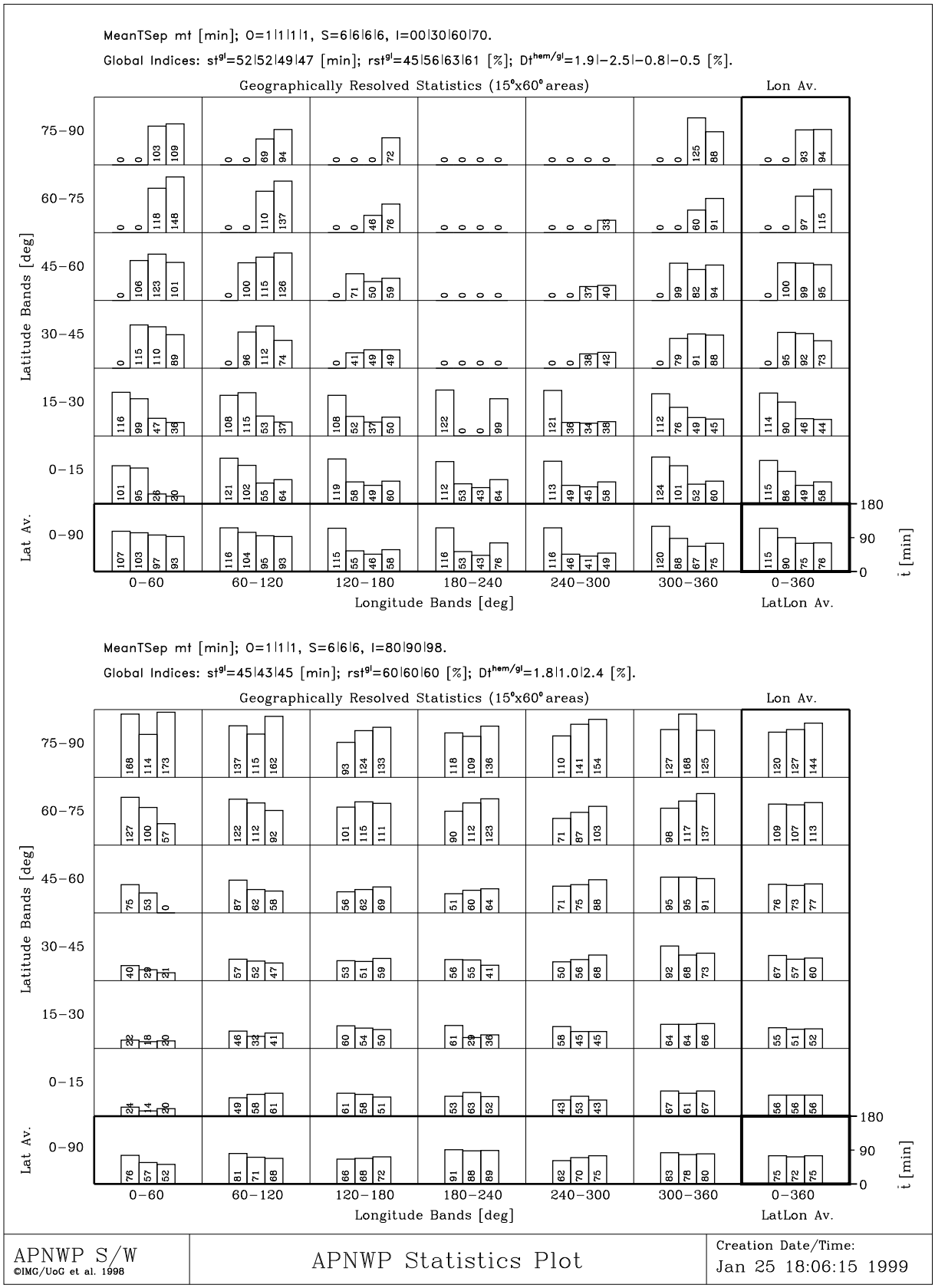

Figure 4.14: Mean time separation $\bar{t}$ $[min]$.

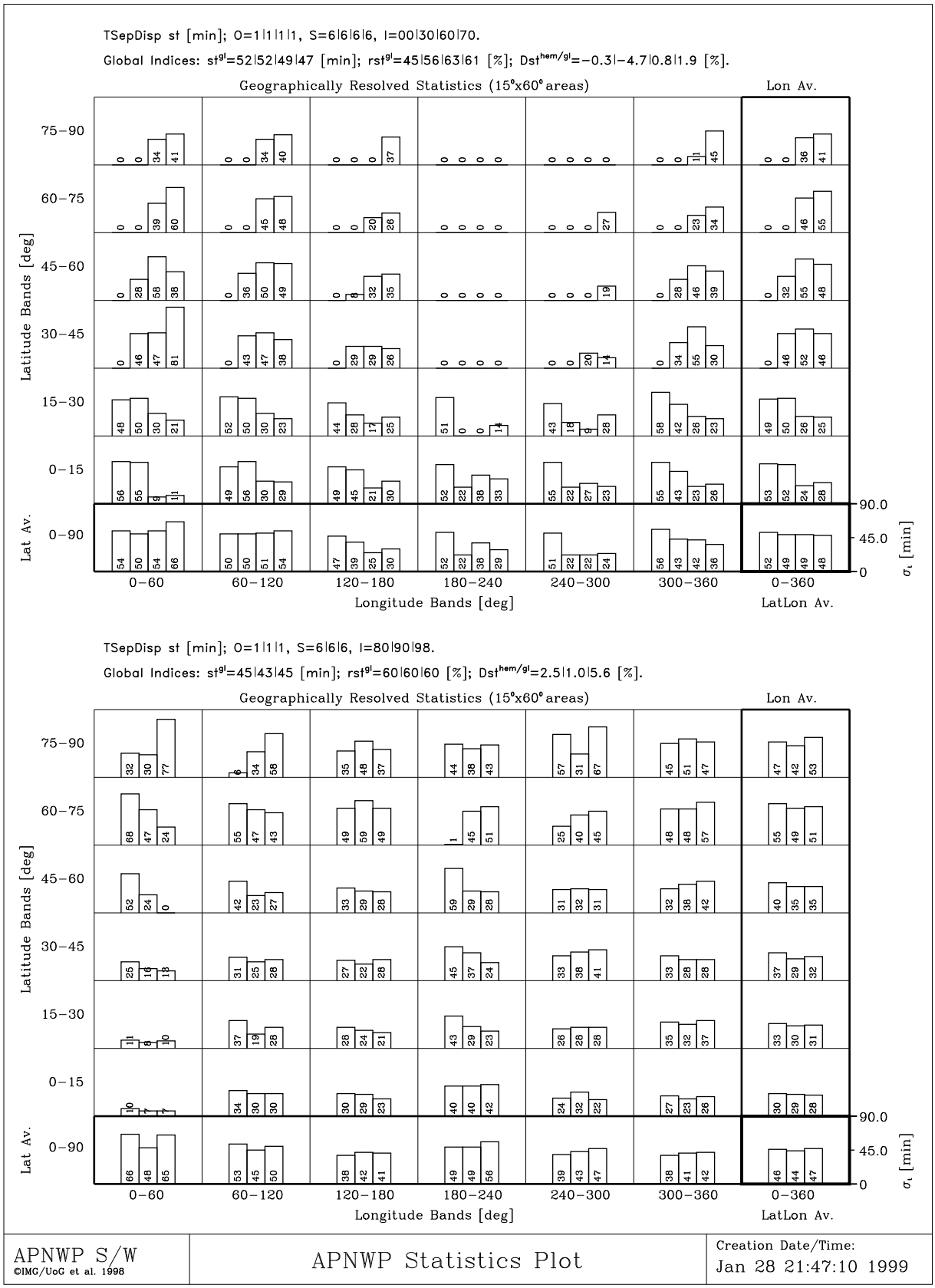

Figure 4.15: Time separation dispersion σ_t $[min]$.

5 Engineering of Realistic Scenarios

5.1 Preliminary Remarks

After carefully analyzing the different aspects of the basic scenario results, it is clear that more advanced constellations are necessary to head towards a reasonable fulfilment of the requirements for operational meteorology, and other needs like climate monitoring. One has to form such more advanced mission scenarios without loosing contact to the more practical determinants like system and operating costs, development time, availability of suitable launching services and so on.

One of the primary disadvantages of the single-plane baseline scenarios studied is certainly their very uneven geographical coverage. The best way to overcome this is by introducing a higher number of orbit planes. Thus we use, for realistic scenarios, a minimum number of two orbit planes (O=2), but we analyze also scenarios with four orbit planes (O=4), the latter for larger constellations. (We do not go to even more planes in this study, since this becomes increasingly far from what may be realized in the not too far future and since we need to keep computational costs under control for the subsequent NWP experiments.)

We basically place the planes as symmetric as possible but as noted above nature destroys this favorite situation due to differential orbital drift given different plane inclinations. We decided to study in such cases, for one and the same constellation, both the "best case" (orthogonal nodes of the planes/maximal separation) and the "worst case" (aligned nodes of the planes/maximal overlap), respectively. This will give us an idea how the geometrical situation, and with it the statistical measures, are changing periodically in time while the constellation repeatedly undergoes its changes from node alignment to node orthogonality.

Also evident is that a larger satellite constellation can crucially improve the situation. Since we found 6 satellites already to be reasonable in terms of number of events we take, for the real scenarios, the size as the minimum constellation. To proceed further towards indeed be able to meet the requirements of Table 2.1, we inspect, in addition larger constellations made of 12 and 24 satellites, respectively. (We do not undertake to study even larger constellations, since with 24 we find that we can already meet the requirements of Table 2.1 and also in order to keep computational costs for the subsequent NWP experiments at an affordable level.)

Clearly with these numbers of satellites, given that we also consider up to 4 planes, a lot of different configurations could be simulated. We limit the total number of realistic scenarios to a reasonable number by selecting a representative sample as defined below. In terms of constellation size, we study sizes of 6, 12, and 24 sats, respectively, as indicated above. In order to get a reasonable sampling going through different numbers of orbital planes and through different numbers of satellites per plane, we use 6 basically different satellite constellations types. 3 of these 6 cases are what we term "symmetric" configurations, namely for O=2 a S=3-3 (6 sat) and a S=6-6 (12 sat) satellite scenario, and for O=4 a 6-6-6-6 (24 sat) LEO constellation. For the other 3 constellation types, "asymmetric" configurations were designed, we used for O=2 a S=4-2 (6 sat) and a S=8-4 (12 sat) scenario, and for O=4 a 8-8-4-4 (24 sat) scenario. Such "asymmetric" orbit filling may be more favorable than a "symmetric" one: the analysis of the basic scenarios (chapter 4) showed that the more inclined orbits gave a much more even coverage (with

a moderate maximum at high latitudes though), therefore most of the satellites should presumably be positioned in higher inclined orbits and fewer into lower inclined ones to optimize towards equal global coverage.

Concerning inclinations and the issue of drifting orbits requiring to look into node orthogonality vs. node alignment of orbit planes we decided to sample these dimensions of basin space by 7 scenarios for each of the three "symmetric" configurations (including one purely sun-synchronous one) and by 6 scenarios for each of the "asymmetric" configurations (no purely sun-sync one).

Given this design we end up with 39 scenarios which involve 21 different constellations (the difference between the number of scenarios and of actual constellations derives from the running several scenarios for one and the same constellatoin to address the node alignment/node orthogonality issue).
With this design we assembled a fair set of promising candidates for heading towards the requirements of Table 2.1 (actually fulfilling them, at least with the 24 sat constellations). For convenience, these 39 realistic scenarios are concisely summarized by Table 5.1, the scenarios grouped there into colums representing the three different constellation sizes (6, 12, 24 sats). As seen, 13 scenarios are to be investigated for each size.

O=2	O=2	O=4
$S\epsilon\{3-3, 4-2\}$	$S\epsilon\{6-6, 8-4\}$	$S\epsilon\{6-6-6-6, 8-8-4-4\}$
$I\epsilon\{98-98\}^*$ $\Delta\Omega$=90	$I\epsilon\{98-98\}^*$ $\Delta\Omega$=90	$I\epsilon\{98-98-98-98\}^*$ $\Delta\Omega$=45
$I\epsilon\{80-55\}$ $\Delta\Omega\epsilon\{90,0\}$	$I\epsilon\{80-55\}$ $\Delta\Omega\epsilon\{90,0\}$	$I\epsilon\{\underbrace{80-80}_{\Delta\Omega_h=90} - \underbrace{30-30}_{\Delta\Omega_l=90}\}$ $\Delta\Omega\epsilon\{45,0\}$
$I\epsilon\{80-30\}$ $\Delta\Omega\epsilon\{90,0\}$	$I\epsilon\{80-30\}$ $\Delta\Omega\epsilon\{90,0\}$	$I\epsilon\{\underbrace{98-98}_{\Delta\Omega_h=90} - \underbrace{30-30}_{\Delta\Omega_l=90}\}$ $\Delta\Omega\epsilon\{45,0\}$
$I\epsilon\{98-30\}$ $\Delta\Omega\epsilon\{90,0\}$	$I\epsilon\{98-30\}$ $\Delta\Omega\epsilon\{90,0\}$	$I\epsilon\{\underbrace{80-60-40-20}\}$ $\Delta\Omega\epsilon\{45,0\}$

Table 5.1: Real Satellite Constellation Scenarios

Notes: * For pure sun-sync scenarios only symmetric satellite constellations were used.

5.2 Description of the Real Satellite Constellation Scenarios

Table 5.1 contains the main input parameters of our 39 different real satellite mission scenarios which were discussed above in short form and which we shall explain here in a little more detail. Tow thirds of the cases use two different orbit planes for positioning the LEO satellites and the last 13 cases are the constellations with 4 separate orbit planes.

For the two orbit plane cases configurations of 6 and of 12 satellites were chosen.

For the symmetric configurations using two different orbit planes (left-hand and middle column of Table 5.1), with 3 or 6 satellites sharing an orbit (orbital spacings of the LEOs 120 or 60 degrees, respectively), scenarios with different orbital plane inclinations were taken (i.e. inclinations of the two plains were 80-55, 80-30, or 98-30 degrees) and one pure sun synchronous scenarios, where both planes had the same inclination of 98 degrees. For cases with different orbit inclinations cases with node orthogonality ($\Delta\Omega = 90°$; "best case") and node alignment ($\Delta\Omega = 0°$; "worst case") were both considered. (For pure sun-sync scenarios only the $\Delta\Omega = 90°$ case was used because no differential precession of both orbit planes will take place.

The setup for the the asymmetric cases is essentially the same as for the symmetric ones. Here 4 or 8 satellites are occupying the higher inclined orbit plane, whereas 2 or 4 of them are located in the lower inclined orbit. We use no sun-sync only scenarios for asymmetric configurations, however, since an unequal orbit filling for two orbits at indentical inclination does not make too much sense.

The 4 orbit plane cases (O=4) were in principle handled in the same manner as the former two orbit scenarios, but we have been somewhat more restrictive with sampling the inclination dimension of the basin space in order to again limit to 7 symmetric and 6 asymmetric scenarios.

For the purely sun-synchronous orbit scenario only the fully symmetrical case (6 satellites in each of the 4 orbit planes, with $\Delta\Omega = 45°$ separated) were used. For the scenarios with $I\epsilon\{80 - 80 - 30 - 30\}$ & $I\epsilon\{98 - 98 - 30 - 30\}$, the two pairs of equally inclined orbits (i.e., 98-98, 30-30 degrees) were spaced 90 degrees in Ω (this spacing is time-independent due to the identical inclination). The pairs, in turn, were split with 45° and 0° against each other to simulate the two extremes of minimal and maximal overlap of nodes. For the last constellation case 4 different orbital inclinations were used, with an orbit plane separation of 45° (orbit nodes maximally dispersed, "best case") and of 0° (all orbit nodes aligned, "worst case"), respectively.

5.3 Calculation and Visualization of the Real Satellite Constellation Scenarios

The calculation and visualization process of the real satellite scenarios is made in the same manner as was documented in chapter 3.3 for the calculation and in chapter 4 for the visualization of the results of the basic scenario.

The visualization process was also handled in the same manner as before. Small differences can be noticed when inspecting the plots in the first header line of the plot panels. Here, having now more than one orbit plane for each scenario means that the satellite and inclination values for a single scenario were growing longer in order to include all information about the individual satellite numbers per orbital plane and about the different orbital inclinations of these planes. Generally, all characteristics of the plots in this chapter (Figures 5.1 to 5.30) are as explained in detail in sections 4.1 and 4.2.

5.4 Figure Caption for Figures 5.1 - 5.10

5.4.1 Contents

Figures 5.1 - 5.10 contain the results for the 6 sat/2 orbit symmetric satellite scenario with 3 sats per orbit (upper panel), as well as the results for its asymmetric complement with 4 satellites in the higher inclined orbit and two in the lower inclined orbit (lower panel).
Figures 5.1 to 5.5 show the cases with node alignment ($\Omega = 0°$), while Figures 5.6 to 5.10 show the cases with node orthogonality ($\Omega = 90°$). As noted before, the pure sun-sync constellation was only calculated for the latter scenario.

5.4.2 Special Remarks

A quick look at Figure 5.1 shows that the number of occultation events is quite unevenly distributed over the globe, the maximum number density reached is 7.6 [Mm^{-2}]. A comparison with Figure 5.6 (the $\Omega = 90°$ case) shows immediately the big difference between the optimum node separation and node alignment. Interesting is also that the symmetric satellite constellation (upper panel case of Fig. 5.6) gives already reasonably smooth average occultation event distribution.

Figures 5.2, 5.3, 5.7, and 5.8, showing the mean distances and their dispersion, apear to be consistent with the number density results of Figures 5.1 and 5.6.

The mean time separations and the time separation dispersions shown in figures 5.4, 5.5, 5.9, and 5.10 are showing no big difference between the best case and worst case scenarios. At higher latitudes the average time separation is generally greater than in the more equatorward regions.

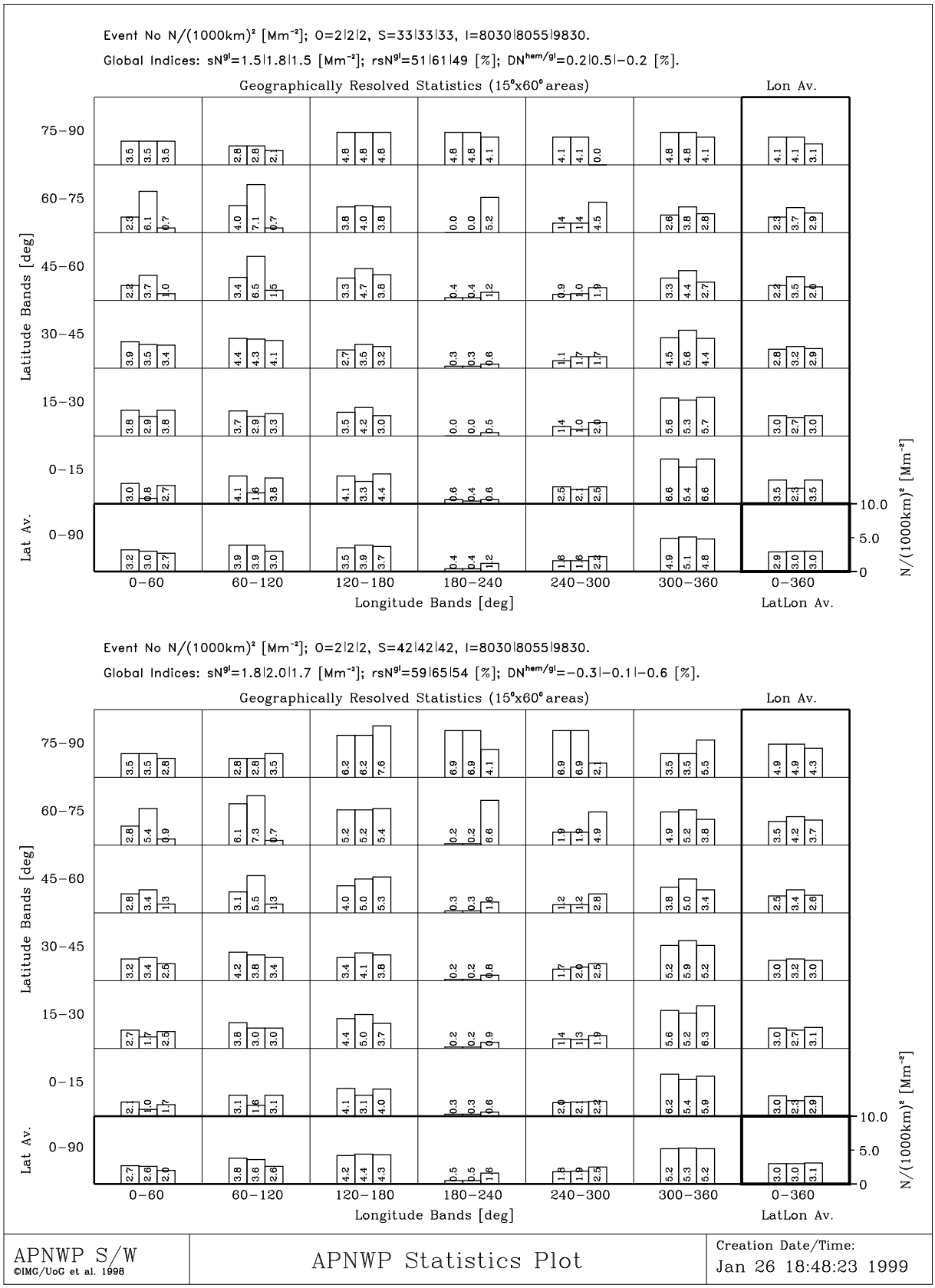

Figure 5.1: Occultation event number densities $N/(1000km)^2$ $[Mm^{-2}]$.

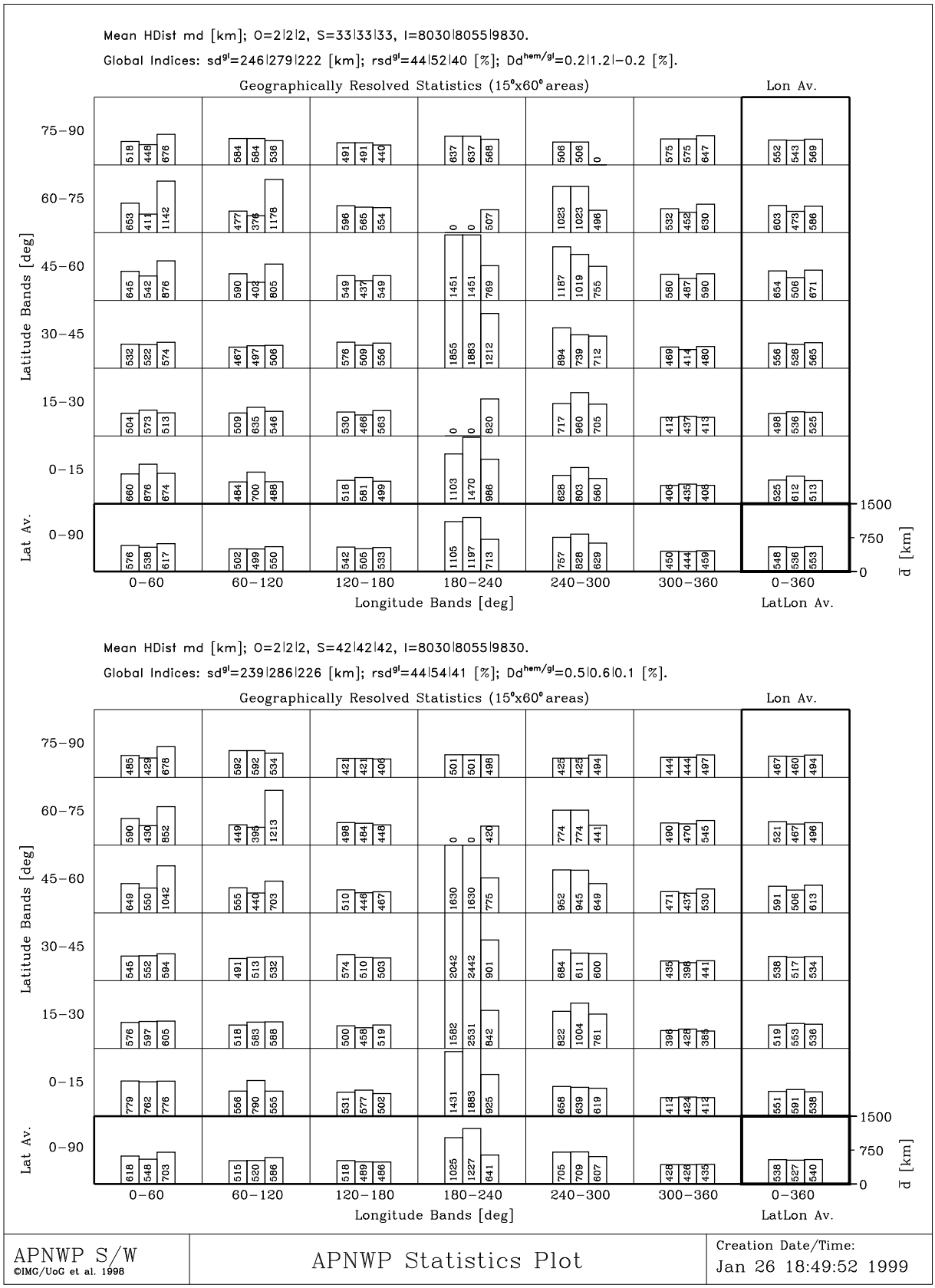

Figure 5.2: Mean horizontal distances $\overline{d}$ $[km]$.

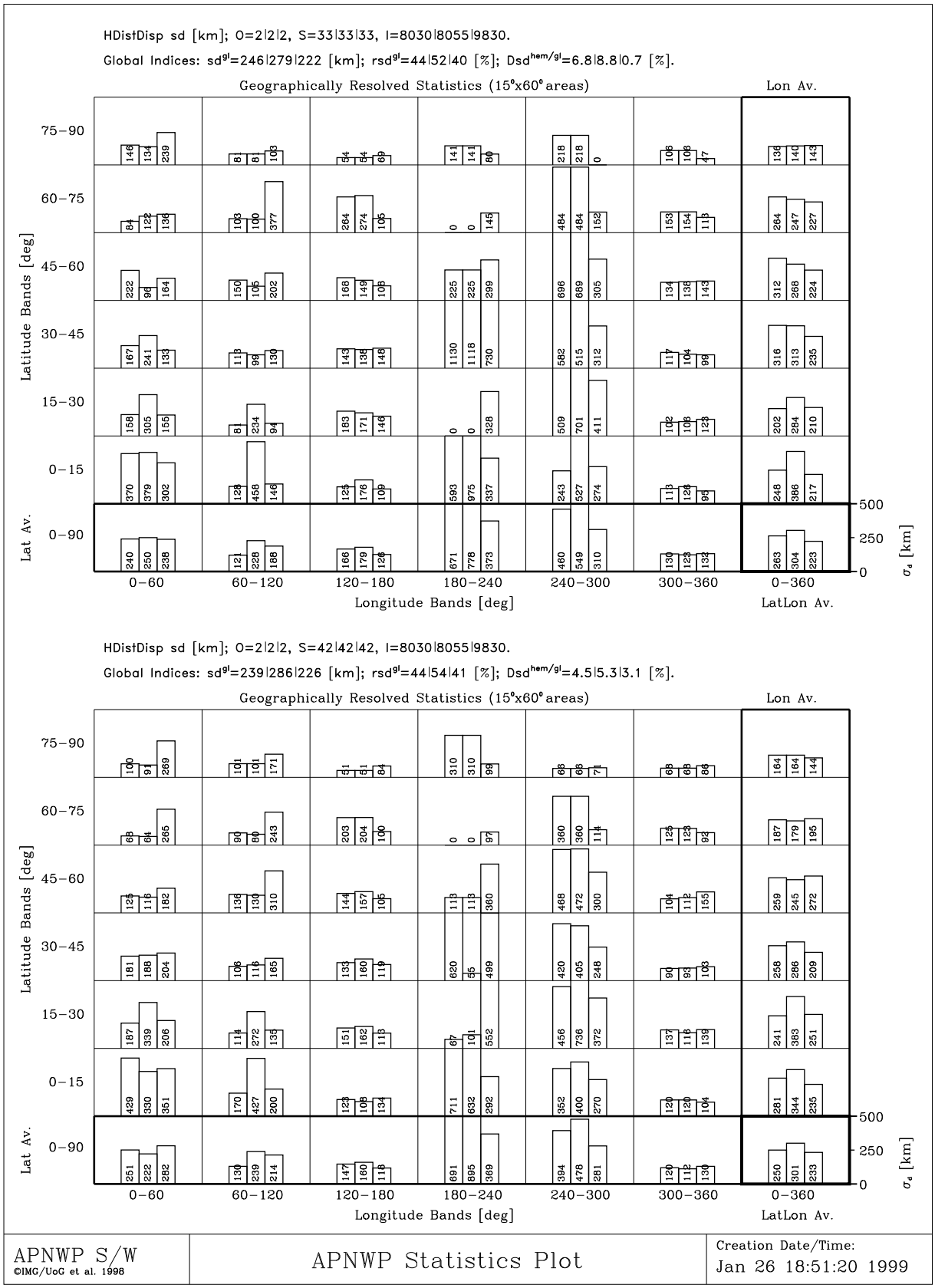

Figure 5.3: Horizontal distance dispersion σ_d $[km]$.

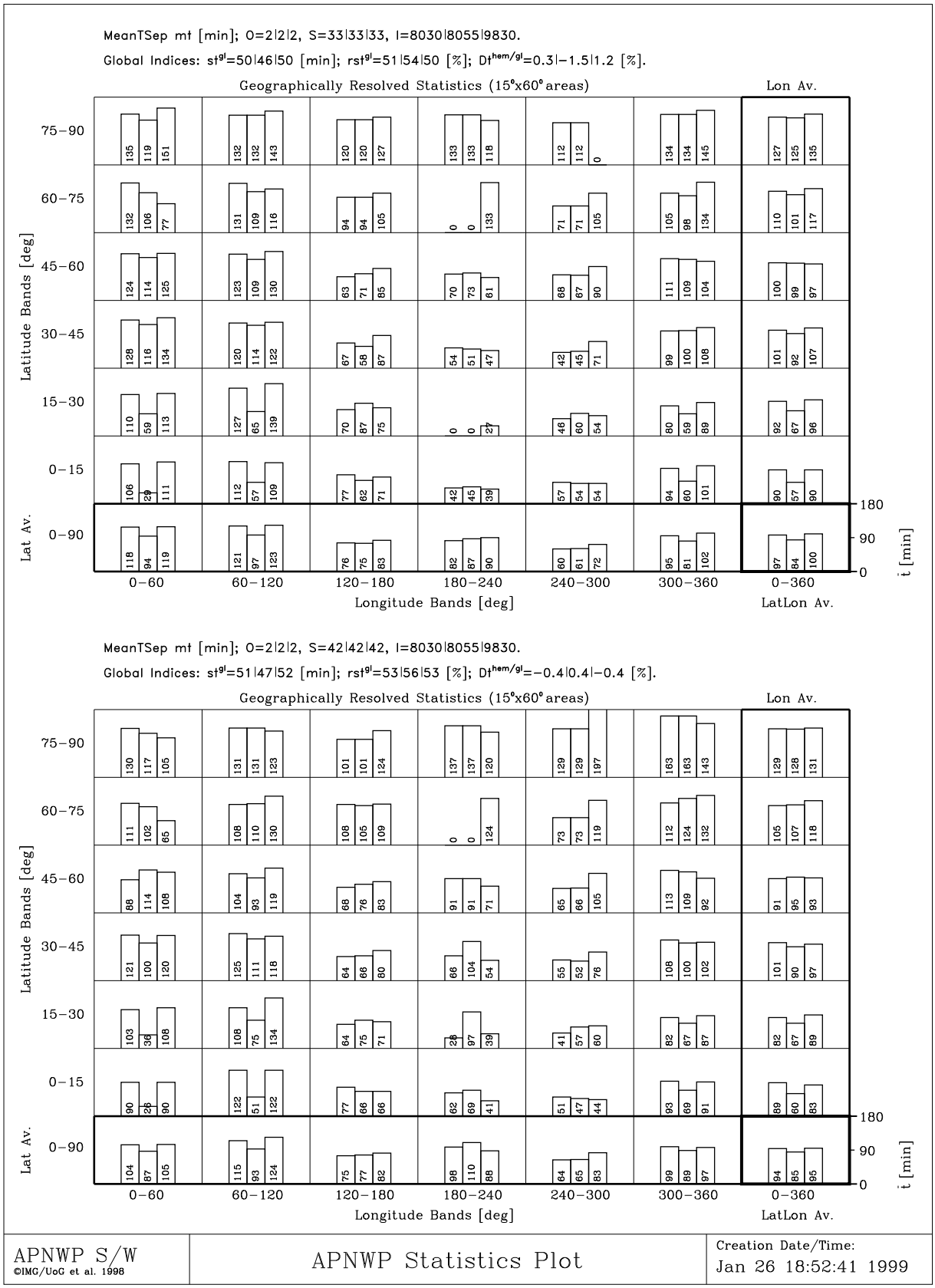

Figure 5.4: Mean time separation $\bar{t}$ $[min]$.

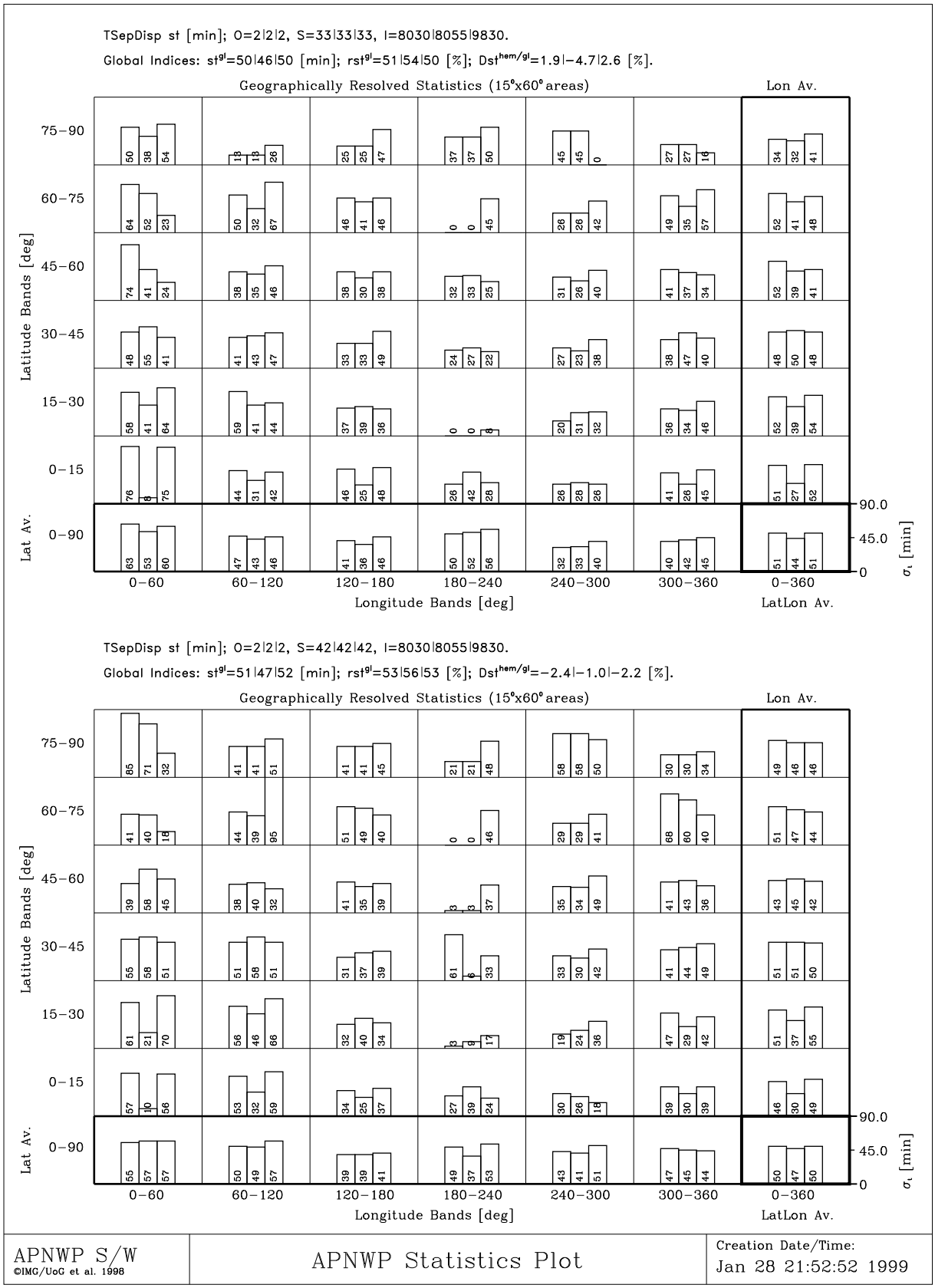

Figure 5.5: Time separation dispersion σ_t $[min]$.

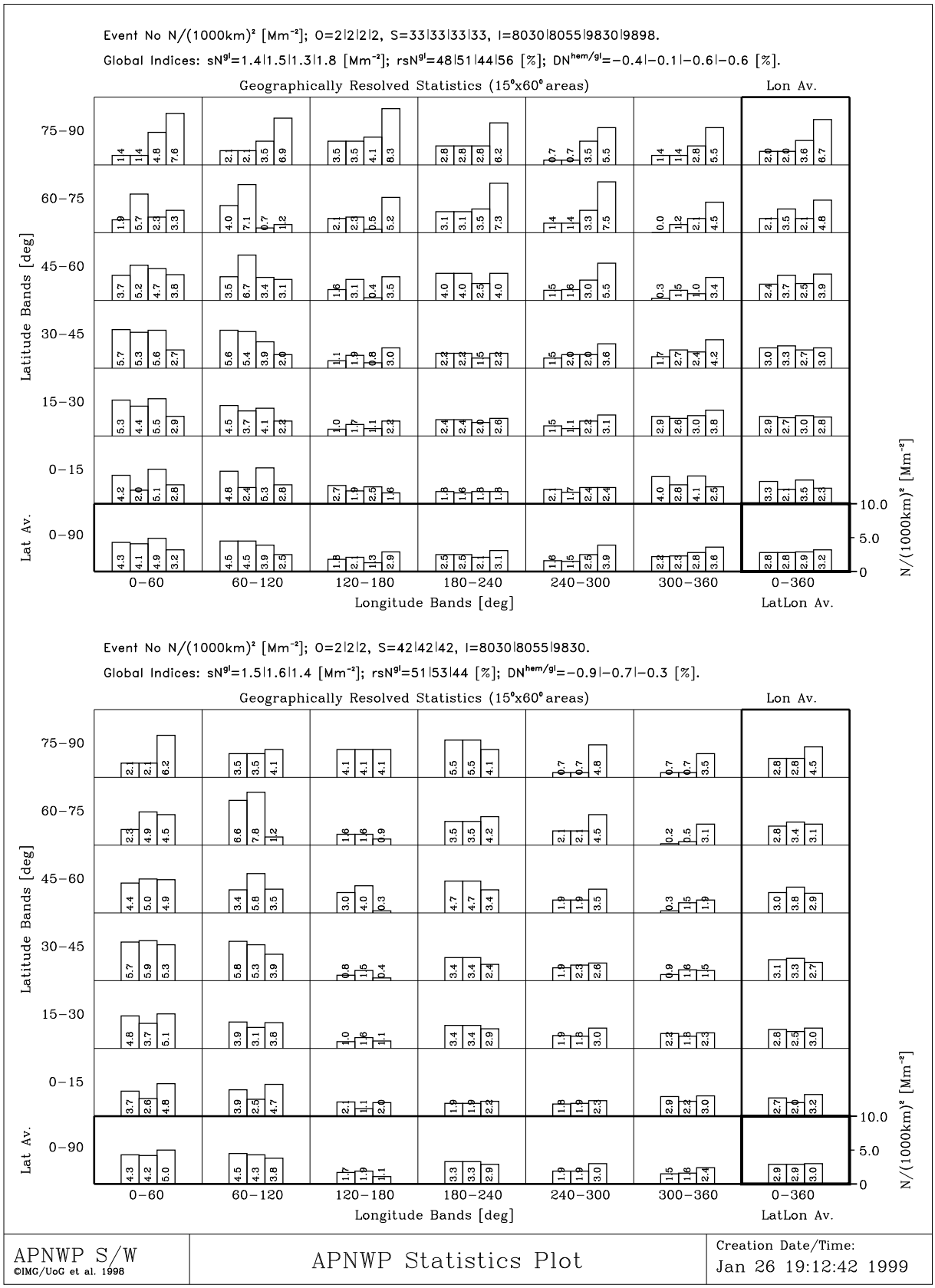

Figure 5.6: Occultation event number densities $N/(1000km)^2$ $[Mm^{-2}]$.

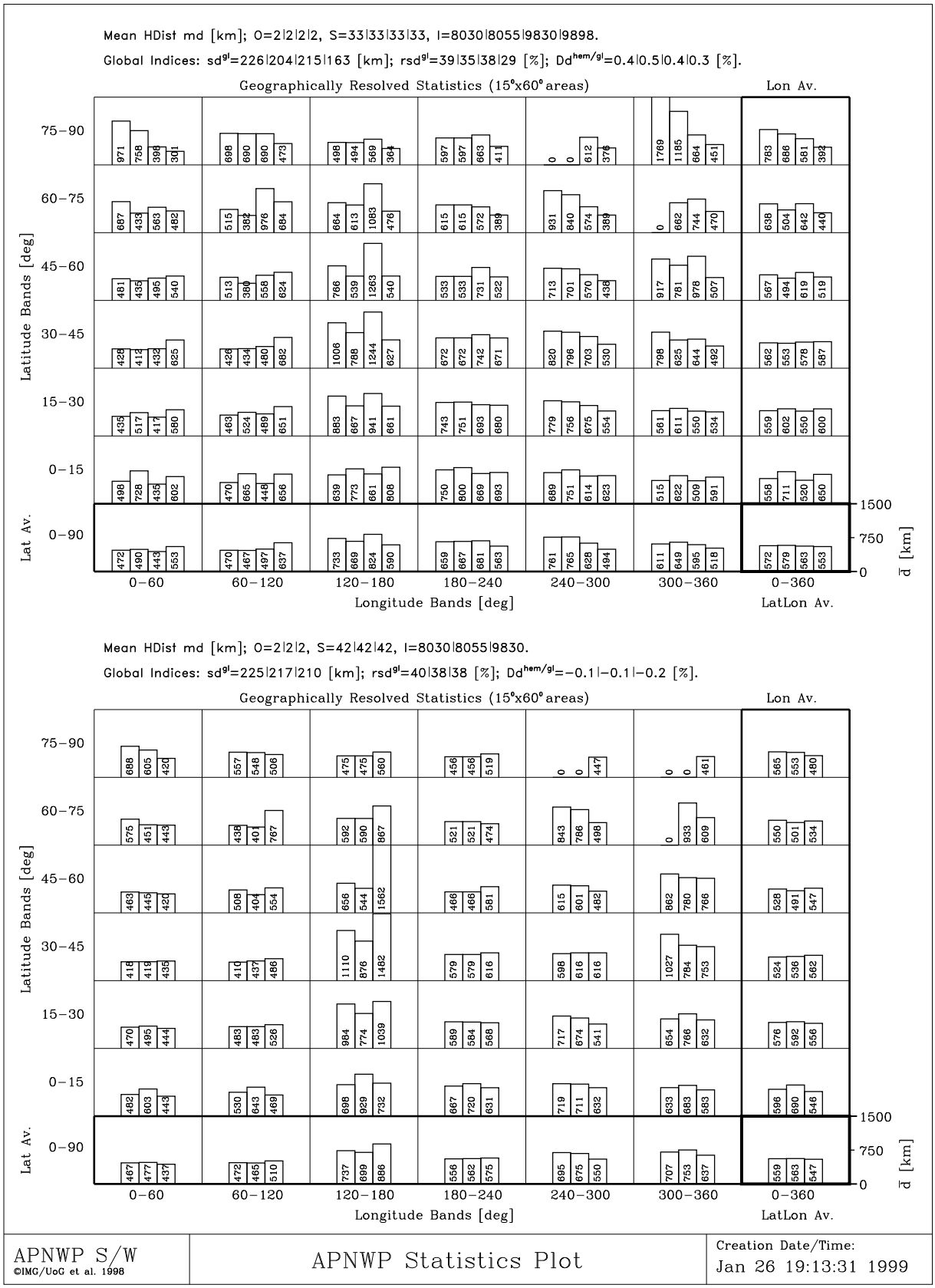

Figure 5.7: Mean horizontal distances $\overline{d}$ $[km]$.

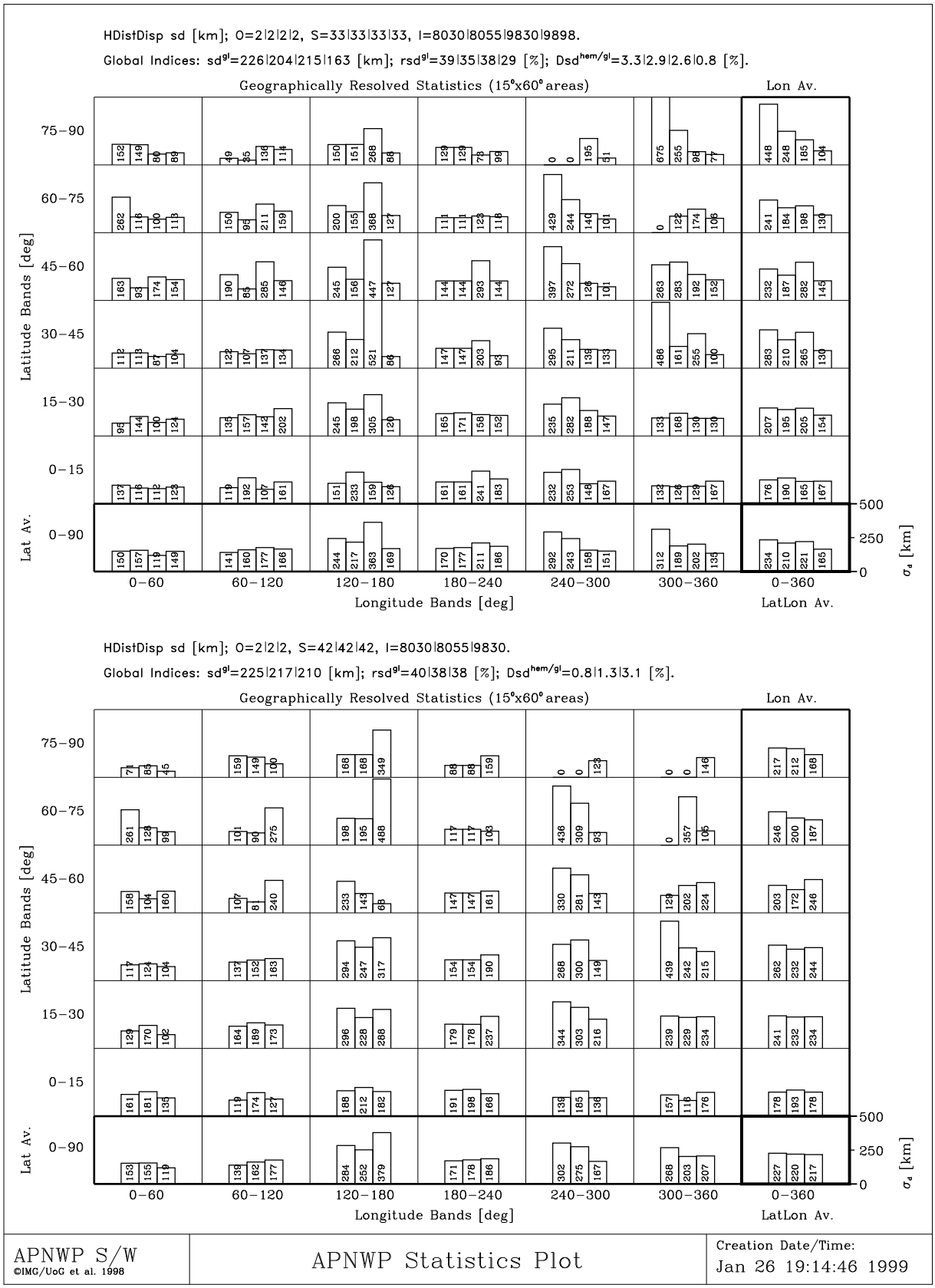

Figure 5.8: Horizontal distance dispersion σ_d $[km]$.

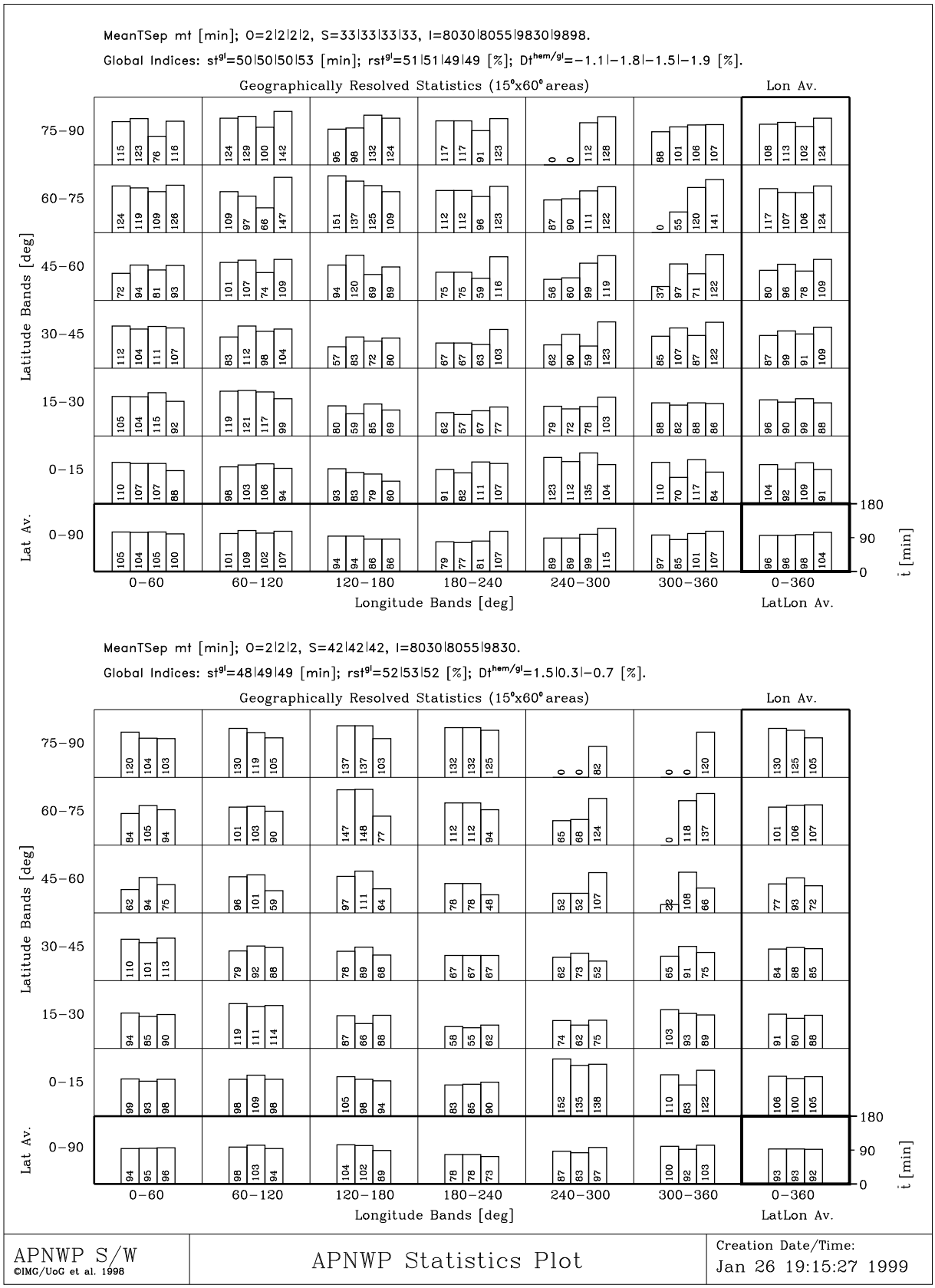

Figure 5.9: Mean time separation $\bar{t}$ $[min]$.

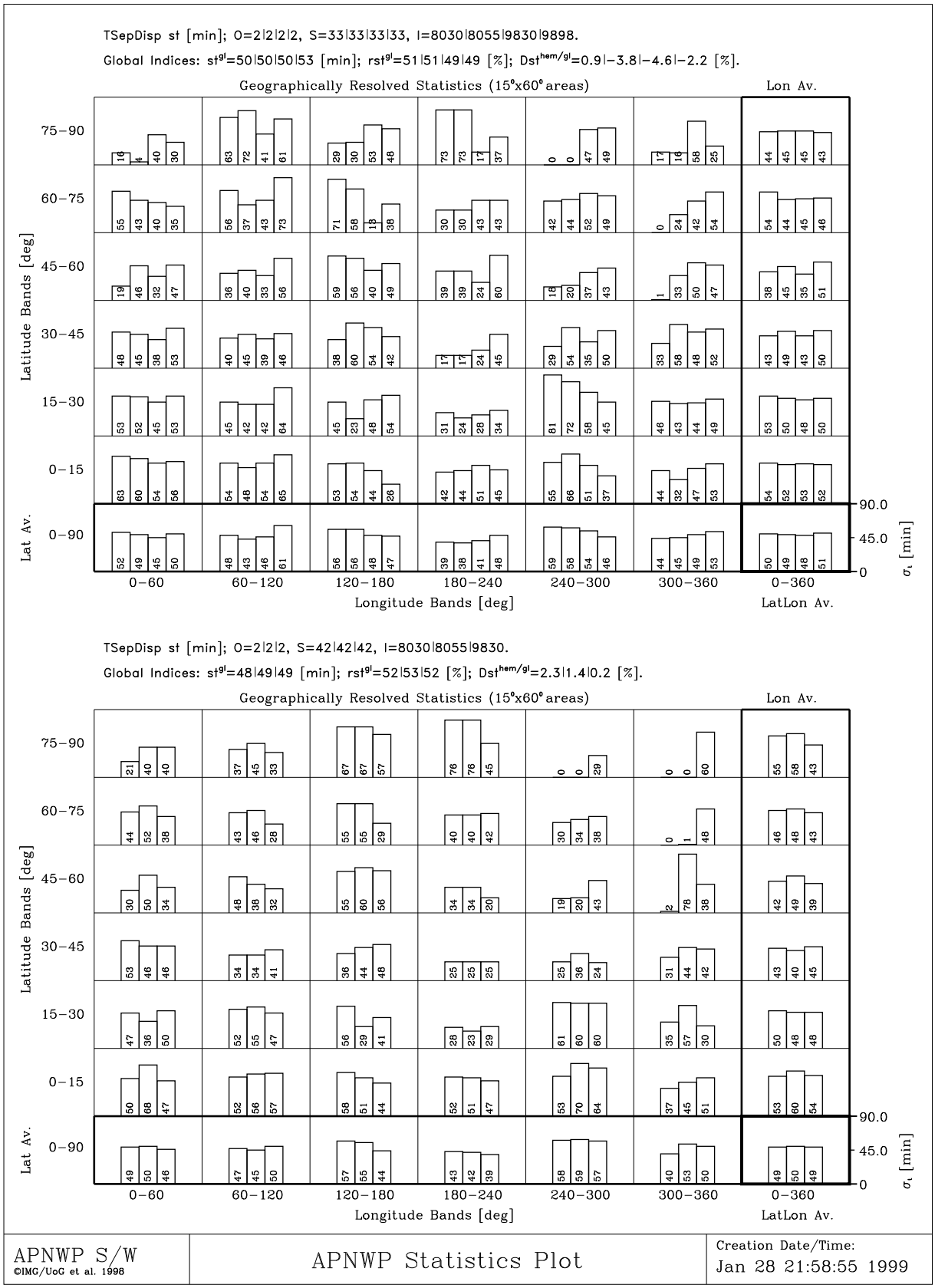

Figure 5.10: Time separation dispersion σ_t $[min]$.

5.5 Figure Caption for Figures 5.11 - 5.20

5.5.1 Contents

Figures 5.11 - 5.20 contain the results for the 12 sat/2 orbit symmetric satellite scenario with 6 sats per orbit (upper panel), as well as the results for its asymmetric complement with 8 satellites in the higher inclined orbit and 4 in the lower inclined orbit (lower panel). Figures 5.11 to 5.15 show the cases with node alignment ($\Omega = 0°$), while Figures 5.16 to 5.20 show the cases with node orthogonality ($\Omega = 90°$). As noted before, the pure sun-sync constellation was only calculated for the latter scenario.

5.5.2 Special Remarks

A quick look at Figure 5.11 shows that the number of occultation events still is somewhat uneven distributed over the globe. The maximum occultation event density reaches here 17.2 [Mm^{-2}].
The comparison with Figure 5.16 (the $\Omega = 90°$ case) shows immediately the significant difference between the optimum node separation and no node separation. Some scenarios give already quite smooth average occultation event distribution during the node-orthogonality situation shown in Figure 5.16. What is also clearly seen is that the pure sun-sync scenario yields significantly higher event numbers in the polar regions than the rest of the constellation scenarios.

Figures 5.12, 5.13, 5.17, and 5.18, illustrating mean distances and distance dispersions, are consistent with the number density results of Figures 5.11 and 5.16, respectively. The mean distances have been reduced compared to the 6-sat scencarios, as expected. In regions with relatively low event number density the distance dispersion is still relatively high, though.

Like for their predecessors for 6 sats, the results for the mean time separation (Figures 5.14 and 5.19) and the time separation dispersion (Figures 5.15 and 5.20) show no big difference between the best case and worst case scenarios. Also at higher latitudes the average time separation is generally greater than in the more equatorwards regions. In absolute values the time measures seem to possess no significant dependence on constellation size.

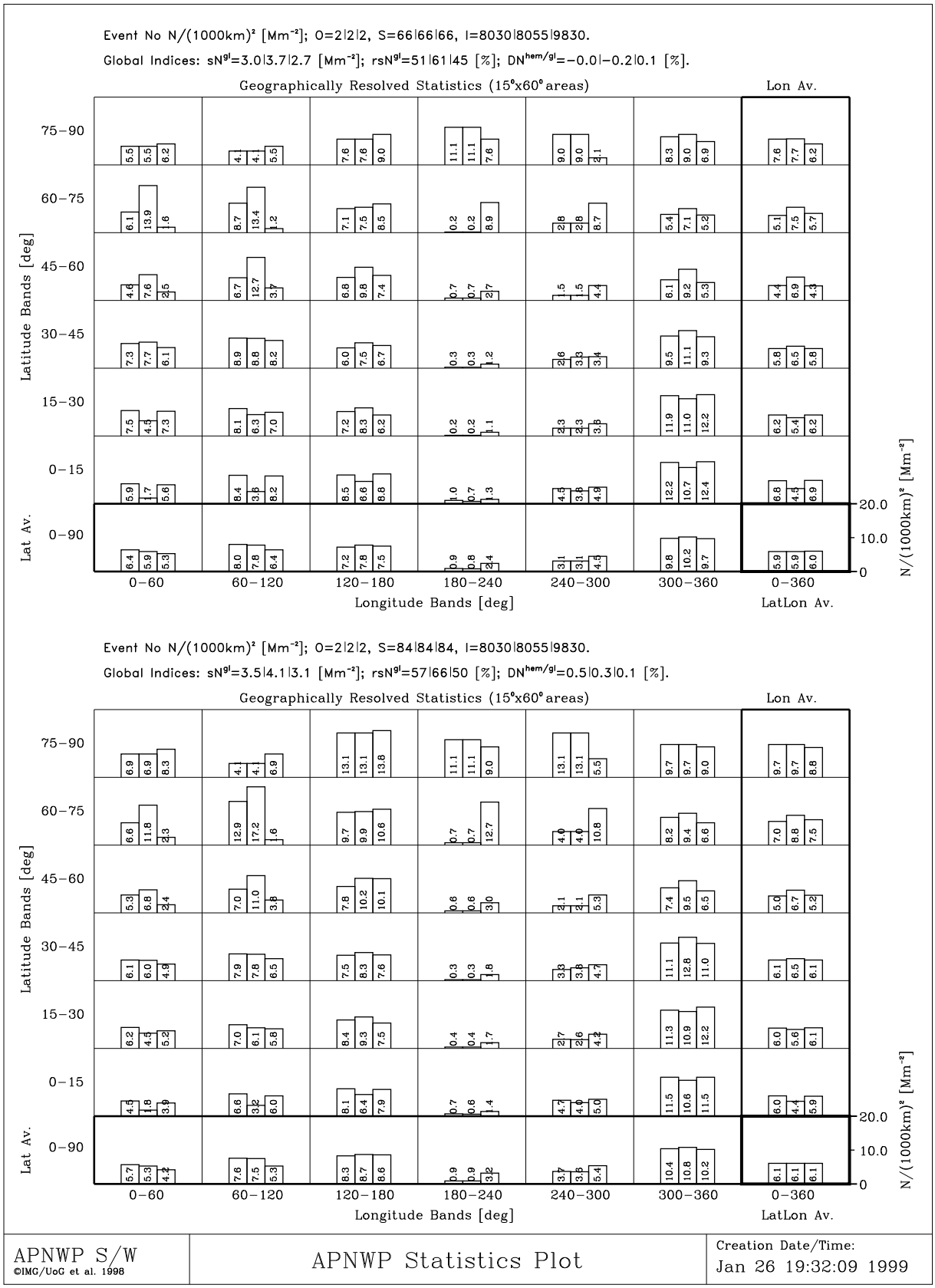

Figure 5.11: Occultation event number densities $N/(1000km)^2$ $[Mm^{-2}]$.

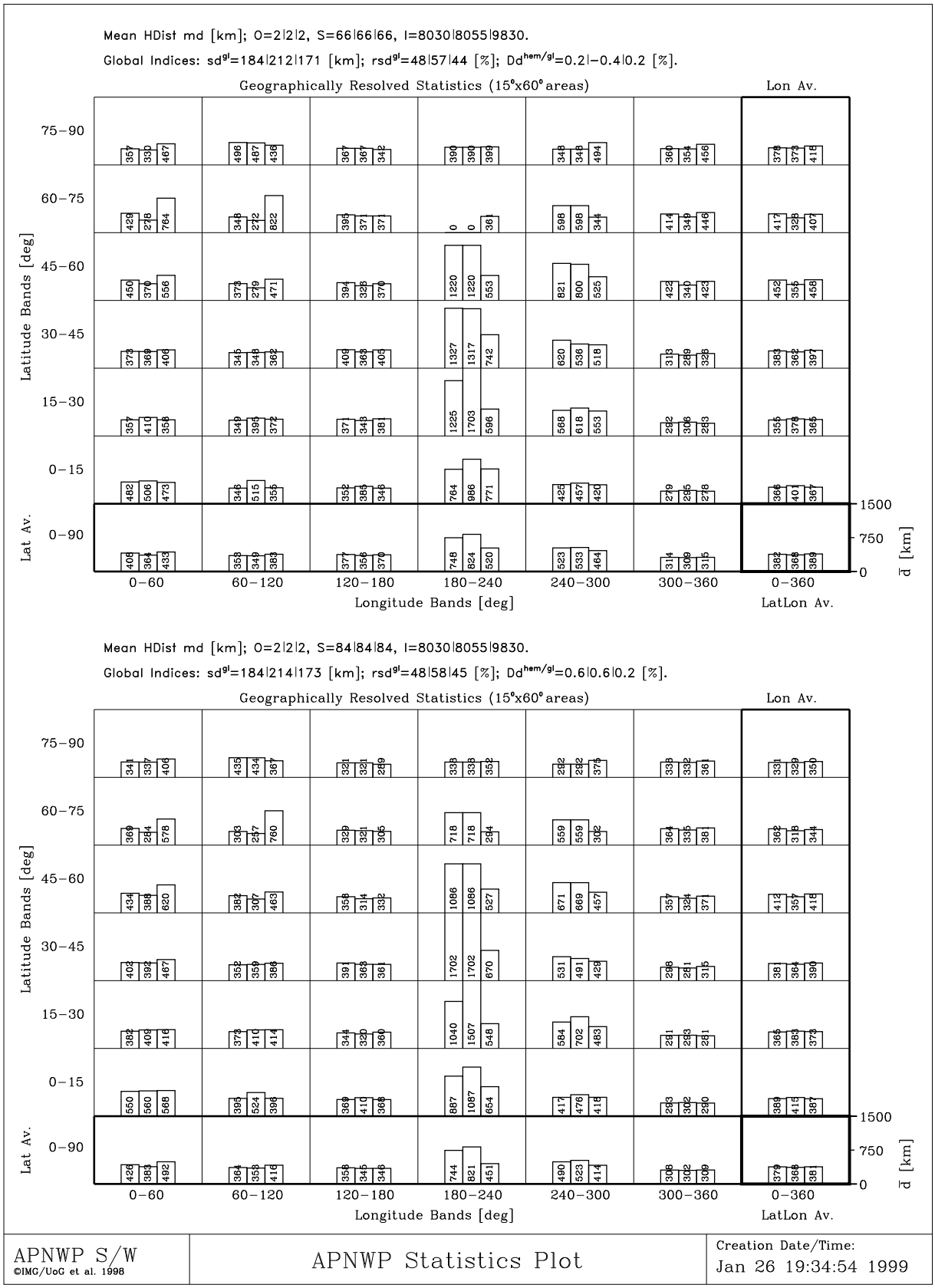

Figure 5.12: Mean horizontal distances $\overline{d}$ $[km]$.

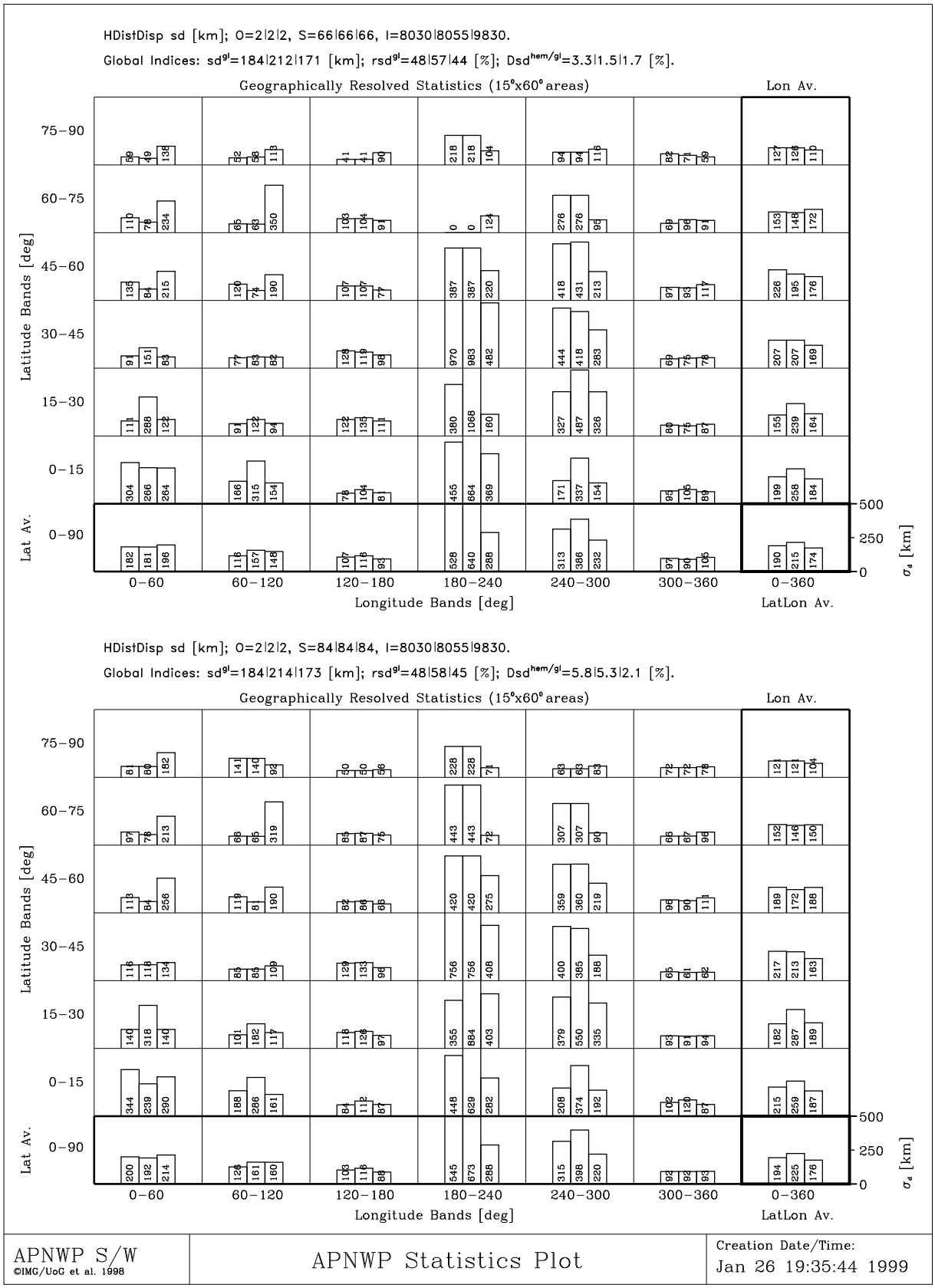

Figure 5.13: Horizontal distance dispersion σ_d $[km]$.

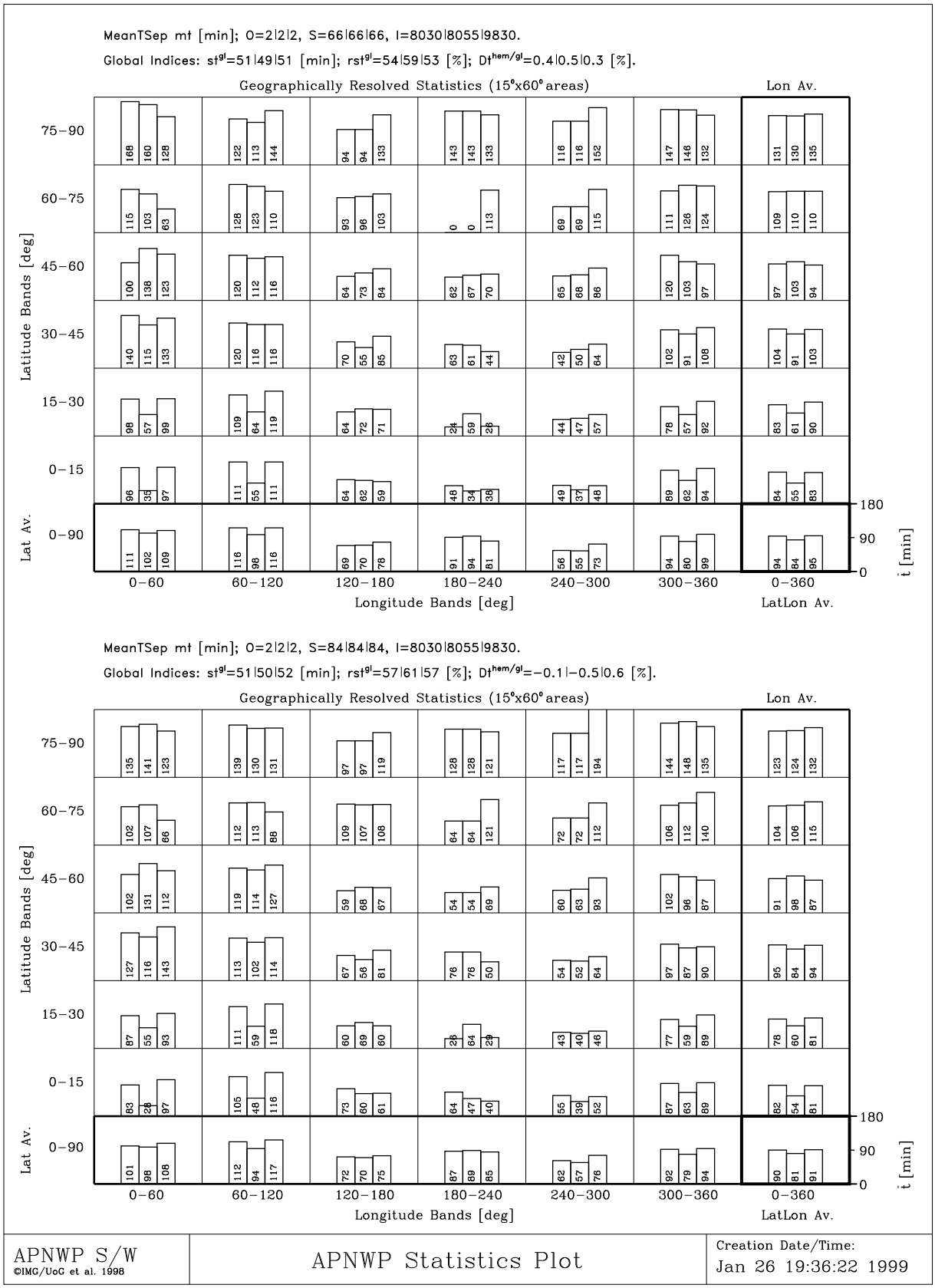

Figure 5.14: Mean time separation $\bar{t}$ $[min]$.

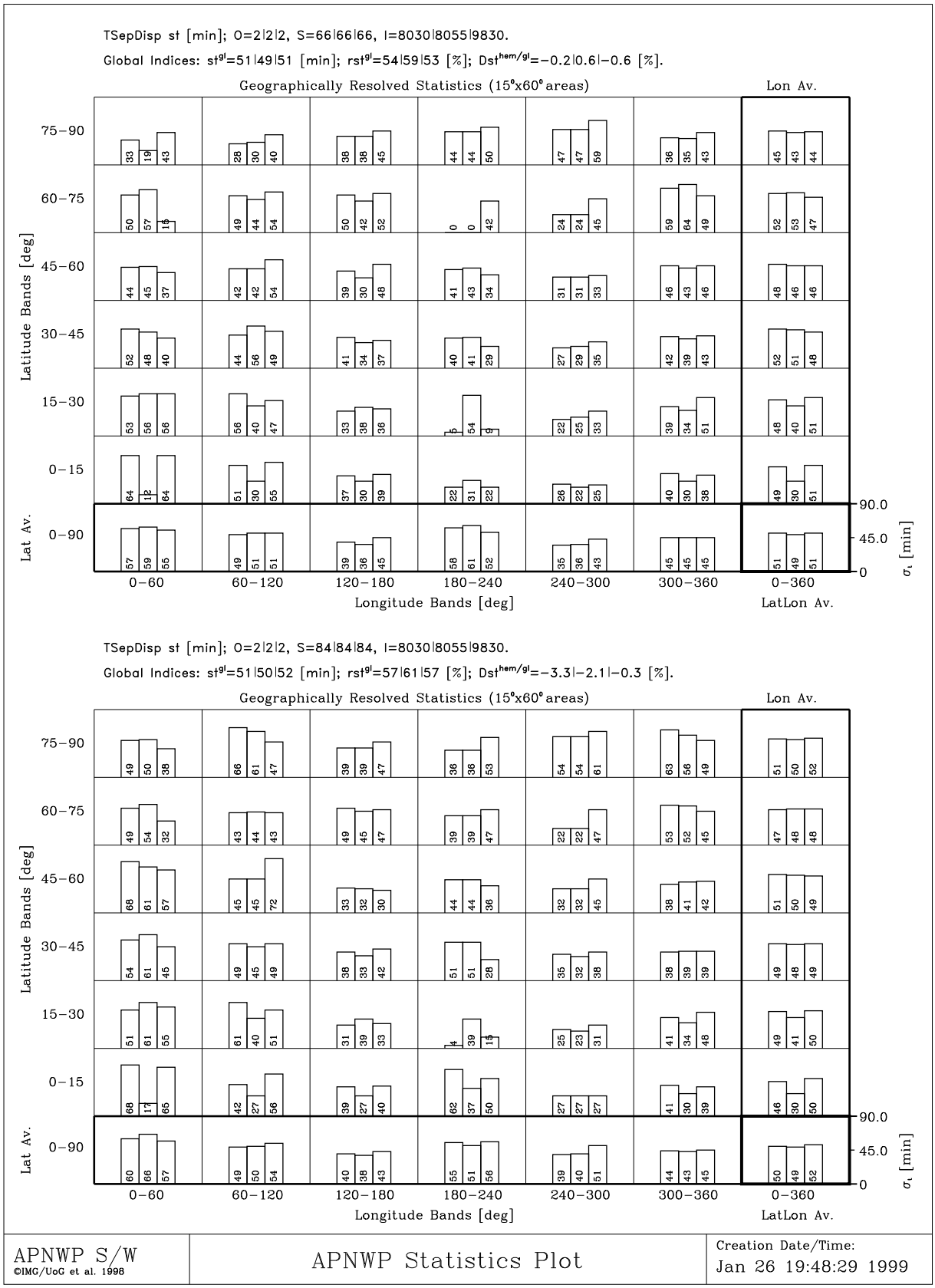

Figure 5.15: Time separation dispersion σ_t $[min]$.

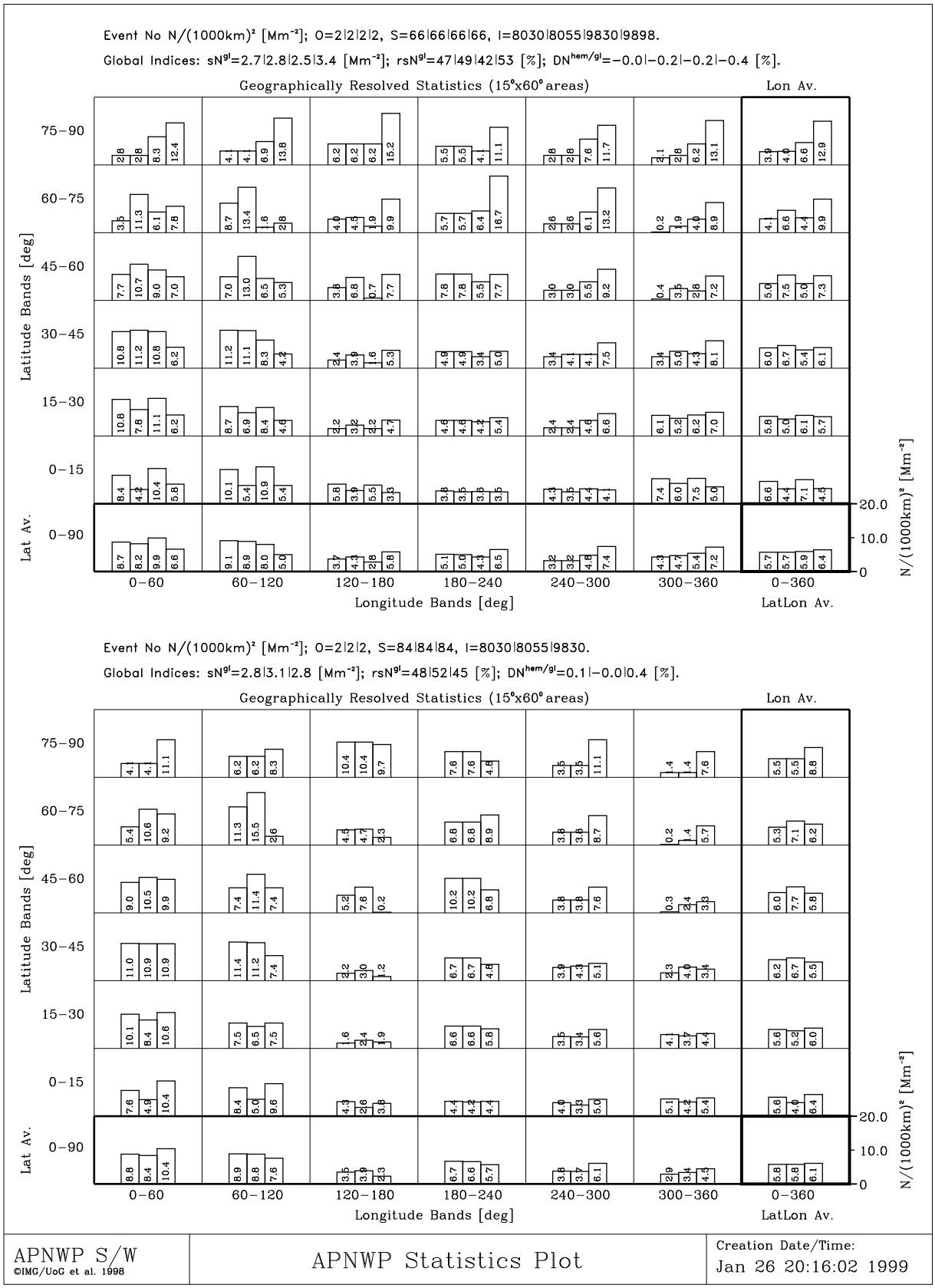

Figure 5.16: Occultation event number densities $N/(1000km)^2$ $[Mm^{-2}]$.

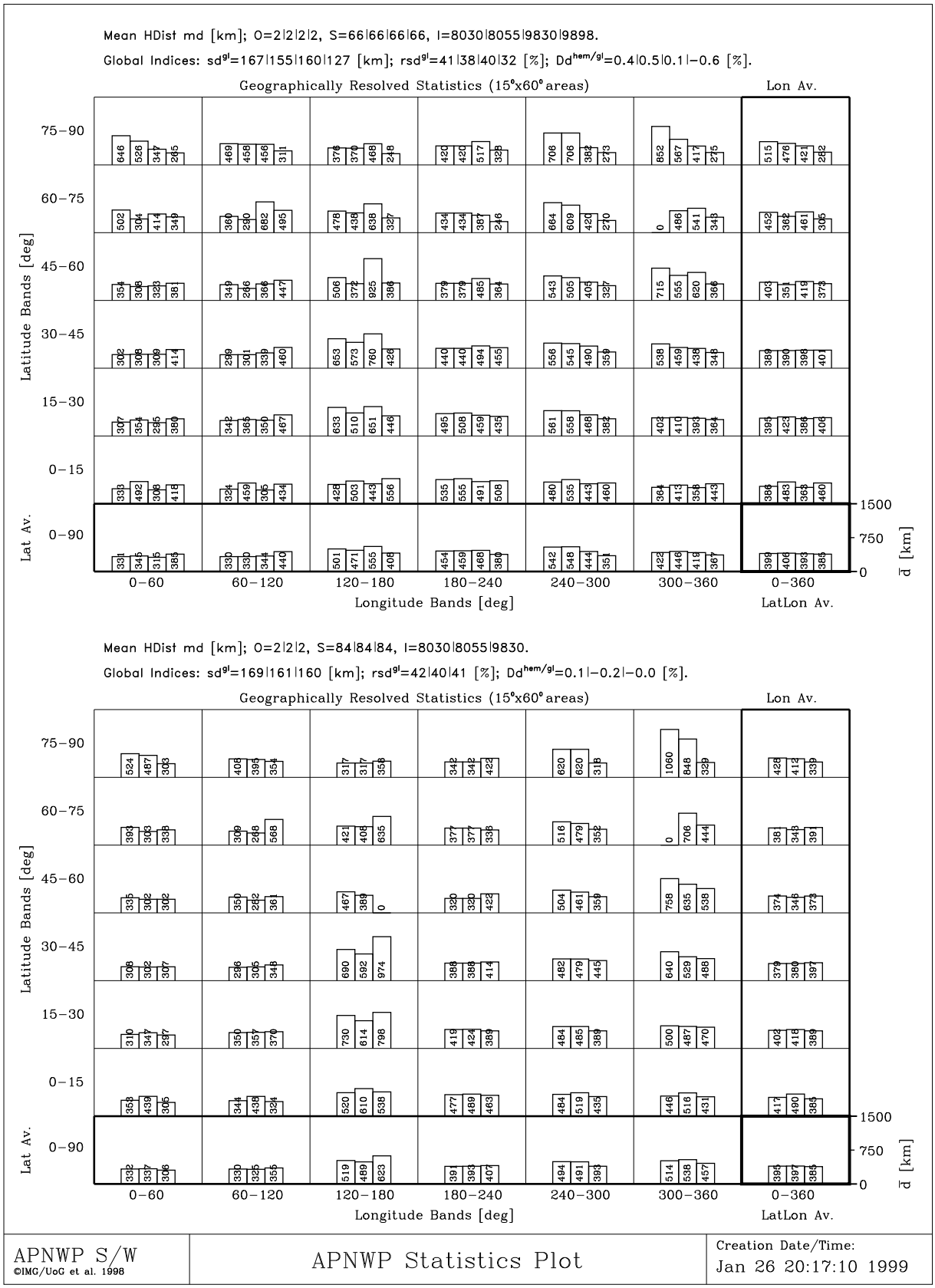

Figure 5.17: Mean horizontal distances $\overline{d}$ $[km]$.

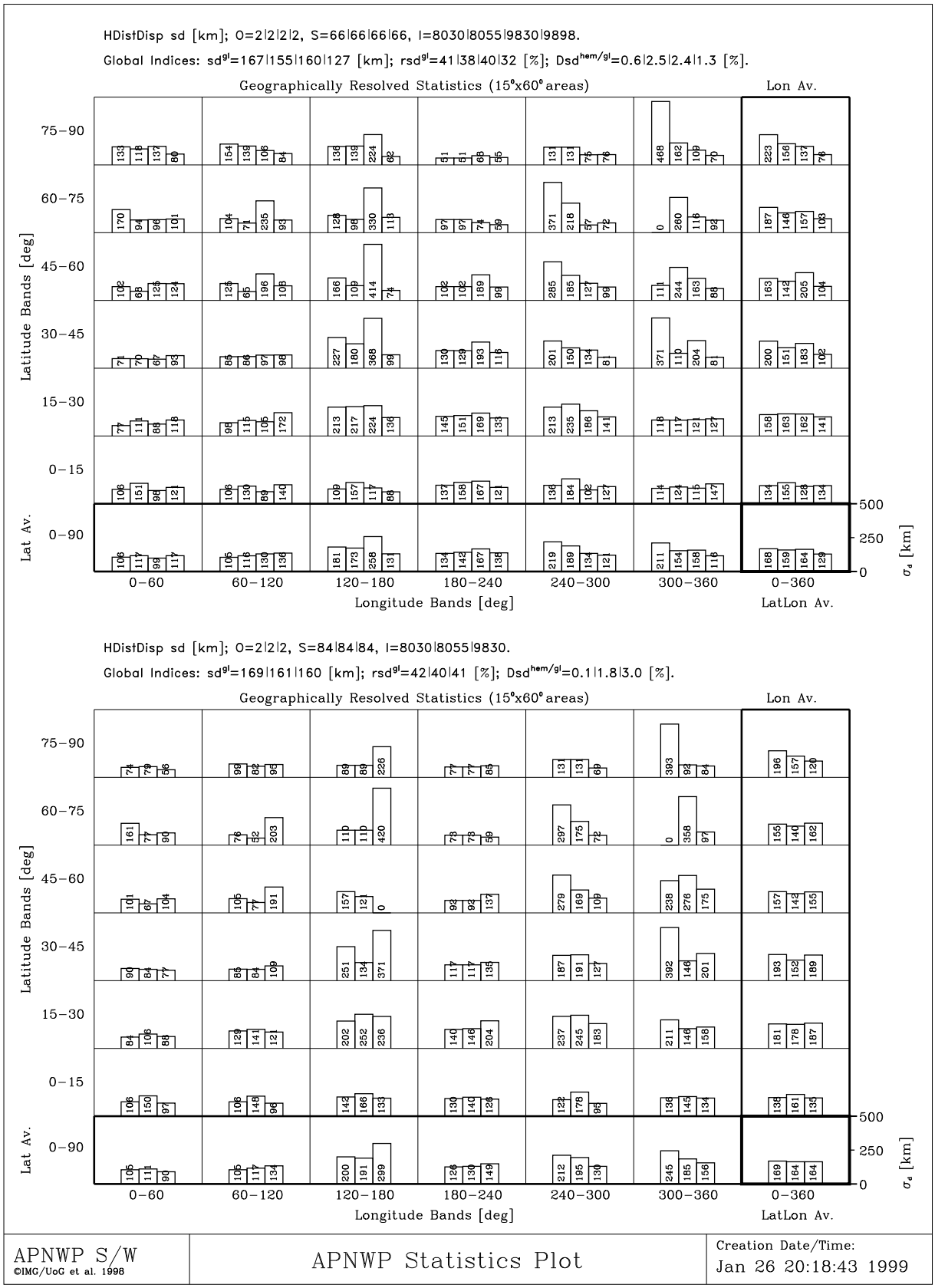

Figure 5.18: Horizontal distance dispersion σ_d $[km]$.

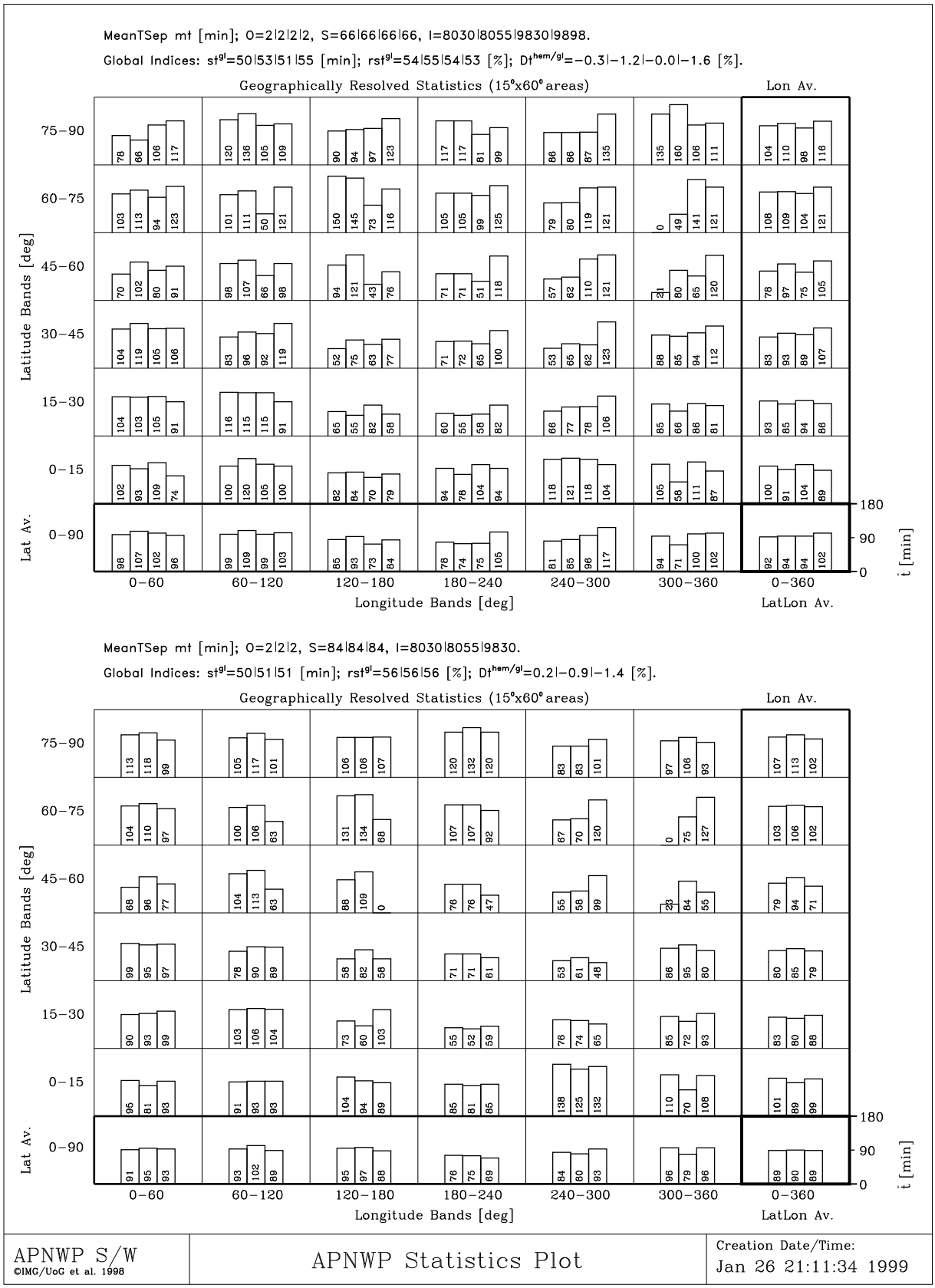

Figure 5.19: Mean time separation $\bar{t}$ $[min]$.

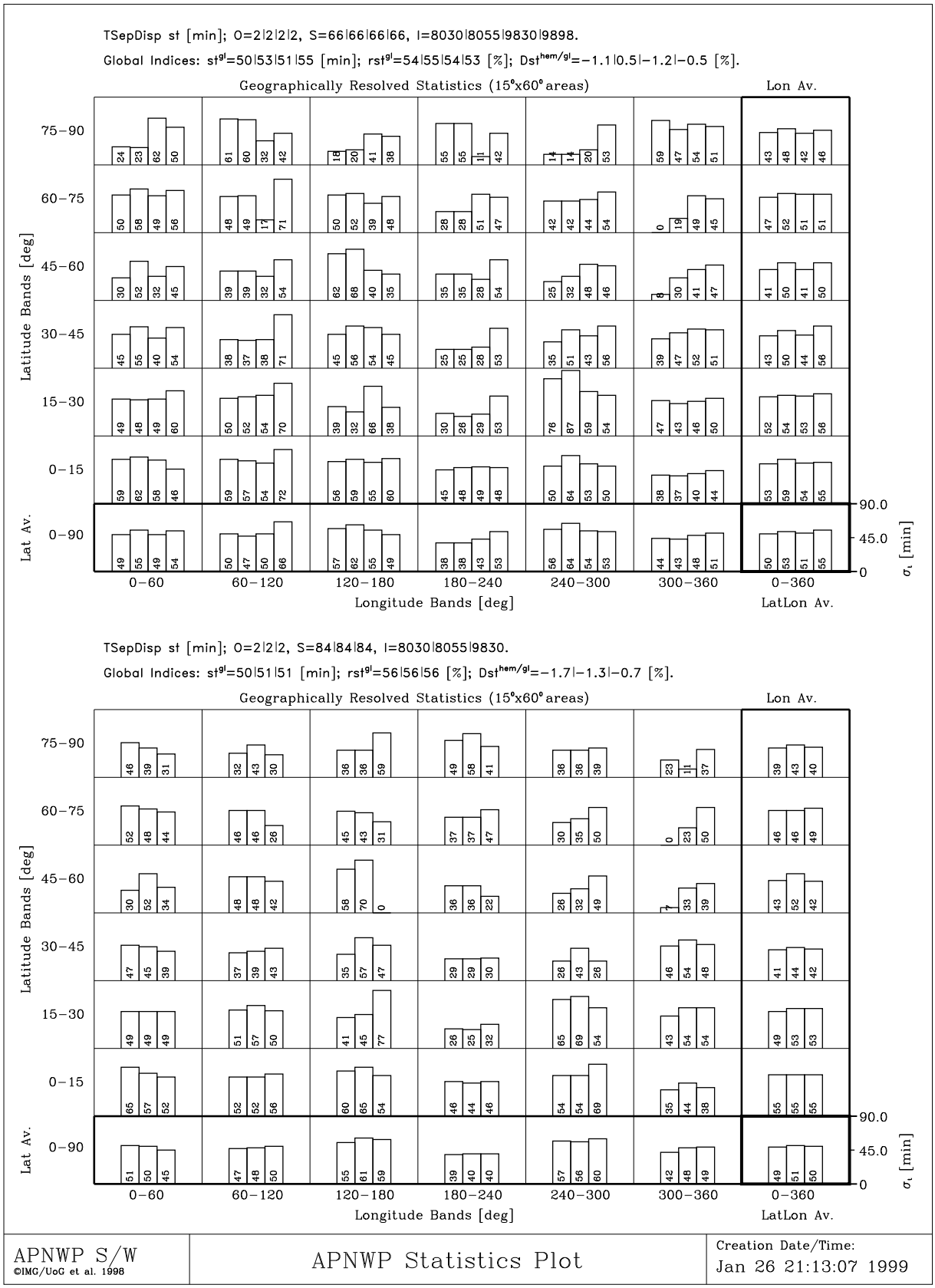

Figure 5.20: Time separation dispersion σ_t $[min]$.

5.6 Figure Caption for Figures 5.21 - 5.30

5.6.1 Contents

Figures 5.21 - 5.30 contain the results for the 24 sat/4 orbit symmetric satellite scenario with 6 sats per orbit (upper panel), as well as the results for its asymmetric complement with 8 satellites in the higher inclined orbits and 4 in the lower inclined orbits (lower panel).
Figures 5.21 to 5.25 show the cases with node alignment ($\Omega = 0°$), while Figures 5.26 to 5.30 show the cases with maximal node dispersion ($\Omega = 45°$). As noted before, the pure sun-sync constellation was only calculated for the latter scenario.

5.6.2 Special Remarks

A quick look at Figure 5.21 shows that with 24 LEOs in orbit symmetrically sharing 4 different orbit planes with different orbit inclinations the number of occultation events is now quite equally distributed over geographic space. A comparison of Figures 5.21 and 5.26 shows that the question of node alignment or dispersion begins to play a more minor role for that large, well distributed constellations. The dependence on the state of the nodes is quite reduced already though still some effect is seen. are d as seen before a distinct improvement over the former worst case scenarios. The global situation is quite acceptable.

Figures 5.22, 5.23, 5.27, and 5.28, showing mean distances and distance dispersions, are again quite consistent with the number density results shown in Figures 5.21 and 5.26. We see that this constellation, showing in average mean distances below 300 km, already meets the requirements of Table 2.1.

For the 24 satellite constellations the overview shows that the mean time separation (Figure 5.24 and 5.29) and the time separation dispersion (Figure 5.25 and 5.30) are more equally distributed than in the former cases with smaller constellations. Especially in the scenarios with equally separated satellites per orbit, the differences between the individual cells are relatively small (for both variables) with average values for the time separation near 2 hours and average value near 50 minutes for the time dispersion, respectively. Note that the absolute values for the time separation definitely do not decrease with constellation size, they stay roughly constant.

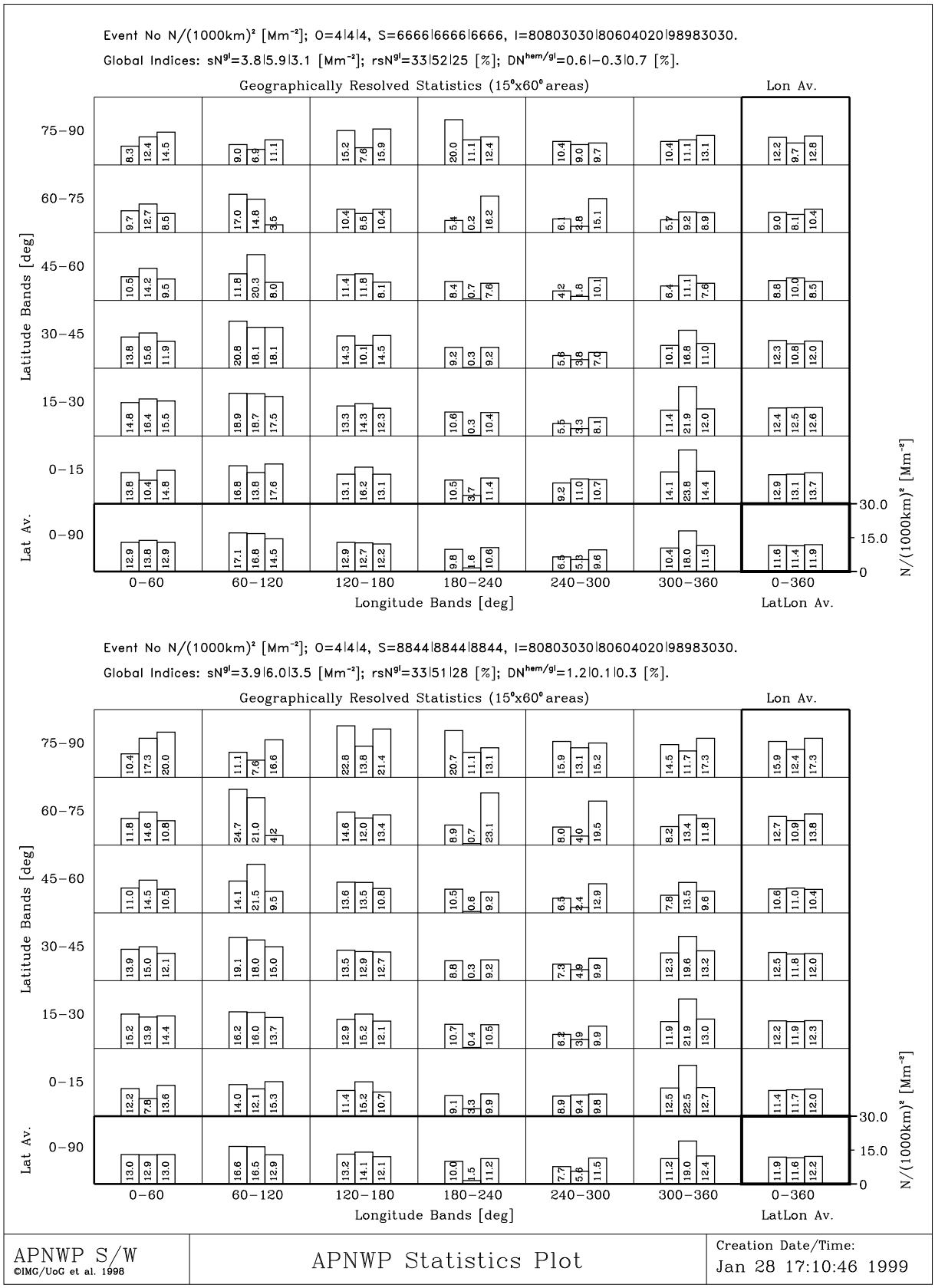

Figure 5.21: Occultation event number densities $N/(1000km)^2$ $[Mm^{-2}]$.

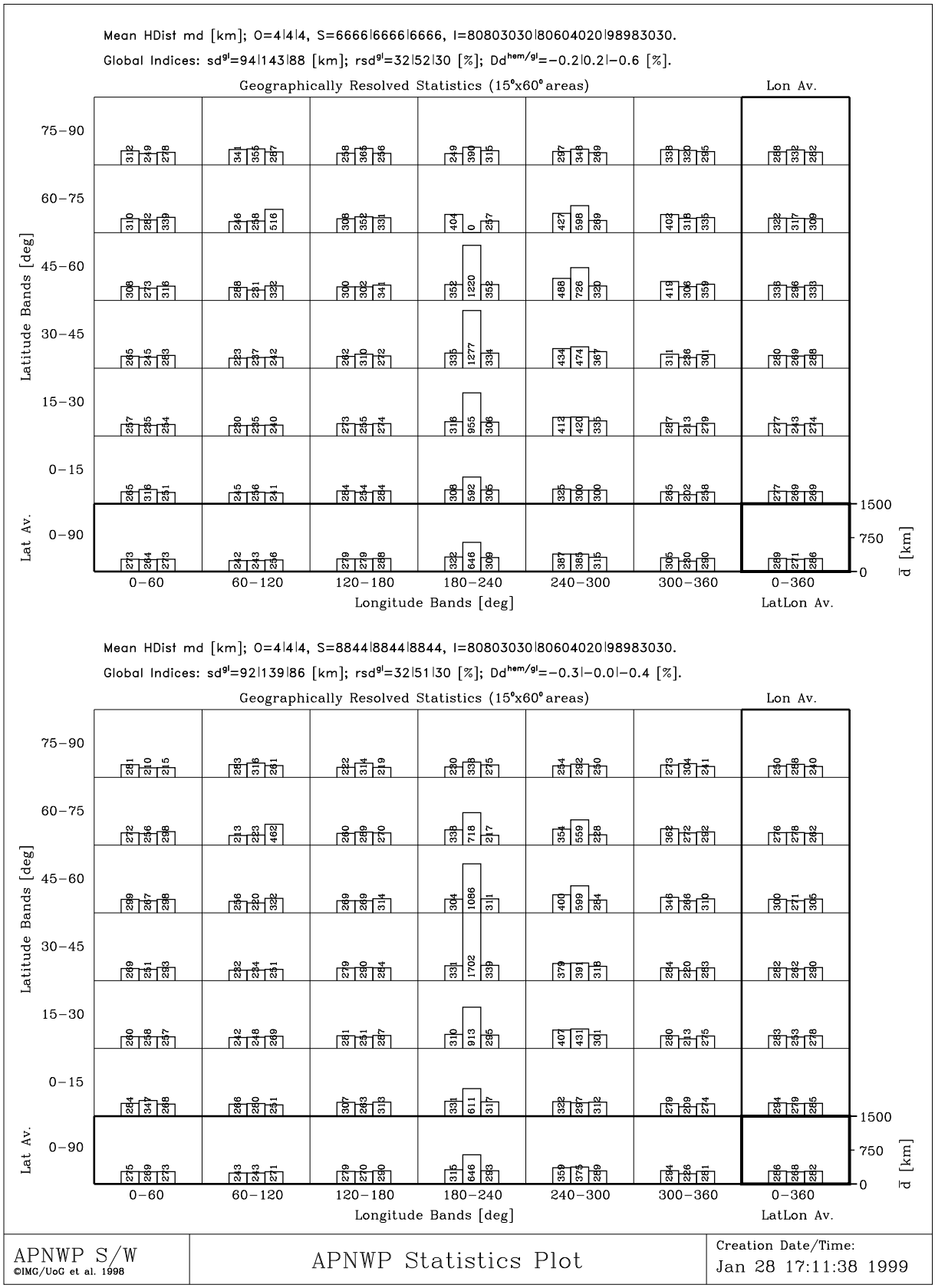

Figure 5.22: Mean horizontal distances $\overline{d}$ $[km]$.

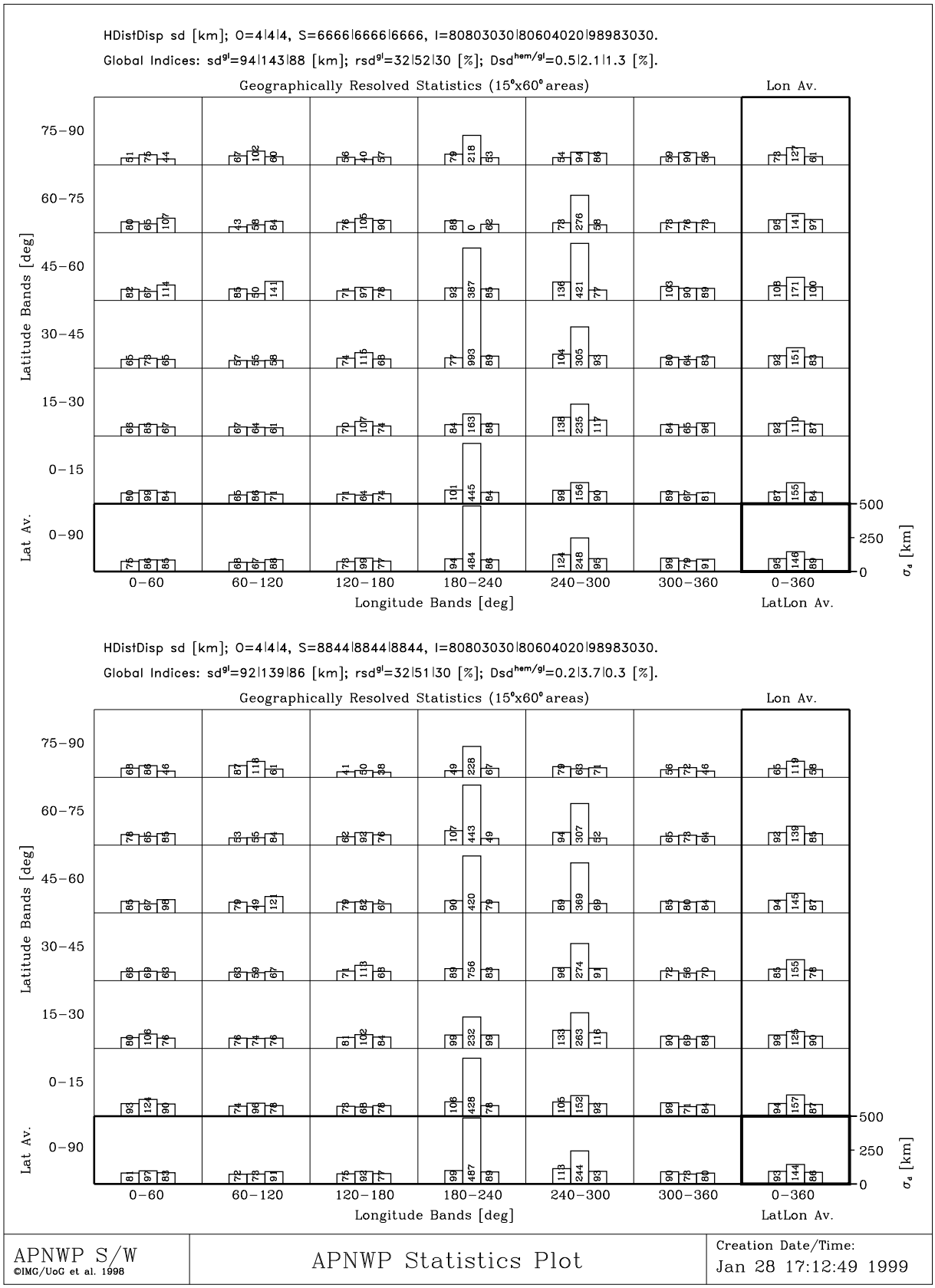

Figure 5.23: Horizontal distance dispersion σ_d $[km]$.

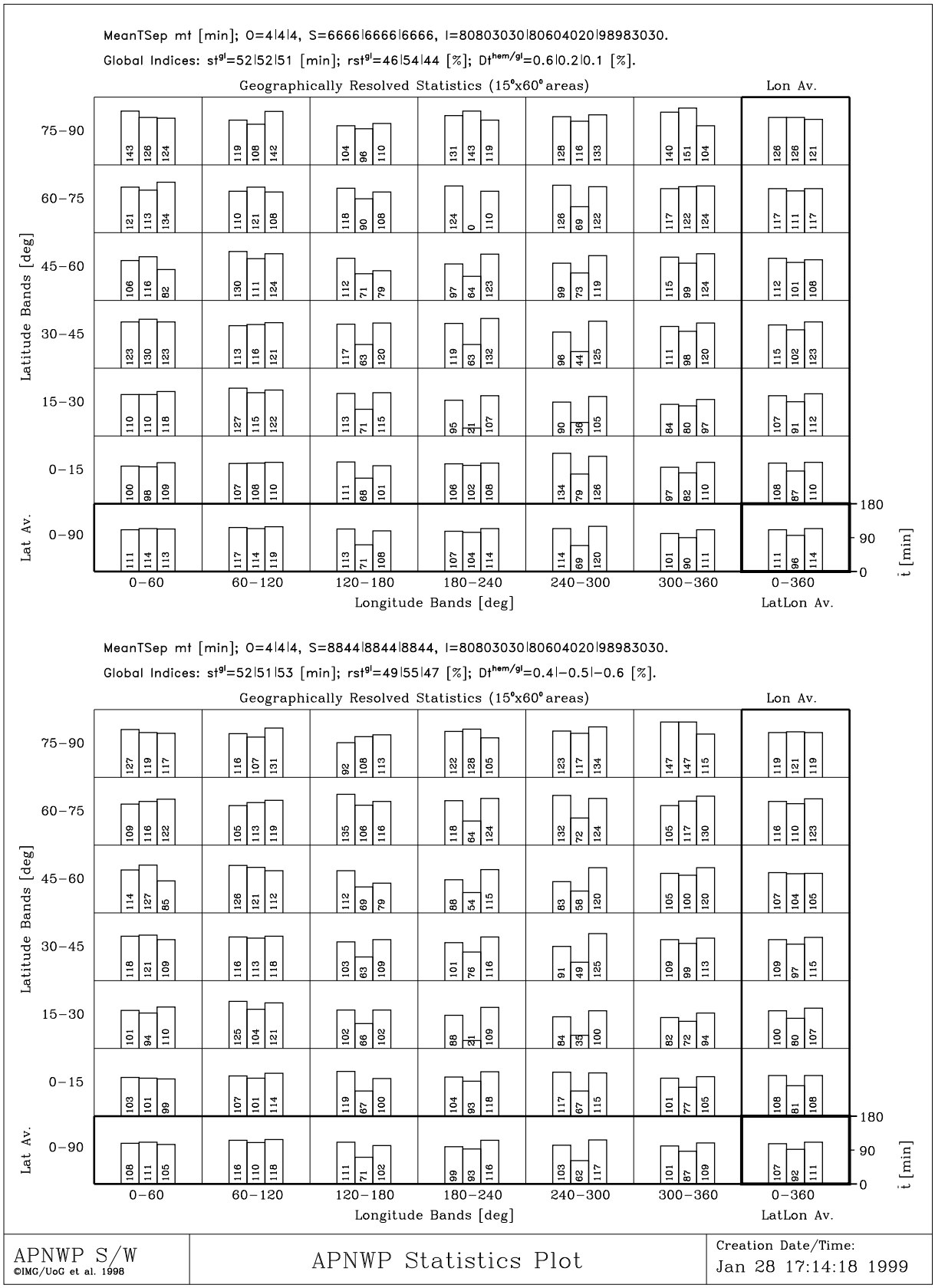

Figure 5.24: Mean time separation $\bar{t}$ $[min]$.

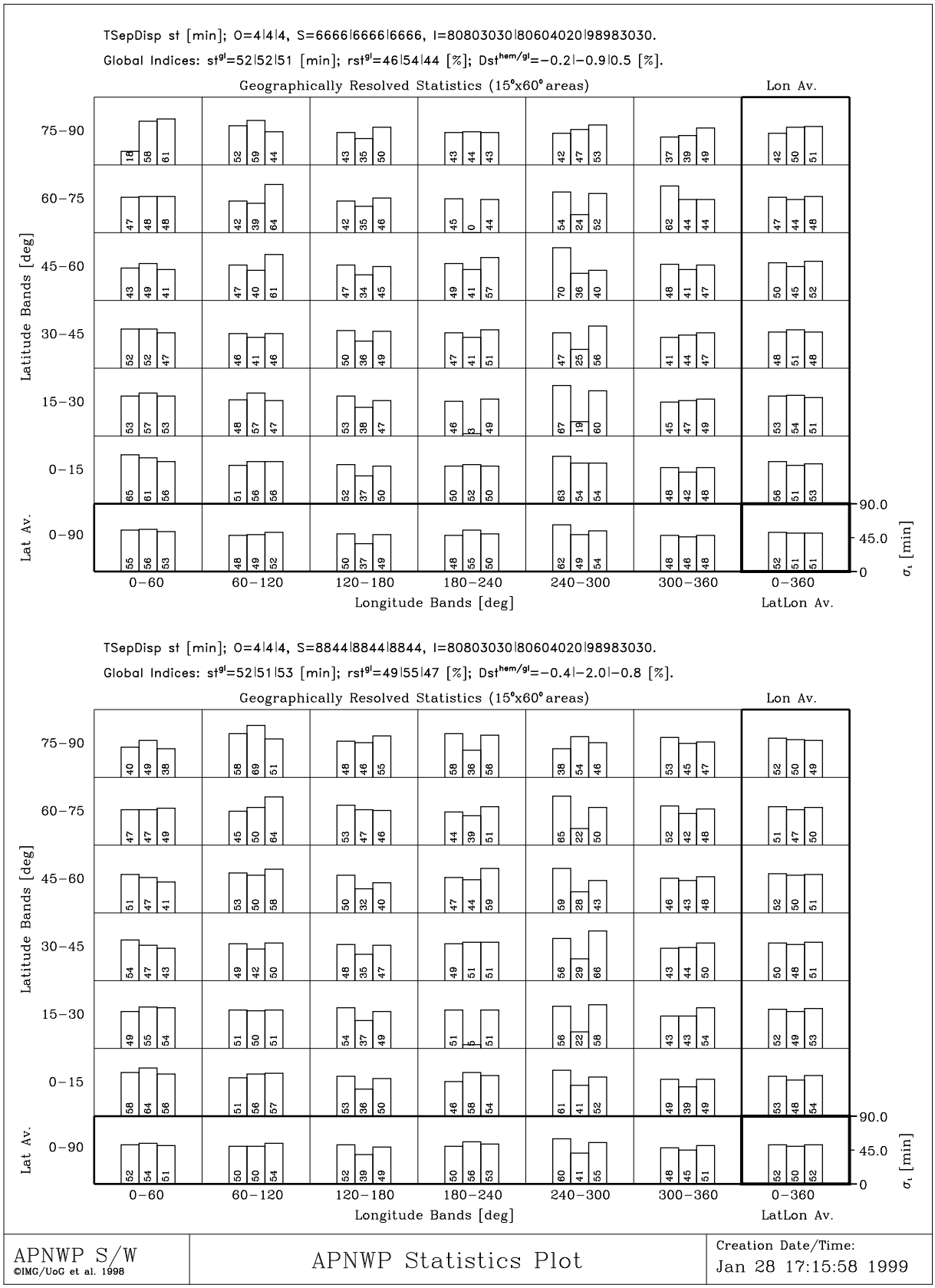

Figure 5.25: Time separation dispersion σ_t $[min]$.

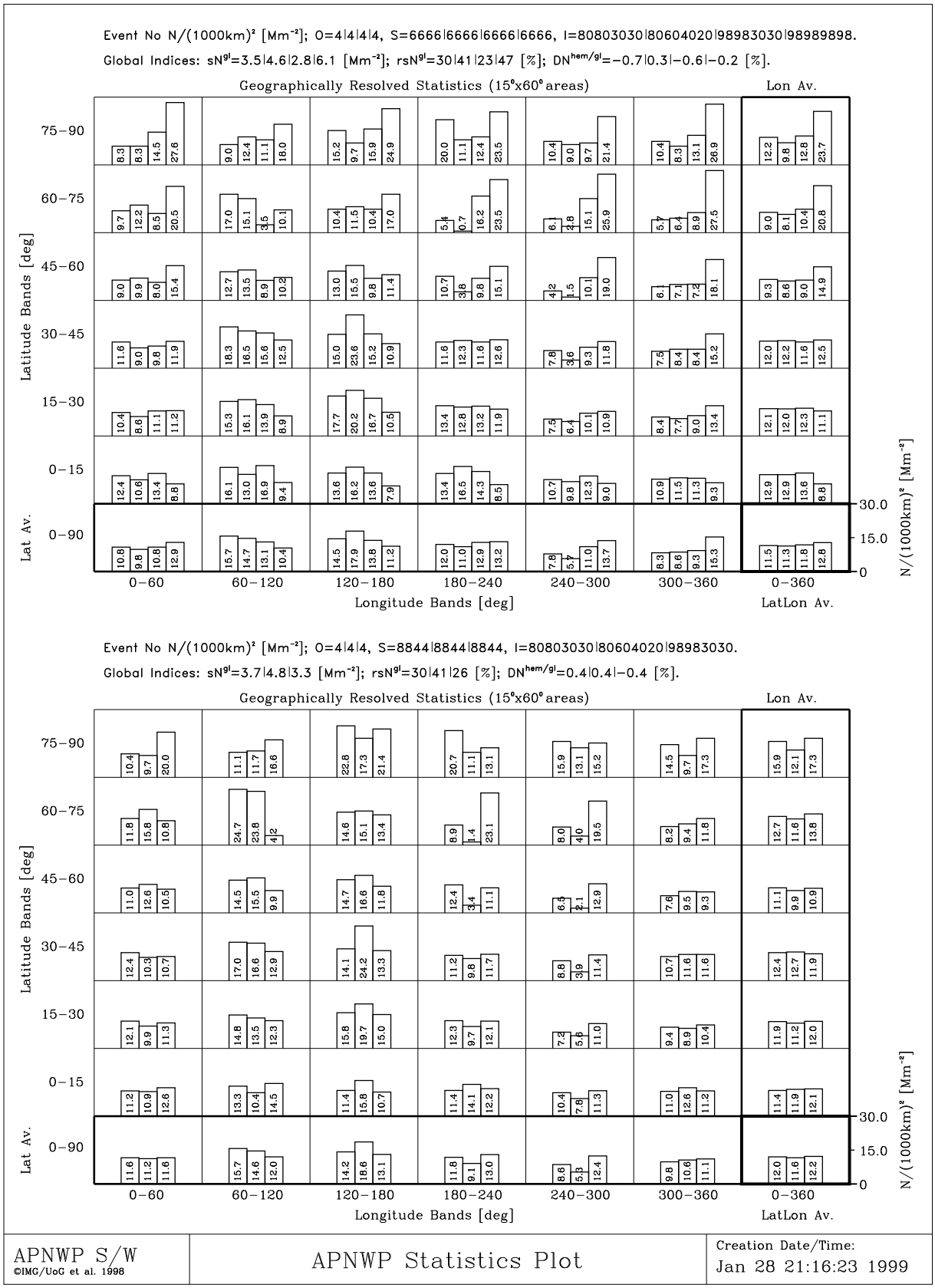

Figure 5.26: Occultation event number densities $N/(1000km)^2$ $[Mm^{-2}]$.

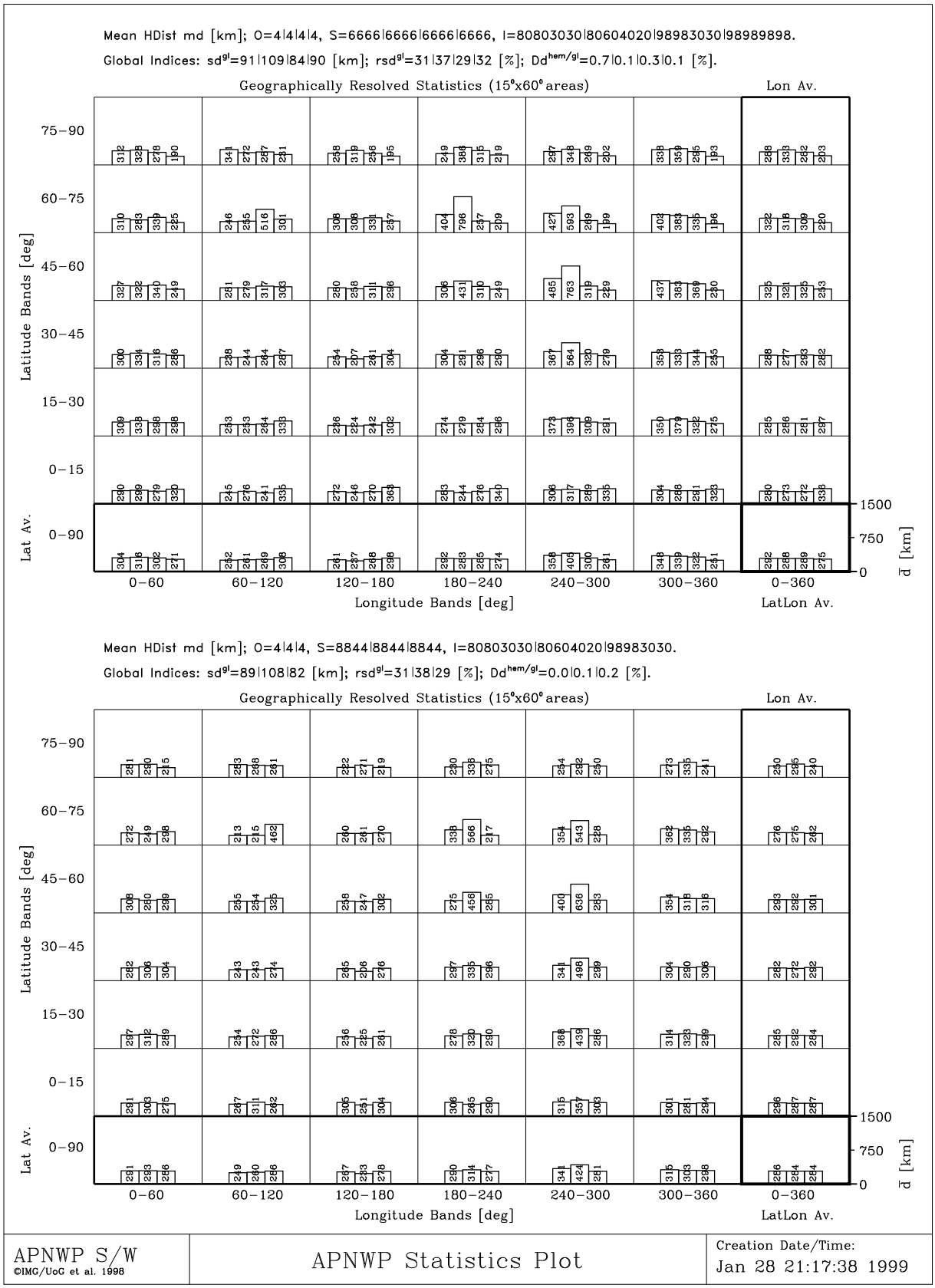

Figure 5.27: Mean horizontal distances $\overline{d}$ $[km]$.

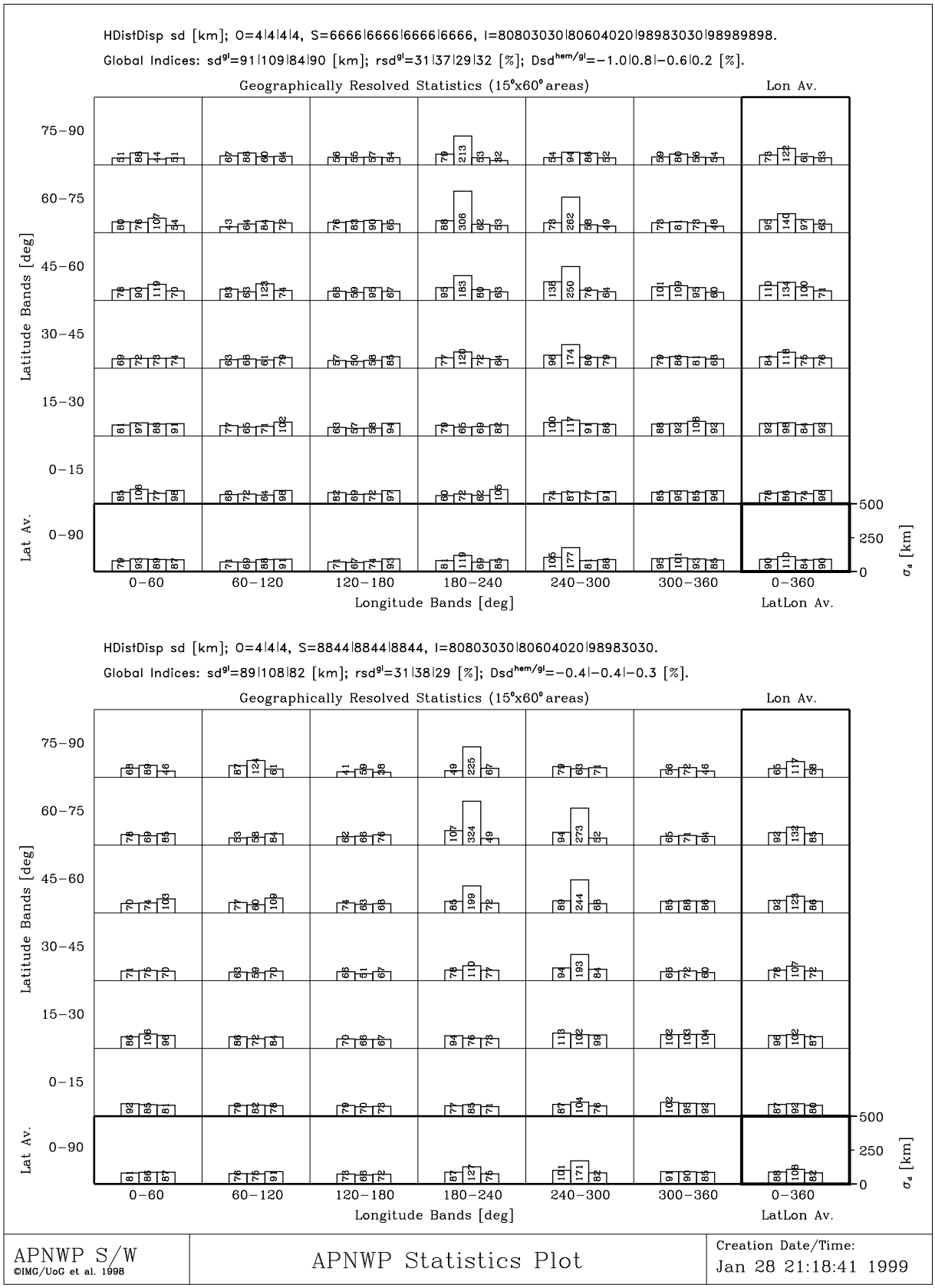

Figure 5.28: Horizontal distance dispersion σ_d $[km]$.

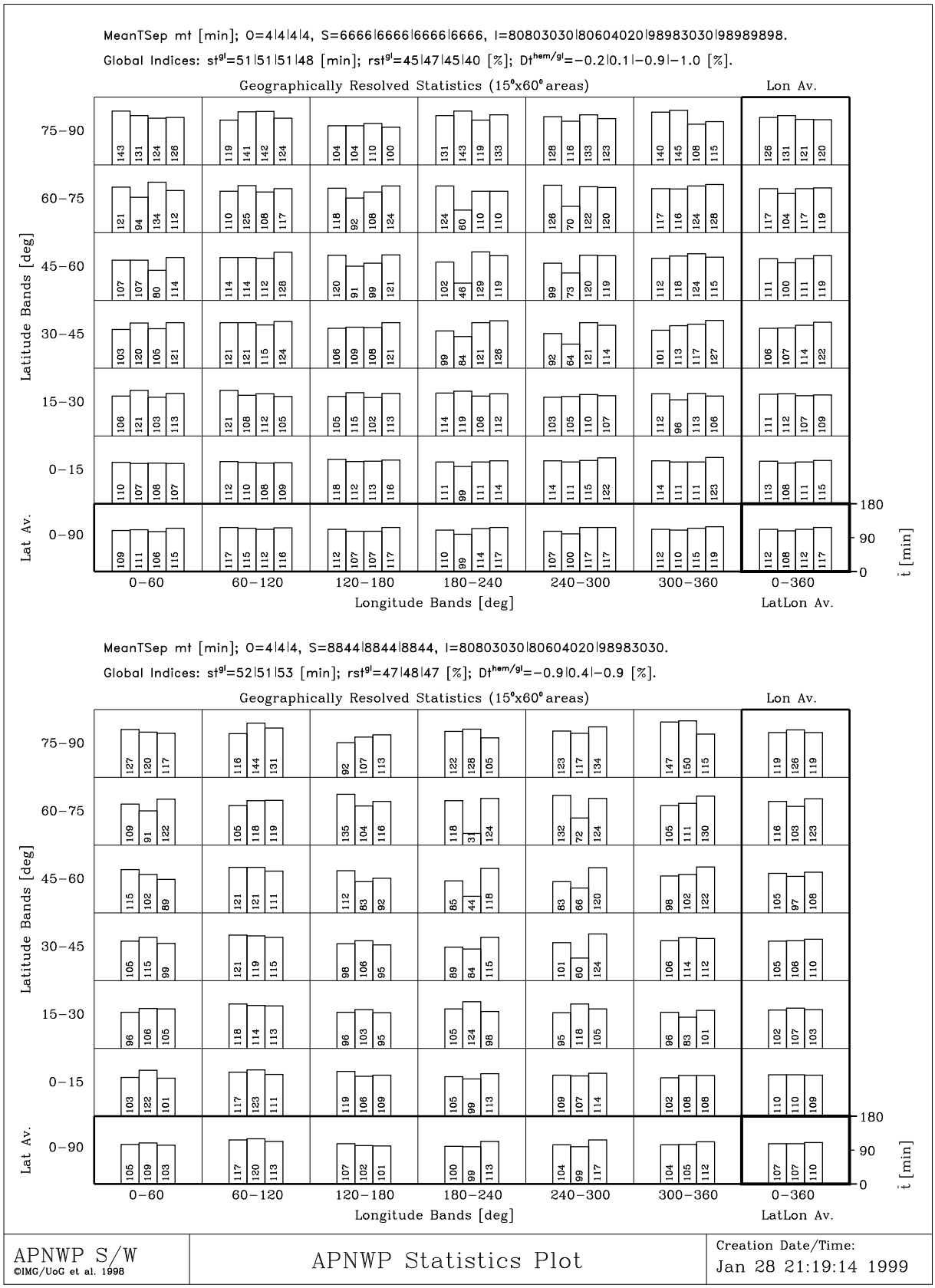

Figure 5.29: Mean time separation $\bar{t}$ $[min]$.

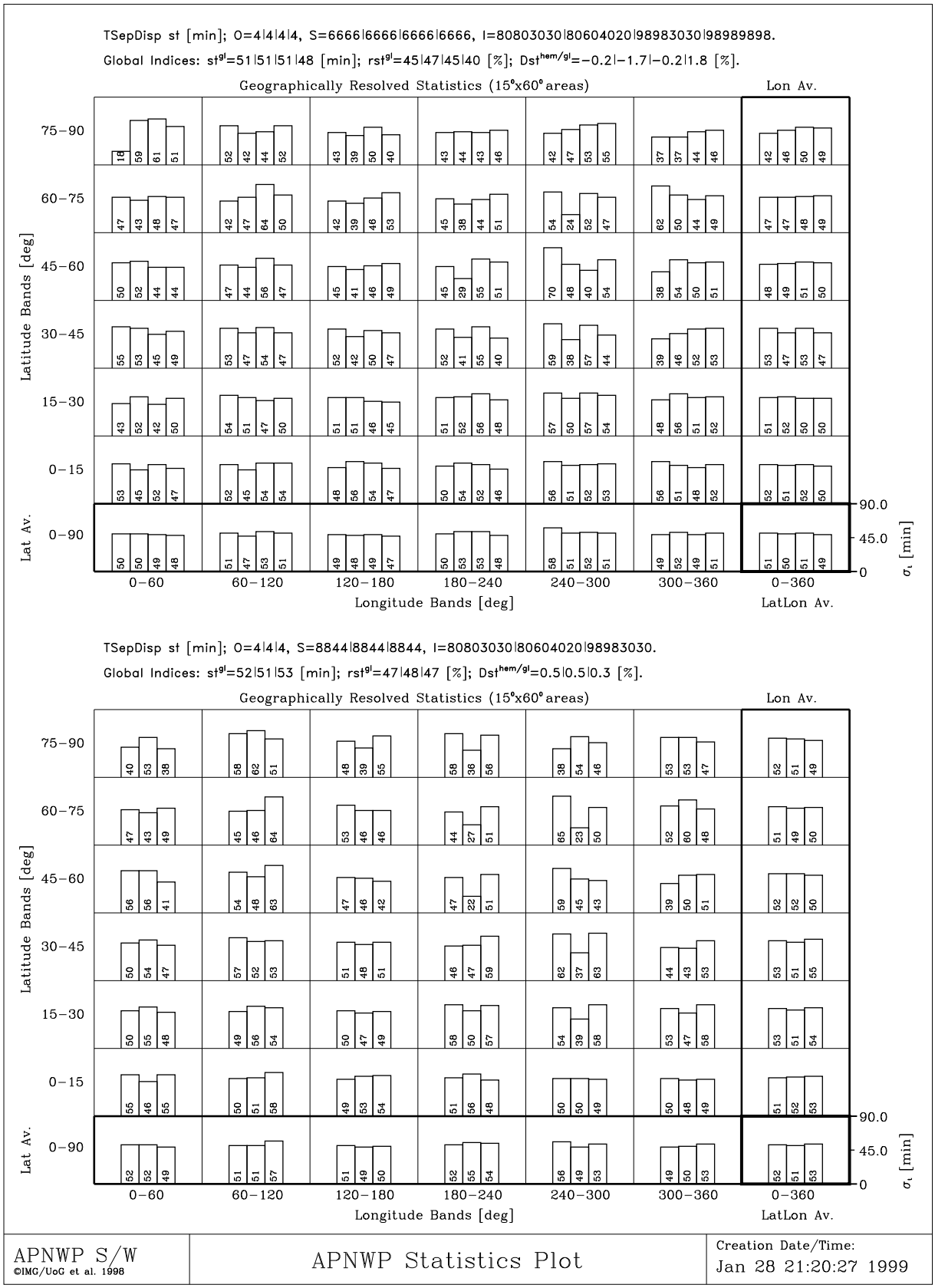

Figure 5.30: Time separation dispersion σ_t $[min]$.

6 Summary and Conclusions

In this report we have, after reviewing and defining observational requirements for NWP, described how we designed a GNSS constellation mission scenario study, how we computed about 60 different relevant simulations, and how we analyzed the results of these different scenarios. Beginning with 21 simple satellite constellation scenarios (the so-called basic cases), we increased the complexity of the satellite constellations, in our 39 real scenario simulations, to configurations of up to 24 satellites orbiting simultaneously in 4 different orbital planes with different inclinations and nodes for the orbits.

Before starting with the satellite constellation simulations, relevant statistical performance measures were defined, including the number of occultation events per unit area, the mean distance between neighbor events, the rms dispersion of distances about this mean, the mean time separation of neighbor events, and the rms dispersion of time separations about this mean, respectively. For getting some expertise on the different influences of typical input variables (mainly orbital elements) on performance measures we first investigated so-called basic scenarios. This provided guidance, besides predefined generic requirements and general constraints which we introduced at the beginning of the report, for the design of more realistic scenarios. These were designed to sensibly sample the basin space of LEO constellations in view of preparing good candidate constellations for a subsequent selection of a few constellations to be used as basis for NWP experiments.

We aimed at reasonably sampling the basin space with an as small as possible number of candidate scenarios and finally selected a pool of 39 realistic scenarios spanning a diversity of satellite configurations with satellites spread out over different orbital planes with different inclinations and satellite numbers per orbit and different orbit node geometries. A lot could and can be learned from analyzing and comparing the individual results of the real scenarios: We provide the results in this report in highly visualized form in an atlas-like manner so that the reader can thoroughly inspect and intercompare the results of all scenarios in all statistical measures computed.

A straightforward result of the scenarios was the confirmation that there is a near linear dependence of the average occultation event number density on the size of the constellation. The regional details in number density are highly dependent on constellation layout, though, as is well illustrated by our result figures. Given the number of satellites, the largest single constellation design action to take is using sensibly placed multiple orbital planes for the satellites (also somewhat straightforward). An interesting result was that the mean time separation between neighbor events is roughly independent of constellation size. Concerning mean distance between neighbor events, the largest constellation considered (24 satellites) was definitely able to entirely fulfil the (geographic space/time) observational requirements set out at the beginning of the study.

Another feature of interest in the results is the significant influence of differential orbital drift, in case of orbit planes with different inclinations. It makes quite a difference whether the constellation is in a phase of maximally aligned nodes (event distribution more uneven) relative to a phase of maximally dispersed nodes (event distribution maximally even). These phases are, for typical constellations, periodically passed with a period of around one month. Larger constellations increasingly reduce the dependence on the state of nodes, with 12 satellites it is still quite well visible, however.
Regarding equal coverage, we should furthermore note that a pure sun-synchronous satellite constellation should be avoided because such a configuration definitely tends to place

too many occultation events at higher latitudes - as we clearly see in both the number density and distance measures - while the lower latitudes are underfilled.

As most favorable scenarios from our analyses of different satellite constellations we can tendatively recommend one of our 24 satellite scenarios with two higher inclined orbit planes and two lower inclined ones (all of them as equally separated in their orbital nodes as possible). These scenarios fulfil the requirements set out at the beginning of the report by using still a relatively small fleet of satellites, and already provide quite homogeneous overall coverage as indicated by the different statistical measures.

In a next step we will make the tendative conclusions presented above more firm by a quantitative performance assessment of realistic scenarios studied here. Based on the quantitative results obtained, we will perform an assessment combining all statistical measures computed, complemented by measures reflecting implementation costs, with a weighting scheme. This will be performed in order to select, from all constellations considered here, a sample of 3-4 "best" constellations as basis for our NWP experiments.